

# Feasibility Study of Integrating a 120MW Photovoltaic Power Plant into the Jamaican Power Grid

O'Neil Jesse Nelson

A thesis submitted to  
Auckland University of Technology  
in fulfilment of the requirements for the degree of  
Master of Engineering (MEng)

2018

School of Engineering



## Abstract

Utility scale photovoltaic (PV) power plants are generally feasible in geographic areas exposed to greater than 3 kWh/m<sup>2</sup>/day of sun irradiance. Jamaica is suited to capitalise on this natural resource, with a reported solar exposure yield of 5–7 kWh/m<sup>2</sup>/day and available lands for the development of a utility-scale PV system to supply the island state's existing grid. Currently, the challenges faced in Jamaica are grid management issues such as difficulties managing frequency and determining the reserve margin. These issues are deterrents to increasing the penetration of utility scale renewable generation. This research aims to combat these and other technical challenges through micro-grid simulations on a country scale. This thesis presents a comparison between the technical outcomes of the conventional network configuration and the technical outcomes when conventional sources are replaced with PV integration. Three different model simulations were conducted using technically accepted parameters to assess system performance, feasibility of network integration and abnormal system responses. From the results obtained, a quantitative assessment was compiled to project technical recommendations. The outcome of phase one shows the optimum performance with 1-axis tracking. Results from phases two and three indicate that the insertion of utility-scale PV into the network corresponds with technical tolerance values that presently exist under the conventional system. The data suggest that the incorporation of grid reinforcement options will mitigate any congestion concerns due to reactive power compensation, as well as strengthen fault mitigation schemes. The major implication of this study is to offer technical guidance in the process of increasing the penetration of utility-scale PV installations in Jamaica. This study is the first of its kind to incorporate these three assessment components to assess the integration of a utility-scale PV system.

**Keywords:** Photovoltaic (PV); Solar Irradiance; Grid Reinforcement

## Attestation of Authorship

I hereby declare that this submission is my own work and that, to the best of my knowledge and belief, it contains no material previously published or written by another person (except where explicitly defined in the acknowledgements), nor material which to a substantial extent has been submitted for the award of any other degree or diploma of a university or other institution of higher learning.

O'Neil J Nelson

## Acknowledgments

Firstly, I would like to sincerely show my appreciation and gratitude to the government and citizens of New Zealand and the New Zealand Development Scholarships Committee of the Ministry of Foreign Affairs and Trade, who are responsible for facilitating and funding my New Zealand Aid Development Scholarship 2017–2018. This opportunity ensured that, as a student from a developing country, I could train in the New Zealand engineering education system. In addition, I would like to thank Sacha Pointon, Margaret Leniston and the other members of the NZ Aid Scholarship Team at Auckland University of Technology. You were extraordinary pillars of strength and support.

I thank my supervisors Dr Adam Taylor, my primary supervisor, and Professor Tek-Tjing Lie, my secondary supervisor, for your excellent guidance and support throughout my research process. The ability to have evolved as an engineering researcher is duly noted and appreciated and this will prove invaluable as I continue my engineering journey. Adam always afforded me the time for face-to-face meetings to assess the structure of the research and to provide high quality feedback. In addition, Professor Tek has been a source of encouragement and motivation during challenging periods.

I acknowledge the Auckland University of Technology and the Electrical and Electronic Engineering Department for providing me access to world-class research resources. The Library services and Employability and Careers who have been efficient and indeed invaluable. I was fortunate to have been able to participate in numerous academic and career development workshops, seminars, webinars, lecture series and the AUT Edge Award to find the self-confidence to express my professional opinion.

I also acknowledge freelance proofreader David Parker, who efficiently proofread the final version of my thesis in keeping with the Auckland University of Technology guidelines for proofreading of Postgraduate Theses and Dissertations.

Finally, I express heartfelt appreciation to my family, friends, colleagues and everyone who has supported me throughout the life-changing and exciting journey. I thank you all.

# Contents

Abstract .....	ii
Attestation of Authorship .....	iii
Acknowledgments .....	iv
Contents .....	vi
List of Figures .....	viii
List of Tables .....	x
List of Symbols, Abbreviations and Acronyms .....	xii
Chapter 1    Introduction .....	1
1.1    Introduction .....	1
1.2    Background .....	2
1.3    Aim .....	3
1.4    Research Questions .....	3
1.5    Specific Research Objectives .....	4
1.6    Research Project Timeline .....	4
1.7    Scope .....	5
1.8    Structure of Thesis .....	6
Chapter 2    Literature Study .....	8
2.1    Literature Review .....	8
2.1.1    Introduction .....	8
2.1.2    Photovoltaic (PV) Technology .....	9
2.1.3    Integrating a Photovoltaic Power Plant into a Power Grid .....	11
2.1.4    PV System Site Selection in Jamaica .....	15
2.2    A Generic Photovoltaic Cell .....	16
2.3    Solar Power .....	22
2.4    Short-Circuit Analysis .....	26
2.5    Summary .....	27
Chapter 3    Research Design .....	29
3.1    Introduction .....	29
3.2    Research Methodology .....	30
3.3    Data Collection Instruments .....	31
3.3.1    Computer Modelling .....	31
3.3.2    Simulation Study .....	31
3.3.3    Summary .....	32
3.4    Data Collection Process .....	33
3.4.1    PV Plant Dynamic Modelling .....	33
3.4.2    Load-Flow Analysis .....	34
3.4.3    Short-Circuit Study .....	35
3.5    Data Analysis Procedures .....	35
3.5.1    PV Plant Dynamic Modelling .....	36

3.5.2	Load-Flow Analysis .....	36
3.5.3	Short-Circuit Study .....	37
3.6	Summary .....	40
Chapter 4	Simulation Results and Analysis.....	41
4.1	Introduction .....	41
4.2	PV Plant Dynamic Modelling .....	41
4.2.1	General Description of a Solar PV System .....	41
4.2.2	System Performance.....	43
4.3	Load-Flow Analysis .....	55
4.3.1	Modelling of Transmission Network .....	56
4.3.2	Load-Flow Calculation.....	60
4.3.3	Contingency Analysis .....	62
4.4	Short-Circuit Study.....	63
4.4.1	Building the 20% Scale Model Transmission Network.....	63
4.4.2	Fault Current Calculation.....	67
Chapter 5	Discussion and Implications .....	78
5.1	System Performance Implications.....	78
5.1.1	Site Analysis .....	79
5.1.2	Implications of the Results of Single Site.....	80
5.1.3	Implications of the Results from Four Distributed sites .....	81
5.2	Implications of Technical Analysis .....	83
5.2.1	Grid Infrastructure Improvement .....	84
5.2.2	Technically Feasible Grid Reinforcement for Jamaica.....	84
5.2.3	Technically Infeasible Grid Reinforcement for Jamaica .....	86
5.2.4	Establish a Cap on PV Penetration .....	87
5.3	Summary .....	88
Chapter 6	Conclusions and Recommendations .....	91
6.1	Conclusions .....	91
6.1.1	Limitations of the Study.....	92
6.2	Recommendations .....	93
References	.....	94
Appendix A	PV Plant Data .....	102
Appendix B	Grid Data .....	106
Appendix C	Short-Circuit Fault Data .....	118



## List of Figures

Figure 2.1: Electricity prices for residential consumers, 2011 [1] .....	9
Figure 2.2 Yearly average solar irradiance for top 5 performing countries for solar energy and Jamaica [6] .....	11
Figure 2.3: PV cell equivalent circuit [20].....	17
Figure 2.4: Characteristic curve of a PV cell [21] .....	18
Figure 2.5: Maximum Power for and I-V sweep [21].....	19
Figure 2.6: Maximum Power Operating Point [21] .....	19
Figure 2.7: Effect of irradiance on the I-V characteristic at constant cell temperature [21].....	20
Figure 2.8: Effect of temperature on the I-V characteristic at constant irradiance [21].....	20
Figure 2.9: Module supplying power to vary the operating point [21] .....	21
Figure 2.10: PV cell operation [22] .....	22
Figure 2.11: Assembly of PV field [22].....	24
Figure 2.12: Principle diagram of a grid-connected PV plant [22].....	25
Figure 4.1: IV and PV characteristics of parallel connected strings at $1000 \text{ W/m}^2$ at $T = 46.2^\circ \text{C}$ .....	43
Figure 4.2: Hourly average plane of array total irradiance for Montego Bay site .....	44
Figure 4.3: Hourly average power generation output of a fixed mounted system located at Montego Bay.....	45
Figure 4.4: Average hourly ambient temperature for Montego Bay.....	46
Figure 4.5: Average hourly wind speed for Montego Bay.....	47
Figure 4.6: Plane of array irradiance for tracking systems .....	48
Figure 4.7: 120MW PV power plant power generation output for tracking systems .....	49
Figure 4.8: Plane of array irradiance data for distributed sites .....	51
Figure 4.9: 120MW PV power generation output from distributed sites.....	52
Figure 4.10: Combination daily load profile for Jamaica .....	54
Figure 4.11: Net daily load profile.....	54
Figure 4.12: Section of the Jamaican transmission network.....	58
Figure 4.13: Section of the Jamaican transmission network with integrated PV system.....	59
Figure 4.14: Scaled network model for short circuit analysis.....	65
Figure 4.15: Scaled network model for short-circuit analysis with integrated PV system .....	66
Figure 4.16: Symmetrical fault analysis of 3-phase bolted fault at Region 5 .....	68
Figure 4.17: Asymmetrical fault analysis of three-phase bolted fault at Region 5 .....	69
Figure 4.18: Symmetrical fault analysis of double-line-to-ground fault at Region 5 .....	70
Figure 4.19: Asymmetrical fault analysis of double-line-to-ground fault at Region 5 .....	71
Figure 4.20: Symmetrical fault analysis of line-to-line fault at Region 5.....	73
Figure 4.21: Asymmetrical fault analysis of line-to-line fault at Region 5.....	74
Figure 4.22: Symmetrical fault analysis of single-line-to-ground fault at Region 5.....	75

Figure 4.23: Asymmetrical fault analysis of single-line-to-ground fault at Region 5 .....	76
Figure A.1: MATLAB Code .....	104

## List of Tables

Table 1.1: Thesis research project timeline .....	5
Table 2.1: Daily average solar irradiance for top 5 performing countries for solar energy and Jamaica [6] .....	10
Table 2.2: Comparison of PV facilities in sun-belt countries .....	14
Table 2.3: Types of PV modules [22] .....	23
Table 4.1: Annual system output of 120MW PV power plant located at Montego Bay .....	46
Table 4.2: Annual system output of 120MW PV power plant for tracking systems .....	50
Table 4.3: Combined annual output of distributed sites .....	53
Table 4.4: Comparison of congested transmission line data.....	61
Table 4.5: Comparison of congested transformer data .....	61
Table 4.6: Comparison of three-phase bolted fault currents at Region 5.....	67
Table 4.7: Comparison of double-line-to-ground fault currents at Region 5.....	70
Table 4.8: Comparison of line-to-line fault currents at Region 5 .....	72
Table 4.9: Comparison of single-line-to-ground fault currents at Region 5 .....	75
Table A.1: Electrical characteristics of SUNARRAY-S6B3613-300T .....	102
Table A.2: Temperature characteristics of SUNARRAY-S6B3613-300T .....	102
Table A.3: Datasheet Information for FS1000CU [CEC 2016].....	103
Table A.4: Net Output Jamaica Daily Load with 120MW Power Plant.....	105
Table B.1 Grid upgrade options available to Jamaica for Utility-Scale PV integration .....	106
Table B.2: Transmission Line Data .....	109
Table.B.3: Load Transformer Data .....	110
Table.B.4: Generating Unit Transformer Data .....	111
Table.B.5: Generation Plant Data .....	112
Table.B.6: Transmission Line Data – Solar System Network .....	113
Table.B.7: Load Transformer Data – Solar System Network.....	114
Table.B.8: Generating Unit Transformer Data – Solar System Network .....	116
Table.B.9: Generation Plant Data – Solar System Network .....	117
Table C.1: Generator Data for 3-Phase Bolted Fault .....	118
Table C.2: Transformer Data for 3-Phase Bolted Fault .....	119
Table C.3: Generator Data for 3-Phase Bolted Fault with Solar Farm .....	120
Table C.4: Transformer Data for 3-Phase Bolted Fault with Solar Farm .....	121
Table C.5: Generator Data for Double-Line-to-Ground Fault .....	122
Table C.6: Transformer Data for Double-Line-to-Ground Fault .....	123
Table C.7: Generator Data for Double-Line-to-Ground Fault with Solar Farm .....	124
Table C.8: Transformer Data for Double-Line-to-Ground Fault with Solar Farm .....	125
Table C.9: Generator Data for Line-to-Line Fault.....	126
Table C.10: Transformer Data for Line-to-Line Fault .....	127

Table C.11: Generator Data for Line-to-Line Fault with Solar Farm .....	128
Table C.12: Transformer Data for Line-to-Line Fault with Solar Farm .....	129
Table C.13: Generator Data for Single-Line-to-Ground Fault.....	130
Table C.14: Transformer Data for Single-Line-to-Ground Fault.....	131
Table C.15: Generator Data for Single-Line-to-Ground Fault with Solar Farm.....	132
Table C.16: Transformer Data for Single-Line-to-Ground Fault with Solar Farm.....	133

## List of Symbols, Abbreviations and Acronyms

AC	Alternating Current
CARICOM	Caribbean Community
CF	Capacity Factor
DC	Direct Current
FACTS	Flexible AC Transmission Systems
GHI	Global Horizontal Irradiance
JPSCo	Jamaica Public Service Company
MPP	Maximum Power Point
MPPT	Maximum Power Point Tracking
NEP	National Energy Policy
NOCT	Nominal Operating Cell Temperature
P	Real power
POA	Plane of Area
PCC	Point of Common Coupling
PR	Performance Ratio
PV	Photovoltaic
Q	Reactive power
SIDS	Small Island Developing States
STATCOM	Static Synchronous Compensator
STC	Standard Test Conditions

# Chapter 1 Introduction

## 1.1 Introduction

Jamaica is endowed with a variety of renewable energy resources which provide a viable and attractive alternative to fossil fuel imports. Globally, as the number of facilities deployed rises and manufacturing costs fall, the economic equation increasingly favours the installation of solar photovoltaic (PV) power generation. This is particularly true for Jamaica, which needs to take significant steps to alleviate its dependence on imported fossil fuels that involve the volatile global market as well as the high cost of local energy distribution. With this potential increase in PV deployment, researchers have become acutely interested in accurate representations of solar PV plant studies in island conditions.

Large-scale solar PV power plants connected to transmission systems are spread over a significant area consisting of multiple small sources of power interfaced with the alternating current (AC) system – a single interconnection point to the grid. The effect of a utility-scale PV power plant on the stability and security of Jamaica's power system must, therefore, be carefully considered. Consequently, modelling the PV plant is essential in order to obtain realistic simulations of the power variations during continuous operation of the PV facility. Additionally, load-flow analysis is an essential analysis tool for power engineers to investigate an electric power system under steady-state operation as well as during abnormal conditions with or without PV integration.

This chapter introduces the background to the technical feasibility of integrating a 120MW solar PV power plant into the existing electricity grid in Jamaica. It describes the aims, research questions and objectives, and scope of this study of utility-scale PV power integration. It also introduces the structure of the thesis report.

## 1.2 Background

Jamaica is a Small Island Developing State (SIDS), located 18° 15' N latitude, 77° 30' W longitude. Jamaica has an area of 10,990 km<sup>2</sup> (4,243 sq mi). The country has an installed electricity capacity of 925.2MW, with its peak demand being 627.5MW. The energy supply mix in Jamaica is approximately 95% fuelled by imported oil, and the escalating cost of oil has resulted in consumers paying US\$ 0.40 per kWh, which is among the highest in the Caribbean Community (CARICOM) [1]. This creates an unsustainable position for Jamaica's national development goals and global competitiveness, and to address this issue the Government of Jamaica has issued a National Energy Policy (NEP) 2009–2030. The mandate of this policy calls for “affordable and accessible energy supplies with long-term energy security” and requires the development of renewable energy in the energy sector [2]. A fundamental priority of the NEP is a goal of 20% renewable energy in the country's energy matrix by 2030.

Photovoltaic (PV) systems are a viable option for Jamaica, as the high global horizontal irradiance (GHI) of 5–7 kWh/m<sup>2</sup>/day provides better opportunities for the deployment of PV systems as a potential energy source. With this potential installation, Jamaica would be joining a global growth trend. The adoption of solar power has been moving at a steady pace, with the generation capacity increasing by approximately 40% per year since 2000. At present, the world is generating 97 times more energy from solar than in 2004, and the cost of energy from a solar module per watt has fallen from US\$ 96 in the mid-1970s to US\$ 0.36 per watt in 2016 [3-5]. This is due to technological advances in PV module production and improved quality materials.

This work investigates the optimal site selection and performance of a 120MW PV power plant to address the need to alleviate Jamaica's dependence on fossil fuel, as outlined above. As part of this process, it is essential to examine the performance of the model of

Jamaica's transmission network. The network is explored under nominal conditions and an analysis of the response to short-circuit faults in the system conducted. Plant performance is investigated for fixed-tilt mounted systems, 1-axis, and 2-axis tracking configurations, and comparative load-flow investigations guide proposed grid reinforcement possibilities and fault mitigation strategies.

### 1.3 Aim

The aim of the thesis is to investigate the technical feasibility of integrating a utility-scale 120MW PV power plant into the existing electricity network in Jamaica. This investigation employs a computer-aided algorithm to: assess the optimal performance of the 120MW PV power plant; identify the optimised site location; and conduct a comparative analysis of an approximate simulation model of Jamaica's transmission network with the PV system integrated, this model being benchmarked against the current network configuration.

### 1.4 Research Questions

The research seeks to answer the following questions:

1. Is it technically feasible for PV generation to be integrated in Jamaica's power grid?
2. How well does the integrated PV system perform in relation to the current configuration of the grid?
3. What are the obstacles to increasing PV utility-scale penetration into the Jamaican grid?
4. What are the possible solutions to these problems?



## 1.5 Specific Research Objectives

In order to answer the research questions in Section 1.4, this study has the following objectives:

1. Assess the use of fixed-tilt mounted systems, and 1-axis, and 2-axis tracking configurations, to determine the optimal performance of a 120MW PV power plant given the GHI.
2. Analyse the technical performance of a utility-scale 120MW PV power plant integrated into Jamaica's transmission network.
3. Identify obstacles to increasing utility-scale PV penetration into the Jamaican grid and propose feasible solutions to these problems.

## 1.6 Research Project Timeline

The Master of Engineering research project is a creative and scientific venture which requires careful planning, execution, monitoring and control of scope, as well as managing schedules, risk, and quality. The tasks of the research study have evolved to follow the research project timeline shown in Table 1.1:

**Table 1.1: Thesis research project timeline**

Month	September (2017)	October	November	December
<b>Tasks</b>	<ul style="list-style-type: none"> <li>- Meet with supervisor to outline research scope and timeline.</li> <li>- Intensive literature review to cover the breadth and depth of the study area.</li> <li>- Formulate research questions and objectives.</li> </ul>	<ul style="list-style-type: none"> <li>- Draft literature review around research questions.</li> <li>- Establish model simulation parameters.</li> </ul>	<ul style="list-style-type: none"> <li>- Refine the research scope and thesis timeline.</li> <li>-Familiarisation with the various engineering software tools.</li> <li>- Data gathering sequence of data typical of that in Jamaica.</li> </ul>	<ul style="list-style-type: none"> <li>- Plan thesis structure and layout.</li> <li>- Initial iteration of algorithm generation.</li> <li>- Implement the collected data typical of that in Jamaica.</li> <li>- Draft Chapter 2 (Literature study).</li> </ul>
Month	January (2018)	February	March	April
<b>Tasks</b>	<ul style="list-style-type: none"> <li>- Develop the final form of the PV power plant algorithm.</li> <li>- Execute the PV power plant algorithm.</li> <li>- Record and organise the output of the algorithm.</li> </ul>	<ul style="list-style-type: none"> <li>- Design the approximate network model of Jamaica's grid.</li> <li>- Implement the simulation parameters into the approximate network model.</li> </ul>	<ul style="list-style-type: none"> <li>- Execute the iterative process to simulate the load flow across the approximate network without PV integration.</li> <li>- Execute the iterative process to simulate the load flow across the PV integrated approximate network.</li> </ul>	<ul style="list-style-type: none"> <li>- Execute the iterative process to simulate the 20% scale model without PV integration.</li> <li>- Execute the iterative process to simulate the PV integrated 20% scale model.</li> </ul>
Month	May	June	July	August (2018)
<b>Tasks</b>	<ul style="list-style-type: none"> <li>- Draft Chapter 3 (Research Design).</li> <li>- Collect and organize all data results.</li> <li>- Analyse the results.</li> </ul>	<ul style="list-style-type: none"> <li>- Draft Chapter 4 (Results).</li> <li>- Draft tables and figures.</li> <li>- Draft references and appendices.</li> </ul>	<ul style="list-style-type: none"> <li>- Draft Chapter 5 (Discussion).</li> <li>- Draft Chapter 1 (Research Objectives).</li> <li>- Draft Chapter 6 (Conclusion).</li> </ul>	<ul style="list-style-type: none"> <li>- Final review of AUT School of Engineering guidelines for formatting a digital thesis.</li> <li>- Review, edit and produce printed copies.</li> <li>- Submit 1x copy to the Engineering Faculty Office.</li> </ul>

**Thesis submission date:****08/09/2018**

## 1.7 Scope

The thesis covers the optimal performance of a 120MW PV system given the high GHI for Jamaica. In addition, the thesis presents a study of the impacts that the integration of the system can have on the existing network configuration in Jamaica. The PV system modelling process will involve algorithm generation and simulation with MATLAB and System Advisor Model (SAM) software environments, and environmental data from Meteonorm.

The integration of the utility-scale PV system is benchmarked against an approximated simulation model of the current configuration of the Jamaican transmission network. The integration process of the 120MW PV system within this scope involved literature studies and the approximate modelling of Jamaica's transmission network in the Xendee cloud computing platform developed by Electric Power Research Institute (EPRI). The Xendee engineering cloud platform integrates EPRI OpenDSS smart grid analytics. The system load-flow is analysed within the Xendee software platform and the integrated PV system load-flow investigated by comparison. This is to ascertain the impacts of the integration and to propose any mitigation solutions where required. The fault response capability of the network is scrutinised to benchmark the fault response for the integrated PV system.

## 1.8 Structure of Thesis

The thesis is organised in a conventional manner. The first chapter gives the background, aim, research questions, specific objectives, tasks and the scope of the execution of the research. The second chapter provides the review of literature and the theoretical background to the research topic. It further explains the technical concepts required in understanding the problem and some of the expected outcomes of utility-scale PV power plants.

The third chapter describes and justifies the methodology and research method chosen to determine the algorithm to assess the optimal performance PV system and the simulation analysis of the approximate network. This chapter also describes the instruments and mechanisms for collection of the output data of the modelling and simulation study. This chapter also outlines the rigorous evaluation and interpretation process of the data post-collection.

The fourth chapter presents the results of the algorithm for the three conditions under investigation, these being fixed-tilt mounted, 1-axis and 2-axis tracking systems. Further, this chapter presents the results of the simulation studies for the approximate current network configuration and for the network with the 120MW PV system integrated. The impacts in terms of the results of fault analyses of a 20% scale model of the current configuration as well as the scenario with solar PV system integration are also presented.

The fifth chapter outlines a discussion of the implications resulting from the outcome of the optimal investigation given the GHI concentration. This chapter further proposes possible solutions to mitigate the potential problems arising from the integration of a 120MW PV power plant with existing network parameters. Finally, fault condition values will be analysed to decide the necessary protection mitigation schemes for the integration of a 120MW PV system.

The sixth and last chapter presents the final conclusions of the study and makes recommendations on the topic addressed here. It is the aim of this study that the recommendations provide a template to help mitigate the technical challenges that could be faced by integrating a utility-scale PV power plant into Jamaica's electricity grid.

## Chapter 2 Literature Study

This chapter provides a review of relevant bodies of knowledge within the scope of the research. Section 2.1 examines PV technology in Section 2.1.2, integrating a PV system in Section 2.1.3 and system site selection in Section 2.1.4. Section 2.2 introduces the PV cell, Section 2.3 discusses solar power, Section 2.4 expands on short-circuit fault analysis, and Section 2.5 summarises the chapter.

### 2.1 Literature Review

#### 2.1.1 Introduction

The public supply of electricity in Jamaica is solely controlled by Jamaica Public Service Company (JPSCo). Jamaica's electricity production is not globally competitive and cannot sustainably meet the country's national development goals. As of 2011, 15% of the nation's gross domestic product (GDP) (US\$ 2.2 billion) was spent on imported fuel. Jamaican consumers pay nearly US\$ 0.40 per kWh, which is amongst the highest electricity costs in the Americas. For comparison, neighbouring island states, Trinidad and Tobago consumers pay US\$ 0.05-0.06 per kWh [1]. The drastic disparity between the prices paid in other countries and that paid in Jamaica is that these other countries have successfully harnessed their natural resources, whether it be oil, as in the case of Trinidad and Tobago, or solar, as in the case of Germany which has nearly half of the world's installed solar PV capacity. Despite having an average GHI of just 2.9 kWh/m<sup>2</sup> per day, Germany has efficiently converted sunlight into energy. Figure 2.1 below shows the comparison of electricity prices of consumers in the region and around the world and confirms the relatively high price paid by Jamaicans for electricity.

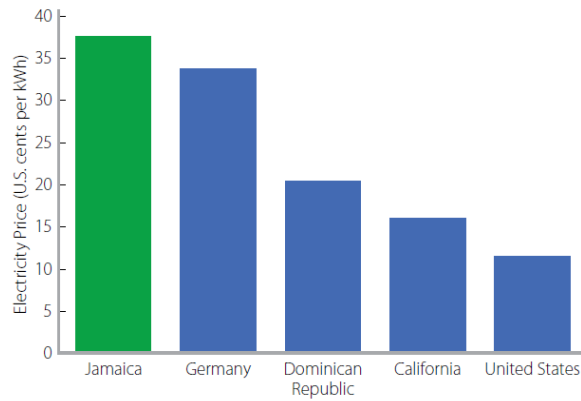


**Figure 2.1: Electricity prices for residential consumers, 2011 [1]**

Imported oil represents approximately 91% of Jamaica's electricity generation fuel source. However, Germany may be used as a blueprint. While not having the highest GHI, Germany has an abundance of PV installations. Jamaica, given its geographical location, should be able to harness a natural resource – sunlight – to utilise solar-based generation as a viable addition to the nation's energy mix.

### 2.1.2 Photovoltaic (PV) Technology

Globally, there is an increased focus on the consumption of electricity from PV, which has been increasing at approximately 40% per year since 2000 [6]. At present, the world is currently generating 97 times more energy from solar than it was in 2004 [5]. Although this still only represents 1.05% of global energy production, the rate of increase of PV generation is encouraging. In 2014 the International Energy Agency projected that solar power could supply 27% of global electricity generation by 2050 [7]. The equatorial position of Jamaica means it has the relative sun position to relate to other top performing countries for PV installations. As shown in Table 2.1 below, the country is well positioned to capitalise on the high concentration of solar irradiance [1, 6].

*Table 2.1: Daily average solar irradiance for top 5 performing countries for solar energy and Jamaica [6]*

Country	Solar Irradiance (kWh/m <sup>2</sup> /day)
China (Shanghai)	3.81
Germany (Berlin)	2.73
Japan (Tokyo)	3.80
USA (Phoenix, AZ)	5.34
Italy (Florence)	3.91
Jamaica	5.60

Jamaica boasts consistently high GHI levels, signalling the possibility of supporting solar PV generation at any scale. Solar generation is viable as observed by comparison with these nations and should be central in investigations into diversifying the country's energy mix.

Figure 2.2 below illustrates solar irradiance data for Jamaica and the top 5 performing countries employing solar energy [6]. Jamaica has consistently high values of solar irradiance throughout the year with a maximum of 6.55 kWh/m<sup>2</sup> per day and a minimum of 4.24 kWh/m<sup>2</sup> per day.

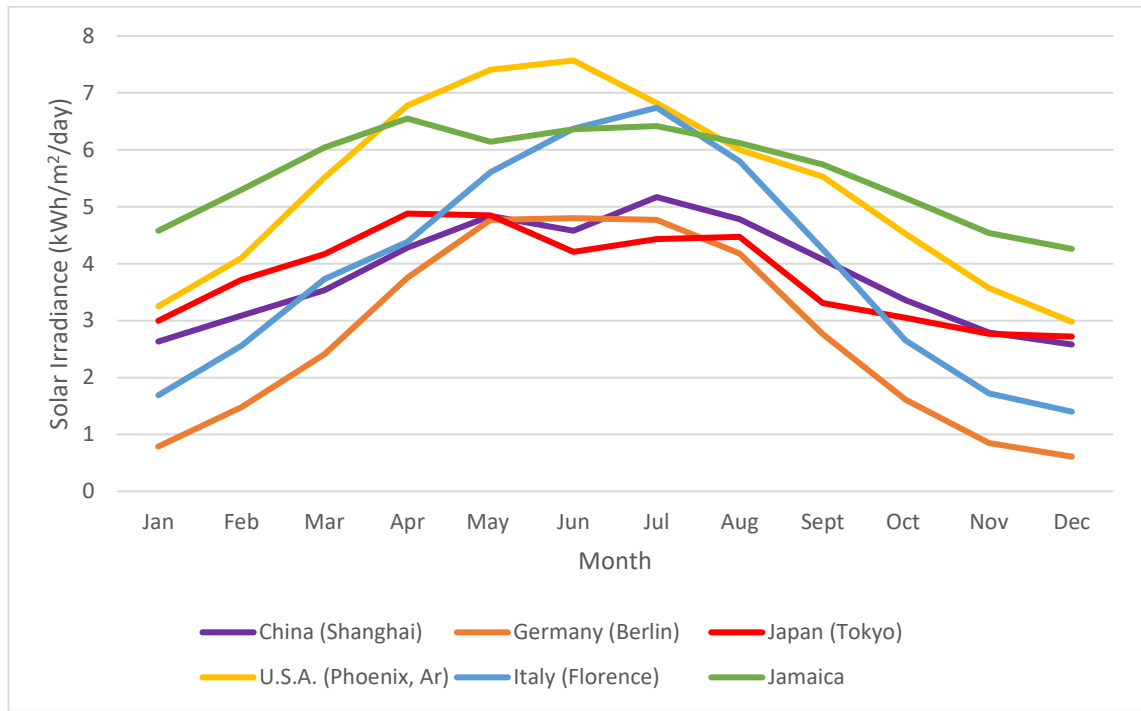


**Figure 2.2** Yearly average solar irradiance for top 5 performing countries for solar energy and Jamaica [6]

Only two other countries have similar irradiance values of Jamaica: the USA (Phoenix, Arizona) and Italy (Florence). However, this is only around the time of the summer solstice and is attributed to geographical situation of the selected locations in the two countries at that point in the year. Germany has the lowest annual value and yet has been able to successfully implement PV technology, representing a significant component in its energy sector. Jamaica's geographical position allows greater consistency of solar insolation and this, as well as other technical parameters, represents the possibility of for large-scale PV generation as compared to these other countries.

### 2.1.3 Integrating a Photovoltaic Power Plant into a Power Grid

The primary focus when integrating a PV power plant into an existing grid is to ensure the smooth transition of power being generated from the generating source to the end user. Research has shown that while the cost associated with implementing utility-scale PV power plants has significantly decreased, the operational challenges involve the



clustering of distributed generation. However, integrating a plant is more feasible than small distributed sites as evidenced in an extensive simulation [8]. This study concluded that incorporating an active power filter with multi-functional capability improved the power quality at the point of common coupling (PCC) by introducing a compensation current and balanced load current harmonics, as well as managing load reactive power demand and the load neutral current. An optimal combination of this technology improves the reliability of the integration of utility-scale PV systems and allows the network to operate efficiently [8].

Jamaica has an issue pertaining to the standard of power delivery via the transmission network. Transmission and distribution losses on the Jamaican grid totalled 22.3% in 2011 [1], which indicates the constraints in terms of grid readiness for the deployment for renewable sources. Grid codes and tolerance values reviewed highlighted the technical requirements of both PV systems and grid side requirements [9]. To support the utilisation of utility-scale PV generation, there must be a focus on system losses, low and high frequency harmonics, DC offset, unintended islanding, under/over voltages, or power fluctuations [9]. Similarly, the adoption of a steady-state voltage operation deviation of  $\pm 5\%$  has been recommended as a grid standard, to protect against network faults [10].

Additionally, there is a push for an increased adherence to the requirements of increased grid performance with the increase a power generation from utility-scale PV power plants. The development of grid codes with respect to PV system integration has been assessed in Germany, the USA, Puerto Rico, Romania, China, and South Africa; with consideration for fault ride through capability, frequency and voltage regulation and active and reactive power support [11]. Further considerations, such as the use of static synchronous compensators (STATCOMs) and capacitor banks as well as energy storage units, diesel generators or flywheels and ultra-capacitors, would support reactive power

fluctuations and comply with power curtailment and power reverse and ramp rate requirements [9].

The redesign or reconfiguration of an electrical network is a complex process due to the multi-variable characteristics of the existing configuration and the requirement that the system continues to satisfy the daily energy demand. Hence, software tools have been designed to produce the models necessary to optimise the usage of the network, such as a numerical analysis model in MATLAB which simulates the power loss analysis of grid-connection PV systems [12]. The parameters presented are considered fundamental for the deployment of a utility-scale PV power plant. The model analyses the power loss of both single-stage and two-stage grid-connected systems. A single-stage connection has the PV array output power directly injected into the electricity network through an inverter; however, the two-stage configuration has a boost converter functioning as a Maximum Power Point Tracking (MPPT) method. Critical to the analysis were factors such as non-uniform solar cell characteristics, loss factors of double line frequency voltage ripple and fast irradiance variation. Therefore, these factors can be incorporated into the recommended technical equipment and improved grid standards to find optimum solutions for the power system in a Jamaican context.

In contrast to the earlier focus on technical factors, it has been recommended that non-technical issues such as the Net Present Value (NPV) and Life-Cycle Costing (LCC) must also be considered for the optimised integration of a utility-scale PV system [13, 14]. The study in [14] assessed a 20MW utility-scale PV power plant and concluded the cost per kWh of PV generation is very competitive in comparison to gas turbines operation after six years and given the overall life-cycle reduction of approximately 541,798 tonnes of CO<sub>2</sub>. This aligns with Jamaica's sustainability goals regarding renewable energy and the nation's investment to mitigate the effects of climate change [15]. The authors in [16]

identified a daily solar insolation index estimated at 5–6 kWh/m<sup>2</sup> per day which led to the installation of a 1MWp system. This is comparable to conditions in Jamaica ranging from 5–7 kWh/m<sup>2</sup> per day. However, the analysis of energy production has been adversely affected by non-technical factors such as ambient temperature, prevailing wind, shading, and low solar irradiance which are categorised as environmental factors and site conditions. Therefore, it must be understood that technical factors respond to non-technical factors; technical factors result from the interaction between the output of the PV system and the transmission network, whereas non-technical factors influence the balance of the system and the overall efficiency of all the components of the plant. Consequently, these indicators prove relevant to study to determine the feasibility of utility-scale PV systems in Jamaica.

PV technology has proven to be a valuable type of renewable energy resource due to its zero emissions, zero noise, and reliability for sunny locations. Table 2.2 below represents solar developments with a sun-belt topography and electricity infrastructure comparable to that of Jamaica.

*Table 2.2: Comparison of PV facilities in sun-belt countries*

<b>Locations</b>	<b>Size of plant</b>	<b>Irradiance</b>	<b>Reference</b>
Bali, Indonesia	1 MWp	5 to 6	[16]
Adam City, Oman	1 MW	7.4	[17]
Bisha, Saudi Arabia	10 MW	3.5 to 7	[18]
Sahab, Jordan	20 MW	3.8 to 8	[14]

The reports referenced in Table 2.2 outlined the performance of each design and incorporated several of the technical standards recommended for safety and power quality. A techno-economic evaluation with various numerical simulations developed in different power system analysis software tools was used to determine the feasibility of

each system [14, 16-18]. This canvasses a wide range of procedures to identify optimal site location as well as the technical specifications of the installation of a PV system. These measures align with the NEP goal of expanding Jamaica's renewable generation contributing to the nation's international competitiveness. To accurately estimate the energy produced by a PV power plant, information is needed on the solar resource and temperature conditions of the site, in addition to the layout and technical specifications of the plant components. Hence, selecting a suitable site is a crucial component of the development of a viable PV project, and equally important as technical standards to such a project.

#### 2.1.4 PV System Site Selection in Jamaica

A factor that must be taken into consideration is the best location to access the highest GHI, which, being at very high levels, favours PV electricity generation in Jamaica. Optimal location in the form of shading factor must be considered, and this is coupled with the overall footprint of the utility-scale PV system. Optimisation means taking the entire PV plant as a whole, not just the majority of panels at the cluster centre. In a study conducted by 3TIER it was stated that a significant hurdle for Jamaica is in fact that, "As in most countries, the primary factors limiting the use of solar power in Jamaica are not meteorological, but infrastructure related. The access to transmission capacity as well as availability of land are the primary impediments to solar development." [1] [3TIER p.12]. This demonstrates that solar irradiance is not the only factor to be considered and highlights the need for optimum site selection, ideally with more than 75% sunlight exposure [19]. It has been evidenced that Jamaica more than satisfies the minimum hypothetical requirements. Thus, minimising shade is an important criterion in project optimisation. Another criterion outlined for suitable site selection is the gradient of the terrain, with the important consideration being for flat surfaces and rocky sites only being

used in unavoidable situations [19]. Considering the need for ideal site locations, Jamaica may be examined for these required conditions for the optimum site selection for a utility-scale PV facility. Given the country's topography, it is paramount to consider potential changes in the landscape that may alter the longevity of the project, and ultimately affect the project's success for the next 25 years.

The need for an assessment of land market value following basic economic principles, serves as the foundation of the valuation process for PV site selection. The goal is to estimate the market value of all land sites as well as specify all related land attributes. This is done by collecting the relevant data and verifying and analysing the data against market estimates. This can be generated using the land-use formula for Jamaica listed in Equation 2.1 below.

$$LV_{PV} = \left[ (Rate_{UT} \times Land_A) + (Rate_{SCR} \times Land_A) \right] \times INF \quad 2.1$$

where	$LV$	=	Land value
	$Rate_{UT}$	=	Special utility rate for land sold to utility entities
	$Rate_{SCR}$	=	The demand rate (scarcity) of the land plots surrounding the projected location
	$Land_A$	=	The land area that is sized to accommodate the PV plant
	$INF$	=	The country's economic inflation

This assessment will ensure the land procurement specific to immediate deployment of a PV plant as well as future site selection.

## 2.2 A Generic Photovoltaic Cell

The equivalent circuit model for a PV cell is shown in Figure 2.3 below and is defined by Equation 2.2 below [20]:

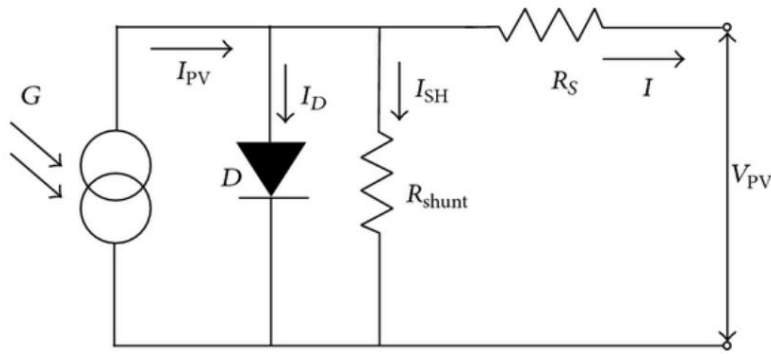


Figure 2.3: PV cell equivalent circuit [20]

$$I = I_{PV} - I_D - I_{SH}$$

$$I = I_{PV} - I_o \left\{ e^{\left[ \frac{q(V_{PV} + I.R_s)}{nKT} \right]} - 1 \right\} - \left( \frac{V_{PV} + I.R_s}{R_{SHUNT}} \right) \quad 2.2$$

where	I	=	Output current [A]
	$I_{PV}$	=	Short-circuit current [A]
	$I_D$	=	Diode current [A]
	$I_{SH}$	=	Shunt current [A]
	$I_o$	=	Saturation current [A]
	$V_{PV}$	=	Terminal voltage [V]
	n	=	Ideality factor
	k	=	Boltzmann's constant
	q	=	Electron charge [C]
	T	=	Junction temperature [K]
	$R_s$	=	Series resistance [ $\Omega$ ]
	$R_{SHUNT}$	=	Shunt resistance [ $\Omega$ ]

The two important components which determine the output of each PV cell are  $I_{PV}$  and  $V_{PV}$ . The operating characteristic curve of a typical PV cell at a certain solar irradiance and temperature is shown in Figure 2.4 below.

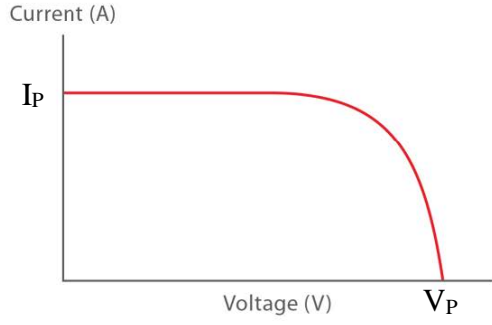


**Figure 2.4: Characteristic curve of a PV cell [21]**

The short-circuit current ( $I_{PV}$ ) is equal to the light-generated current and, at this operating point, the series resistance ( $R_s$ ) is neglected [21]. Therefore, the output must be equal the magnitude of  $I_{PV}$ ; this can be represented by Equation 2.3:

$$I = I_{PV} \quad 2.3$$

$I_{PV}$  occurs at the beginning of the forward-bias sweep and is the maximum current value in the power quadrant. For an ideal cell, this maximum current value is the total current produced in the solar cell by photon excitation:

$$I_{SC} = I_{MAX} = I_{\ell} \quad 2.4$$

Conversely, if the PV cell is operating at  $V_{PV}$  this establishes the open circuit condition. Under this open circuit condition, the leads are left open forming the open circuit voltage ( $V_{OC}$ ) and the shunt current ( $I_{SH}$ ) is neglected [21]. When the leads are left open,  $I = 0$ , therefore  $V_{OC}$  can be represented by the equation shown in 2.5 below:

$$I = I_{PV} - I_o \left[ e^{\left( \frac{qV_{oc}}{kT} \right)} - 1 \right]$$

$$V_{oc} = \frac{kT}{q} \ln \left( \frac{I_{pv}}{I_o} + 1 \right) \quad 2.5$$

The load characteristic of a PV cell can be determined by the product of the current and voltage. The product at  $I_{SC}$  and  $V_{OC}$  will be zero; however, the maximum power point

corresponds with  $V_{MP}$  and  $I_{MP}$  as shown in Figure 2.5 below. This is the power that can be delivered to the external circuit.

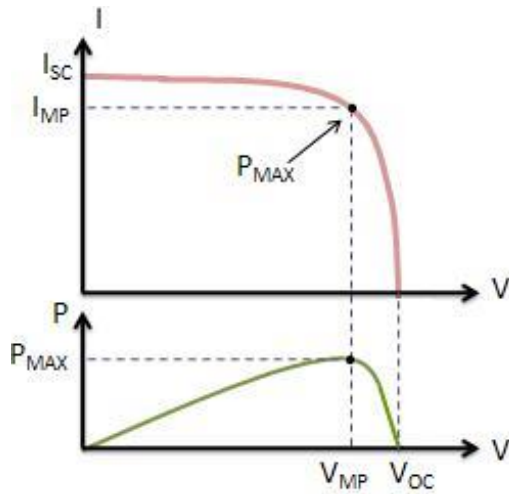


**Figure 2.5: Maximum Power for and I-V sweep [21]**

Under constant irradiance and cell temperature, the operating point of a PV cell is determined by the intersection of the I-V characteristic curve and the load characteristic curve as shown in Figure 2.6 below. At this point, the area under the I-V characteristic curve, which is equivalent to the output power is maximum. This point is referred to as the maximum power point (MPP) and is the optimal operation point of the PV cell.

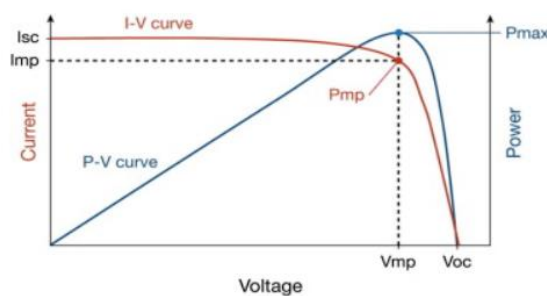


**Figure 2.6: Maximum Power Operating Point [21]**

The effect of solar irradiance and cell temperature on  $I_{SC}$  and  $V_{OC}$  is shown in the I-V curves in Figure 2.7 and Figure 2.8, respectively, below. As irradiance reduces, the short-circuit current decreases in direct proportion as well as the maximum power. There is also a logarithmic decrease in  $V_{OC}$  which contributes to the decrease in the power output.



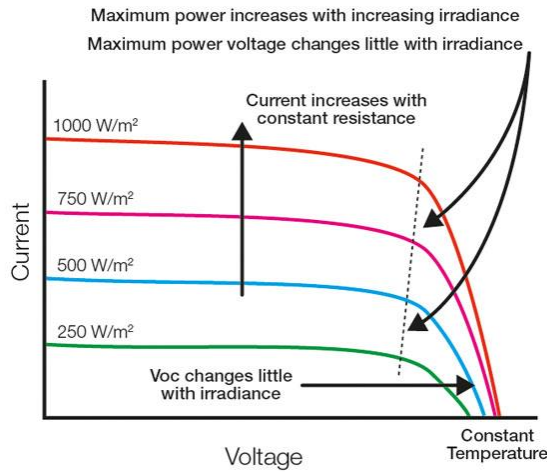


**Figure 2.7: Effect of irradiance on the I-V characteristic at constant cell temperature [21]**

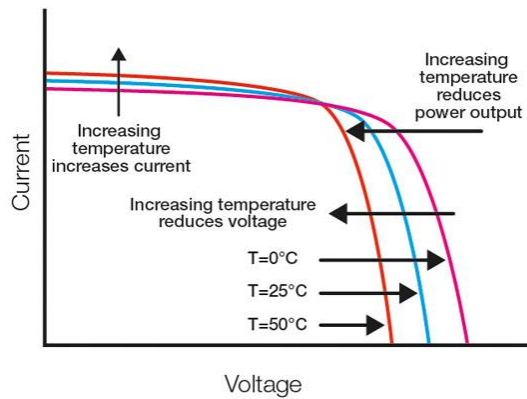


**Figure 2.8: Effect of temperature on the I-V characteristic at constant irradiance [21]**

As can be seen in Figure 2.8, as cell temperature increases,  $V_{OC}$  has a sharp decrease while  $I_{SC}$  has a slight increase. The overall change results in a direct proportion decrease in output power. This indicates that photovoltaics would perform better on cold clear days rather than hot days.

The load characteristic of the PV array is shown in Figure 2.9 below, in the case where the array supplies power to a resistive load. The load characteristic is represented by a straight line with the slope  $= \frac{1}{R}$ . The operating point moves along the I-V curve as the load resistance increases from 0 to  $\infty$ .

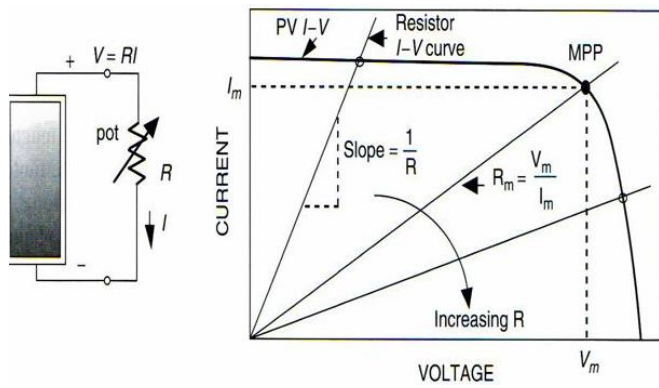


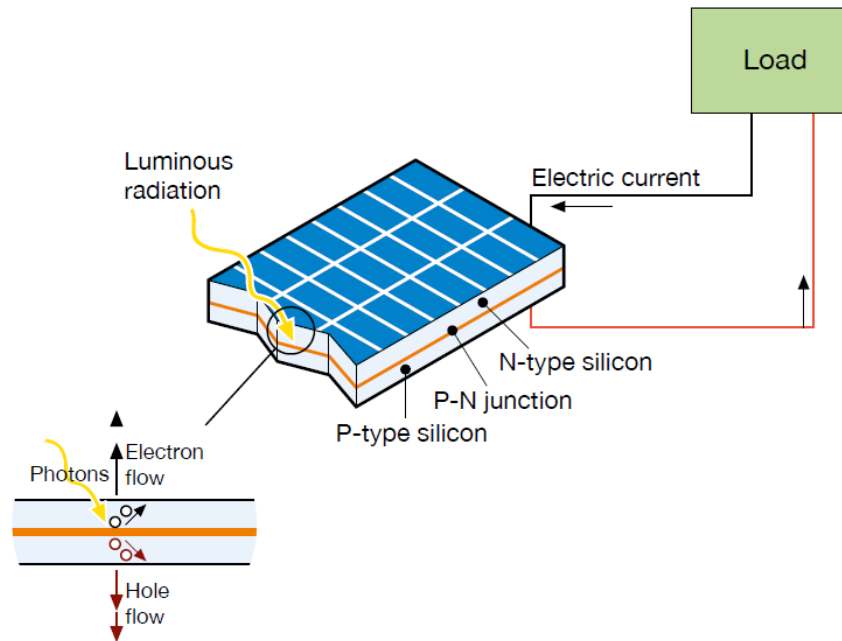
**Figure 2.9: Module supplying power to vary the operating point [21]**

The maximum power delivered occurs when  $R = R_m = \frac{V_m}{I_m}$  at the MPP. At this point, the area under the characteristic curve, which is equivalent to the output power, is at a maximum.

In terms of efficiency, most commercial PV cells have an efficiency of 14–20% which means a large area would be needed for high power output values [21]. Furthermore, the PV array output power varies with irradiance and operating temperature of the cell. As a result, the MPP varies through the operation of the array. With this variation it is not possible to assign a fixed voltage, fixed current or fixed resistive load, and therefore it is not possible to extract the maximum power out of the array. Within the power conditioning devices in solar PV systems, the DC-DC converter incorporates a maximum power point tracking (MPPT) system. The MPPT always ensures that the solar cell is operating at the MPP. There are several MPPT methods, each of these require an algorithm to specify the location of the operating point with respect to the calculated MPP. An optimum MPPT technique should produce high efficiency at a low cost due to PV systems being mass produced.

## 2.3 Solar Power







In a solar PV system, the elementary component is a solar cell, which converts the sun's photon energy into electrical energy [21]. Figure 2.10 below represents the process of conversion from solar irradiance to direct current (DC) power.



**Figure 2.10: PV cell operation [22]**

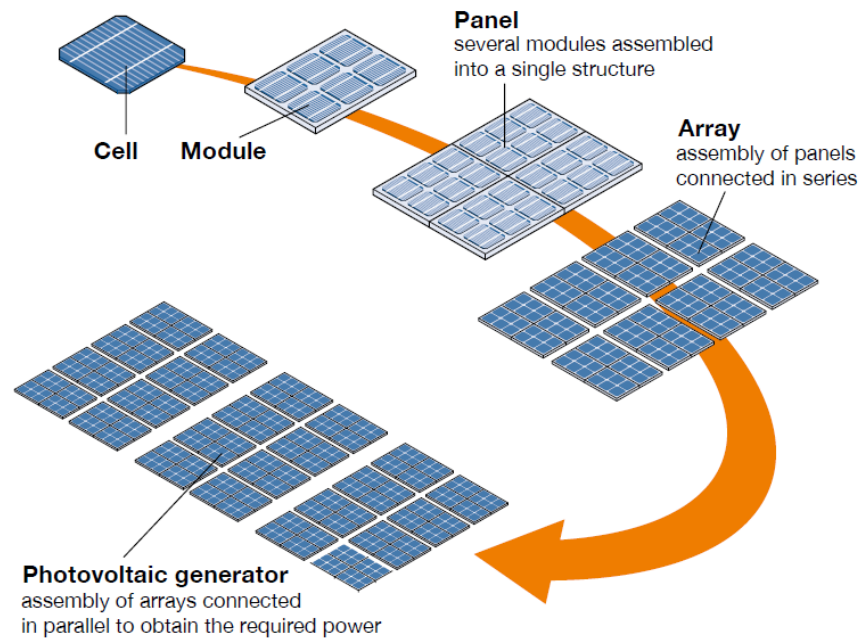
The material used in this solar cell is doped silicon. This is semi-conductive in nature and, given the reaction with photons, produces an electric current which provides useable output power. Table 2.3 below represents the various technologies employed in PV modules, module efficiency, and representative surface area required per kWp.

Table 2.3: Types of PV modules [22]

CELL MATERIAL	MODULE EFFICIENCY		SURFACE AREA NEED FOR 1 KWP
Monocrystalline silicon	14-20%	5-8 m <sup>2</sup>	
Polycrystalline silicon	11-15%	7-9 m <sup>2</sup>	
Micromorphous tandem cell (a-Si/μc-Si)	8-10%	10-12 m <sup>2</sup>	
Thin-film – copper-indium/gallium-sulfur/diselenide (CI/GS/Se)	10-12%	8-10 m <sup>2</sup>	
Thin-film – cadmium telluride (CdTe)	9-11%	9-11 m <sup>2</sup>	
Amorphous silicon (a-Si)	5-8%	13-20 m <sup>2</sup>	

In comparison with crystalline silicon modules, thin film modules show a lower dependence of efficiency on operating temperature and a good response also when the diffused light component is greater, for example, on cloudy days. Similar to thin film modules, amorphous silicon modules have reduced the influence of temperature and diffused light on high power output but require larger dimensions than crystalline silicon modules.

The electrical values (current and voltage) from a single cell are very small and it is impractical to use a single cell on its own. Therefore, for useable power values, the cells are connected in series to increase the output voltage and then arranged in parallel to increase the output current.



**Figure 2.11: Assembly of PV field [22]**

A combination of cells constructs a solar module and, a combination of modules results in a solar array or string. As seen in Figure 2.11 above, to achieve the required power values for large-scale generation, arrays are connected in parallel.

Since the generated output of the PV system is direct current power, it can be used in either of two ways. The first way is to have a grid of DC loads that can utilise the generated DC power. The second way is to connect power conditioning devices (power electronics converters) to transform generated DC power to AC power. This is because most of the electrical loads today operate with AC power. Figure 2.12 below shows a complete arrangement of a solar PV array with power conditioning devices for conversion to alternating current output power and the electrical grid coupling.

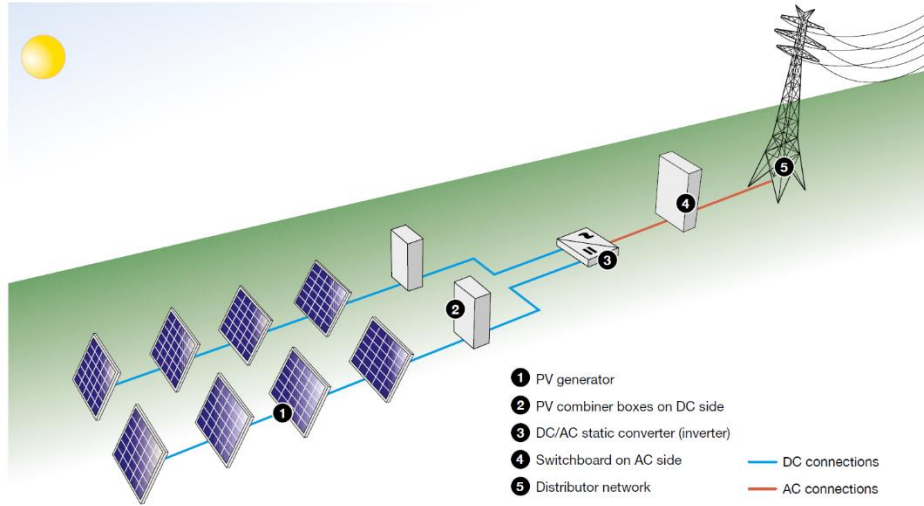


**Figure 2.12: Principle diagram of a grid-connected PV plant [22]**

The DC output of the PV system varies directly in proportion to the solar irradiance received by the array and temperature fluctuations. The DC-DC converter ensures the DC signal to the DC/AC inverter is stable. The static converter inverts DC to three-phase AC, matching the requirements of the electrical grid. For the integration to a power grid, there are other components, such as filter circuits and transformers, and relevant cables are added at the output of the switchboard.

The operational performance of the PV plant may be quantified by the performance ratio (PR) as well as the specific yield and the capacity factor of the facility. The PR is the parameter commonly used to quantify PV plant performance and provides a benchmark to compare the relationship between actual and theoretical energy outputs. It may be expressed by Equation 2.6 below:

$$PR = \frac{AC_{yield} (kWh) \times 1 \left( \frac{kW}{m^2} \right)}{DC_{InstalledCapacity} (kWp) \times PlaneofArrayIrradiation \left( \frac{kWh}{m^2} \right)} \times 100\% \quad 2.6$$

The PR quantifies the overall effect of system losses on the rated capacity, including losses caused by modules, temperature, low-light efficiency reduction, inverters, cabling,

shading, and soiling. The specific yield is the total annual energy generated per kWp installed. The specific yield of a plant depends on the total annual irradiation falling on the collector plane, as well as the performance of the module and system losses, including inverter downtime. The capacity factor (CF) of a PV plant is the ratio of the actual output over one year and its output if it had operated at nominal power the entire year. The CF is described by Equation 2.7 below:

$$CF = \frac{\text{EnergyGeneratedperAnnum}(kWh)}{8760\left(\frac{\text{hours}}{\text{annum}}\right) \times \text{InstalledCapacity}(kWp)} \quad 2.7$$

The CF is affected by the requirement of daylight from the sun that is unobstructed by clouds, smoke, smog, or shade from trees or building structures.

## 2.4 Short-Circuit Analysis

Power system faults which occur on any transmission line are categorised as balanced faults and unbalanced faults, which are referred to as symmetrical and asymmetrical faults. The majority of the faults that occur on power systems are not balanced three-phase faults, but unbalanced faults. In the analysis of a power system under abnormal conditions, it is necessary to make the distinction between the types of faults to ensure the best results possible in the analysis.

The detection and study of these faults are necessary to ensure that the reliability and stability of the power system will not be reduced because of a critical event. The task here is to be able to calculate the fault conditions and to provide the requisite protective equipment designed to isolate the faulted zone from the remainder of the network in the appropriate time. In the analysis of power systems under fault conditions, it is necessary to distinguish between the types of faults to ensure the best mitigation strategy in the analysis. However, in this study, only shunt faults are analysed. Shunt faults are the most

commonly occurring faults in the field. They involve power conductors to ground or short circuits between conductors. Shunt faults are classified in the following four types [23]:

Short-circuit faults on a power system are divided into three-phase balanced faults and unbalanced faults. Different types of unbalanced faults are single line-to-ground faults, line-to-line faults and double line-to-ground faults. 70% of all transmission lines faults are classified as single line-to-ground faults. This type of fault exists when one phase of the set of transmission lines establishes contact with the ground. 15% of all transmission lines fault are classified as line-to-line faults. This type of fault is due to one phase contacting another phase. 10% of all transmission lines fault are classified as double line-to-ground faults. This type of fault occurs where two phases come in contact with the ground. Balanced or symmetrical three-phase faults are the least likely to happen with an occurrence share of 5% of all transmission lines faults. This type of fault occurs where all three phases are contacting each other.

## 2.5 Summary

This literature study has identified some of the important technical considerations which must be considered in order to be able to deploy the most effective and optimal PV system for Jamaica. This chapter has outlined the technical and operational building blocks of the PV system. The current trends in global PV systems regarding cost and technology, coupled with other national policies and other incentives, are tested in this research study. The empirical field reports and actual deployment of PV systems on a global scale provide strong indicators of Jamaica being able to reap positive benefits. Furthermore, the instances of PV systems in the Caribbean and other tropical countries have redoubled to the benefit of the nation's energy security and the country's economic outlook. Not only will the installation of PV systems augment the current power system in Jamaica by making it more efficient and cost-effective, it will also reduce Jamaica's carbon footprint



on the worldwide scale. Sustainable development and achievement of parts of Jamaica's Vision 2030 to reduce energy cost will be realised through the implementation of alternative PV systems.

## Chapter 3                      Research Design

### 3.1 Introduction

This chapter presents the quantitative methodology used in this investigation and justifies its use on the ground to determine the optimal solar energy capacity subject to the system reliability requirements for electricity network integration. Due to the stochastic characteristic of solar irradiation, the reliability performance of a power system with PV generation is quite different from networks with only conventional generation and will be factored into this methodology. Modern power systems are complex and large in nature, containing thousands of PCCs. Analysing such systems in real-time is beyond human capacity, and therefore highly sophisticated computer programmes have been developed to analyse, design, and operate current power systems. The increased global energy demand and sustainable environment requirements necessitate the integration of renewable energy resources into these existing electricity networks, adding to their complexity. Moreover, the deployment of these non-conventional energy resources such as solar, wind, hydro and other renewables introduces technical challenges of stable and reliable operation due to the intermittent nature of the sources as well as the increased distributed nature of energy generation [11].

It is essential to simulate the real-world example of Jamaica, and the impact of the transmission network, and analyse the potential problems of integrating a 120 MW PV power plant to find optimum solutions before it is physically realised. Understanding and finding optimal solutions within the framework of this scenario require simulations of what may occur, and then the solution that best suits the specific situation will be applied. Section 3.2 proposes the research methodology, Section 3.3 discusses the data collection

instruments used during the data collection process which is examined in Section 3.4, and the data analysis procedures are presented in Section 3.5.

## 3.2 Research Methodology

The effective assessment of the technical feasibility of integrating a 120MW PV power plant into the electrical transmission network in Jamaica demanded the collection of relevant data and a rigorous method for analysing them. This research utilised a quantitative approach involving computer modelling and simulation because it aligned with previous studies and best enabled the attainment of my research objectives. This research used computer-based models to optimise the performance of the PV power plant and to create a simulation which was analysed for potential technical problems at the utility-to-customer interface. In summary, these quantitative approaches enabled the systematic collection and analysis of data that increased the robustness of the research process and the conclusions derived.

As a strategic quantitative approach, simulation broadly involves the construction of an artificial and controlled environment enabling data generation, observation of system or sub-system dynamic behaviour, and test runs using defined parameters and exogenous variables. In view of this, simulation is ideal for testing an electricity grid – a large-scale man-made system that facilitates commercial generation and transmission of electric power. These power systems comprise generation plants, electrical loads, and other interconnected dynamic components that are digitalised. As such, they require complex analysis, which falls outside the capacity of analog methods. Furthermore, it is necessary to understand the nonlinear dynamics of the grid to provide technical solutions concerning power quality and system stability. Simulation addresses these considerations and provides a safe way to test and explore different operating conditions within power networks and forecast system problems. For these reasons, practitioners and academics

use simulation widely to analyse power systems and build models for understanding future conditions [24].

### 3.3 Data Collection Instruments

This section discusses the computer modelling of the 120MW PV system in Section 3.3.1 and outlines the components of the simulation study in Section 3.3.2. Data collection involved a three-stage process comprising PV plant modelling, load-flow analysis, and short-circuit study. Phase one of this process involved the use of a computer model algorithm developed in MATLAB to calculate the net energy savings. As well as SAM was used for the designing, sizing, and simulation of the solar system using the mathematical equation of a PV cell to study the behaviour of the PV system. Phase two, comprised a simulation of an approximate three-phase single line diagram. Finally, phase three involved building and analysing a 20% scale model of the system used in phase two of the Jamaica electricity grid, developed using the computer-aided engineering tool on a cloud computing platform.

#### 3.3.1 Computer Modelling

In order to analyse the performance of the PV power plant, a model was developed in SAM in addition to calculating the net energy savings in MATLAB of the 120MW rating of the system. The sun position per hour was assigned a multiplying factor to act as a variable and, with a derating factor of 0.85 of the PV system rating, the output power was calculated [25, 26]. The aim of this was to calculate output power for fixed-tilt mounted, 1-axis and 2-axis tracking systems for environmental conditions experienced in Jamaica.

#### 3.3.2 Simulation Study

The aim of the grid model was to generate load-flows to benchmark the approximate operating real-time data of the electricity network with all elements currently installed.

With the benchmark model complete, this then could be edited to replace 120MW of fossil fuel generating units with the PV system. The networks were designed by means of power system objects categorised within the software interface. The components were assembled with the typical parameters from the library of data found within the cloud platform. This was done to determine how the grid operates and to itemize the prediction of its working condition [27]. The fundamental function of the grid models was to perform a load-flow studies to analyse the steady state operating condition of the practical network. A similar process was carried out to create two smaller scale models for the analysis of short circuit faults for the respective installation conditions.

### 3.3.3 Summary

The decision to use load-flow and short-circuit fault techniques is in line with the aims of this project which are to analyse the technical feasibility of integrating utility-scale PV generation into the Jamaican transmission network. The appropriateness of the decision is further evident with the scale of this project and the areas it would affect. Simulations can be animated, which allows for the concepts and ideas to be more easily verified, communicated, and understood. This also provides increased accuracy and greater precision in forecasting.

An advantage of using this approach is that the virtual environment of a computer-based model is less expensive and utilises less time than the initiation of real-world assets. Now, unlike spreadsheets or solver-based analytics, simulation modelling allows for the observation of system behaviour over time, at any level of detail. This reduces the uncertainty of the system operating conditions, leading to greater risk mitigation and allowing more robust solutions to be found.

### 3.4 Data Collection Process

When integrating a utility-scale PV power plant into an existing power system, a primary concern is the potential security problem of the system performance. Considering the power transfer capacity and stability limits of the system, the failure of a single component in the system could have severe consequences for system operation [23]. Data collection involves the monitoring of the output reports of each phase of the simulation. This section presents the PV power system model used in the optimisation model which will be discussed in Section 3.4.1, with the load-flow analysis simulation model procedure explained in Section 3.4.2 and the short-circuit fault analysis presented in Section 3.4.3.

#### 3.4.1 PV Plant Dynamic Modelling

A computer algorithm, as well as a simulation model, was designed to show a large utility-scale PV power plant for environmental conditions typically found in Jamaica. When viewed from a fixed power production standpoint, it is the most basic overall system configuration. Meteonorm is a meteorological database containing climatological data for solar engineering applications [28]. It takes data for Jamaica that was collected from 1991–2010, to provide hourly average irradiance figures. This data was used to generate an algorithm code that was used for the optimisation of PV power plant and the efficient use of the selected land space.

This presents a careful evaluation of the most efficient method to harness solar energy in the form of solar irradiance at a given location in Jamaica. These models were implemented in SAM and MATLAB/Simulink using most common MPPT techniques, to undertake meaningful comparisons with respect to the amount of energy from a fixed-tilt PV panel arrangement and compared against 1-axis and 2-axis tracking panel arrangements.

### 3.4.2 Load-Flow Analysis

The simulation model was designed as a dedicated electrical power system with generation and load data from [1] to give an approximate model of the current situation in Jamaica. The approximation is done to provide the required line, generator and harmonic data for all the equipment within the power system. Within this environment, the execution of the requisite power simulation functions were conducted, such as load-flow and short-circuit calculations. The computer tool allowed for the creation of a single line diagram to accommodate the topology approximately matching the condition under investigation. In this way, the power system database and its single line graphic were built together, and the component information was also accessible in report form. A load-flow calculation was performed to determine the operating state of the system with all loads connected. The load-flow solving algorithm for the whole system was set out in a separate area to afford the analysis of the output components, e.g. voltage and phase angle, real and reactive power, and line losses [29].

The Xendee engineering cloud platform was used to analyse and validate a theoretical PV power plant integrated into the Jamaican transmission network and results were compared against a benchmarked approximation of the current conventional transmission network in Jamaica. Mathematical representations of various load-flow components were given as necessary and were incorporated within the software tool. Then, the underlined theoretical foundations were analysed and validated through the simulation process and the results recorded. Finally, the simulated results were compared with each other and used to select suitable technical solutions to overcome the added complexity of integrating such renewable energy resources.

### 3.4.3 Short-Circuit Study

It is important to study a power system under fault conditions to provide system protection equipment rating and response time, as well as to recommend relevant mitigation schemes. The Xendee software tool provided ANSI C37/IEEE, and Classical calculation to model transmission networks and perform short-circuit simulations on interconnected, meshed balanced and unbalanced topologies [29].

The calculation method employed the use of peak, momentary ( $\frac{1}{2}$  cycle, 1 cycle and  $1\frac{1}{2}$ –4 cycle), interrupting (8 cycle and 30 cycle) faults at three-phase, two-phase and single-phase locations within the transmission network. Granular reporting was made on current flows at both terminals and for all equipment, power values, angles and voltages. The flexibility to simulate virtually any fault scenario offered the extensibility to benchmark conventional electricity network fault mitigation technology which was then compared against fault values of the non-conventional systems. This made it possible to assess whether the technology already employed would be applicable and, if not, to provide the scope for recommended technical options.

## 3.5 Data Analysis Procedures

The evaluation of the performance of a power system is essential to its nominal operation. Regarding the stability requirements of an electric power system, voltage and load flow are two significant factors in monitoring system performance [23]. There were rigorous examinations of the recorded reports and data comparisons to assess the security of the system performance with the integrated PV system. This section examines the output of optimisation model of the PV power system model in Section 3.5.1, with the load-flow analysis simulation model comparison discussed in Section 3.5.2, and the short-circuit fault analysis outcome examined in Section 3.5.3.



### 3.5.1 PV Plant Dynamic Modelling

The report of the simulation provided data that made it possible to recommend the land use associated with the utility-scale ground-mounted PV facility. This quantified the requirements of the capacity of the power plant and generation potential in a year for a given location. Capacity-based results are useful for estimating land area and costs for such a project. The generation basis provides a more consistent comparison between technologies that differ in capacity factor and enables evaluation of land-use impacts that vary from solar resource differences, tracking configurations, and technology.

### 3.5.2 Load-Flow Analysis

Load-flow simulations are an important part of a transmission network analysis as they are necessary for planning, economic scheduling, and controlling an existing system or its future expansion. The analysis involved determining the magnitudes and phase angles of voltages at each PCC and the real and reactive power in each line. The network was represented as a nonlinear system because the power flow into load impedances is a function of the square of the applied voltages. There are several different methods of solving the resulting nonlinear systems, but the most efficient and practical is a Newton-Raphson method [23] which is the referenced option included in the computer engineering tool. The method is initiated by estimating all unknown variables. The next stage involves the formulation of a Taylor series with the higher order terms ignored, for each of the power balance equations involved in the system of equations. In short form, it can be written as:

$$\begin{bmatrix} \Delta\delta \\ \Delta|V| \end{bmatrix} = -J^{-1} \begin{bmatrix} \Delta P \\ \Delta Q \end{bmatrix} \quad 3.1$$

where  $\Delta P$  and  $\Delta Q$  are the mismatch discrepancy formulae:

$$\Delta P_i = -P_i + \sum_{k=1}^N |V_i| |V_k| (G_{ik} \cos \theta_{ik} + B_{ik} \sin \theta_{ik}) \quad 3.2$$

$$\Delta Q_i = -Q_i + \sum_{k=1}^N |V_i| |V_k| (G_{ik} \sin \theta_{ik} - B_{ik} \cos \theta_{ik}) \quad 3.3$$

and  $J$ , - the Jacobian, is a matrix of the partial derivatives:

$$J = \begin{bmatrix} \frac{\partial \Delta P}{\partial Q} & \frac{\partial \Delta P}{\partial |V|} \\ \frac{\partial \Delta Q}{\partial Q} & \frac{\partial \Delta Q}{\partial |V|} \end{bmatrix} \quad 3.4$$

The linearised system of equations is solved to determine the next guess ( $m+1$ ) of voltage magnitude and angles based on:

$$\theta^{m+1} = \theta^m + \Delta \theta \quad 3.5$$

$$|V|^{m+1} = |V|^m + \Delta |V| \quad 3.6$$

The procedure is an iterative process and after a certain standard of convergence is achieved for residual values of the real power and reactive power, the load-flow calculation is successfully completed.

### 3.5.3 Short-Circuit Study

The analysis of symmetrical faults is incorporated within the operating framework of the software tool like that of load flow. The method generates some assumptions. First, all generators are in phase and are operating at the nominal voltage of the system. Also, electric motors are considered to be generators due to the fact that, when a fault occurs, they usually supply rather than draw power [23]. The voltages and currents are then calculated for the *base* representation:

$$Z_{base} = \frac{(V_{LL})^2}{S_{base}} \quad 3.7$$

$$I_{base} = \frac{S_{base}}{\sqrt{3}(V_R)} \quad 3.8$$

Next, the location of the fault is supplied with a negative voltage source, equal to the voltage at that location in the *base* case, while all other sources are set to zero:

$$I_{Actual} = I_{base} \times I_{pu} \quad 3.9$$

To obtain a more accurate result, these calculations are performed separately for three time ranges: a sub-transient period, lasting only for the first few cycles (½, 1½–4 seconds), which is associated with the largest currents; a transient period, covering a relatively longer time, the period between the sub-transient and the steady-state; and, finally, a steady-state period, which occurs after all the transients have had time to settle.

The magnitudes of the currents during unsymmetrical faults are resolved without the use of assumptions as the load is symmetrical on all phases. However, the approach of the one-line diagram simplifies the solution of balanced three-phase systems, and this method resolves the solution of the unbalanced system into three balanced circuits. The three symmetrical components are positive, negative, and zero sequences. The other pertinent information involves identifying the per-unit positive, negative and zero sequence impedances of the transmission lines, generators, and transformers involved.

The analysis of these resolved elements forms three separate circuits which are linked in a specific sequence, depending on the kind of fault encountered. Once the sequenced circuits are properly connected, the network can then be analysed using classical circuit techniques. The resulting system of solutions for voltages and currents exists as symmetrical components, which must be transformed into phase values with use of the *A-matrix*.

Consider the 3-phase unbalanced currents  $I_a$ ,  $I_b$ , and  $I_c$ , we seek to find the three symmetrical components such that:

$$\begin{aligned} I_a &= I_a^0 + I_a^1 + I_a^2 \\ I_b &= I_b^0 + I_b^1 + I_b^2 \\ I_c &= I_c^0 + I_c^1 + I_c^2 \end{aligned} \quad 3.10$$

Rewriting all the terms of  $\alpha$  components:

$$\begin{bmatrix} I_a \\ I_b \\ I_c \end{bmatrix} = \begin{bmatrix} 1 & 1 & 1 \\ 1 & \alpha^2 & \alpha \\ 1 & \alpha & \alpha^2 \end{bmatrix} \begin{bmatrix} I_a^0 \\ I_a^1 \\ I_a^2 \end{bmatrix} \quad 3.11$$

Rewriting the above equation in matrix notation as:

$$I^{abc} = A I_a^{012} \quad 3.12$$

Where the  $A$  matrix defines a phasor rotation operator  $\alpha$ , which rotates a phasor vector counter clockwise by  $120^\circ$ :  $\alpha = e^{\frac{2}{3}\pi i}$ .

$$A = \begin{bmatrix} 1 & 1 & 1 \\ 1 & \alpha^2 & \alpha \\ 1 & \alpha & \alpha^2 \end{bmatrix} \text{ - } A \text{ matrix} \quad 3.13$$

Solving for the symmetrical components of currents:

$$I_a^{012} = A^{-1} I^{abc} \quad 3.14$$

Where the inverse of the  $A$  matrix is given by:

$$A^{-1} = \begin{bmatrix} 1 & 1 & 1 \\ 1 & \alpha & \alpha^2 \\ 1 & \alpha^2 & \alpha \end{bmatrix} \quad 3.15$$

Therefore, the symmetrical components are:

$$\begin{aligned}
I_a^0 &= \frac{1}{3}(I_a + I_b + I_c) \\
I_a^1 &= \frac{1}{3}(I_a + aI_b + a^2I_c) \\
I_a^2 &= \frac{1}{3}(I_a + a^2I_b + aI_c)
\end{aligned}
\tag{3.16}$$

With the similar expressions for voltages, the symmetrical components for unbalanced voltages being:

$$\begin{aligned}
V_a^0 &= \frac{1}{3}(V_a + V_b + V_c) \\
V_a^1 &= \frac{1}{3}(V_a + aV_b + a^2V_c) \\
V_a^2 &= \frac{1}{3}(V_a + a^2V_b + aV_c)
\end{aligned}
\tag{3.17}$$

### 3.6 Summary

This chapter is the backbone of the research as it ensures that the research data presented is reliable and valid. In addition, this chapter provides insight into why the research has been undertaken and why the hypothesis has been formulated. The research methodology has demonstrated the use of a systematic approach to answer the research questions that have guided the study. It has formulated the various steps that have been adopted in studying the research objectives and rigorously assessed the logic behind them. In this section, all instruments and techniques relevant to data collection and data analysis have been outlined and evaluated.

## Chapter 4                      Simulation Results and Analysis

### 4.1 Introduction

The subject of this chapter is the development of an algorithm to simulate the response of a 120MW PV plant to changes in irradiance as well as the response of the PV plant integrated to nominal conditions and with incidents of disturbances. The results presented in this chapter follow the rigorous methodological process outlined in Chapter 3. The electrical generation performance of the 120MW PV system is presented in Section 4.2, with the load-flow analysis of an approximate model of Jamaica's transmission network outlined in Section 4.3. Finally, Section 4.4 presents the results from the simulation of the power system operating during abnormal conditions due to short-circuit faults.

### 4.2 PV Plant Dynamic Modelling

This section assesses the electrical generation performance of the 120MW PV system with environmental conditions typically seen in Jamaica. In addition to this, the optimum performance and land use requirements of the various tracking systems are presented, as well as an analysis of the performance impact of a single site compared to 4 distributed sites. Section 4.2.1 provides a general description of a PV system. It will outline the detailed electrical characteristics of the PV model, the inverter and the environmental conditions. Section 4.2.2 outlines the system performance of 120MW PV power plant in a single site configuration, and contrasts this with a similar 120MW PV plant distributed across four selected sites as well as outlining the net savings of the PV system.

#### 4.2.1 General Description of a Solar PV System

In the present study, the main system design is undertaken based on a 120MW PV system. For the intended system, a large variety of PV panel options were studied in terms of power, efficiency and module area. The California Electrical Commission (CEC)

Sunarray SUNARRAY-S6B3613-300T was selected and adopted for the study. S6B3613-300T is a robust solar module and can be used for grid-connected applications of solar PV facilities. The nominal efficiency of 15.93% for the module was selected to form a baseline performance matrix for the study, as it is deemed a commercially acceptable value. Detailed electrical characteristics of the module were measured under standard test conditions (STC) and are shown in Appendix A Table A.1. At STC irradiance is  $1000 \text{ W/m}^2$ , air mass of 1.5 solar spectrum and an effective cell temperature of  $25^\circ\text{C}$ . Detailed temperature characteristics of the module are shown in Appendix A Table A.2. The module temperature correction is designed for a nominal operating cell temperature (NOCT) at  $46.2^\circ\text{C}$ . An essential part of a grid-connected PV system is the means of converting the DC output of the PV array into an AC power supply to the utility network. Inverters are used to perform this conversion task. No single inverter is ideal for all situations; taking the local conditions of Jamaica into account and matching the specifications of the adopted module, the Power Electronics: FS1000CU [CEC 2016] inverter was adopted. The inverter datasheet is listed in Appendix A Table A.3 and is standardised by EN 50524:2009.

DC-AC conversion efficiency directly affects the annual revenue of a solar PV facility and varies according to a number of factors, including DC input voltage and load. Other factors that should be considered for the selection of an inverter includes site temperature, product reliability, maintainability, serviceability, and cost. For the test case considered in the study, the  $I$ - $V$  and  $P$ - $V$  characteristics shown in Figure 4.1 below demonstrate a constant irradiation intensity of  $1000 \text{ W/m}^2$  is assumed for all modules with 17 modules per string or solar array. The simulations were run with a temperature correction equal to NOCT ( $46.2^\circ\text{C}$ ).

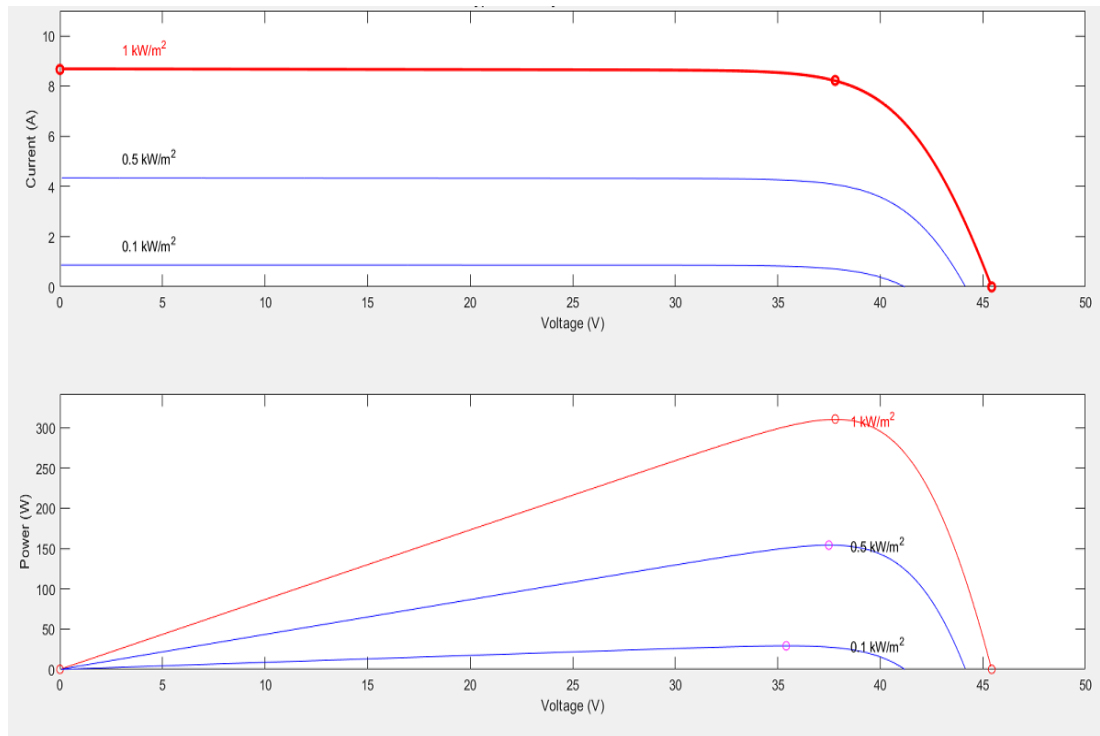


**Figure 4.1: IV and PV characteristics of parallel connected strings at  $1000 \text{ W/m}^2$  at  $T = 46.2 \text{ }^\circ\text{C}$**

It can be seen from the above  $I$ - $V$  curve that, as the solar insolation changes from  $1 \text{ kW/m}^2$  to  $0.1 \text{ kW/m}^2$ , the operation point is reduced. This corresponds to a similar decrease in the output power of the module from a maximum of  $300\text{W}$  to  $25\text{W}$ , as highlighted in the  $P$ - $V$  curve.

#### 4.2.2 System Performance

The aim of this simulation study was to conduct performance analysis of a  $120\text{MW}$  PV system with the input of environmental conditions encountered in Jamaica. The performance analysis was conducted in time steps with SAM software tool developed by National Renewable Energy Laboratory (NREL). It used the Meteonorm meteorological database to obtain irradiation data for the test location. This allowed a detailed simulation of the efficiency with which the plant converts solar irradiance into AC power and the losses in the conversion. It is necessary as well to clarify the net daily energy demand after the inclusion of the  $120\text{MW}$  PV system [25, 30].



#### 4.2.2.1 Concentrated System Facility

Figure 4.2 below shows the hourly plane of area (POA) irradiance data for a fixed-tilt mounted system for the selected site at Montego Bay across three separate months to represent the sample irradiance coverage for the year. Sunlight hours are measured between sunrise at 6 am and sunset at 6 pm on average for the region.

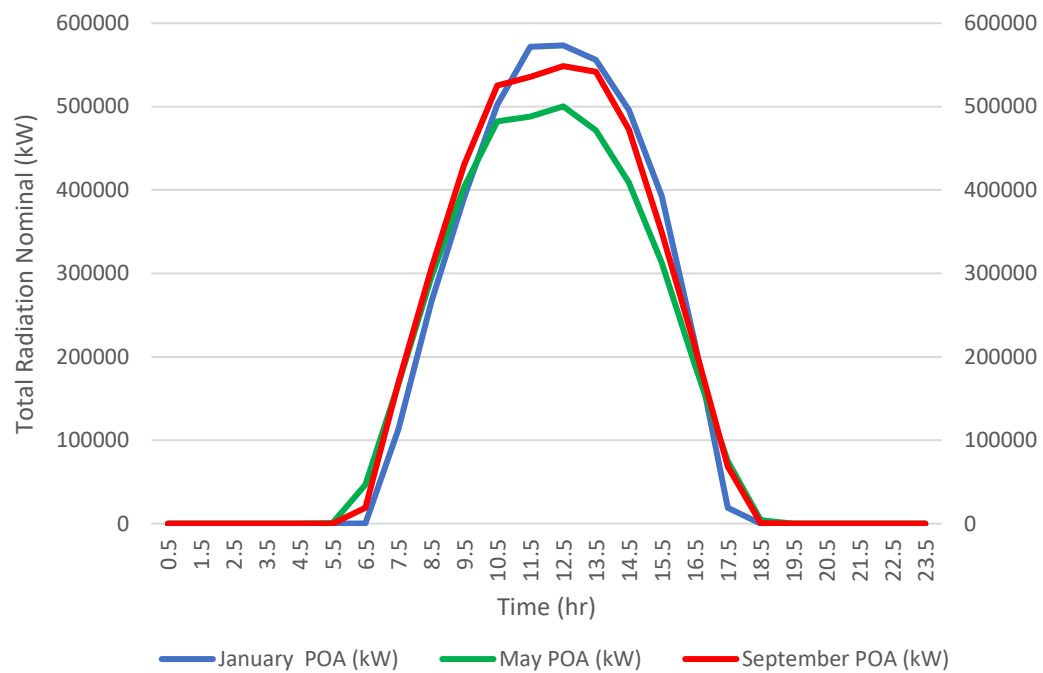


**Figure 4.2: Hourly average plane of array total irradiance for Montego Bay site**

The data shows that in January there is a higher concentration of solar irradiance between 11:30 am and 2:00 pm. September shows the second highest concentration followed by May.

Figure 4.3 below reflects the hourly power generation output of the fixed-tilt mounted 120MW PV plant for the selected site at Montego Bay across three separate months to represent the sample hourly generation across the entire year.

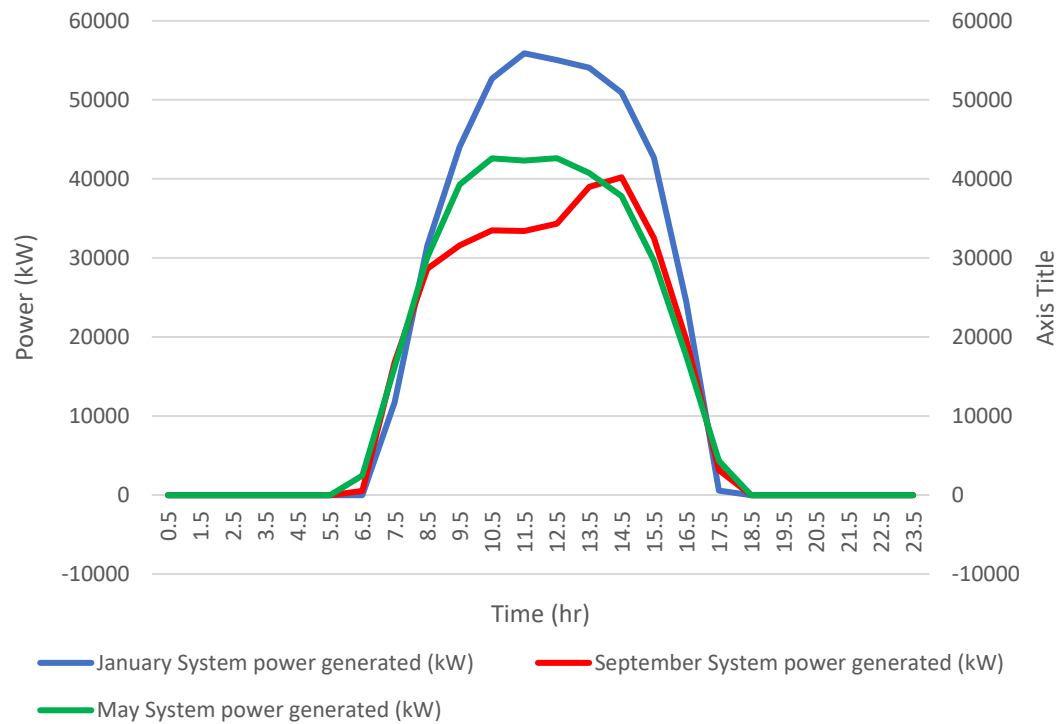


**Figure 4.3: Hourly average power generation output of a fixed mounted system located at Montego Bay**

The data illustrates that January has the highest generation performance peaking at 56MW at 11:30 am. This followed by May showing the second highest generation of 43MW at 10:30 am, whereas September peaked at 40MW at 2:30 pm.

Table 4.1 below outlines the overall annual output for the fixed-tilt mounted 120MW PV system located at Montego Bay after 8,760 hours of operation.

**Table 4.1: Annual system output of 120MW PV power plant located at Montego Bay**

Metric	Value
Annual energy (year 1) (kWh)	136,005,520
Capacity factor (year 1) (%)	12.9
Energy yield (year 1) (kWh/kW)	1,133
Performance ratio (year 1)	0.58

The table reflects the annual energy transmitted to the electricity network, the capacity factor and performance ratio of the facility and the energy yield relative to the installed size of the system.

Figure 4.4 below presents the average hourly ambient temperature at the Montego Bay location across three separate months, January, May and September. This represents the sample for the entire year.

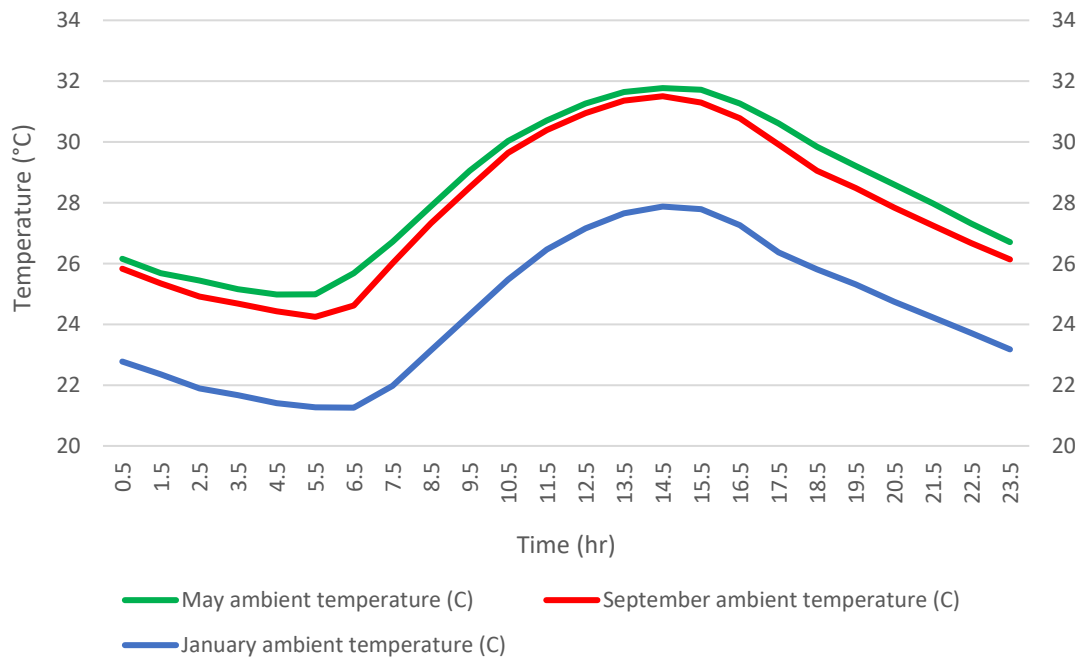


**Figure 4.4: Average hourly ambient temperature for Montego Bay**

May displayed the overall highest temperature profile, with September having almost identical values. January had temperatures consistently below the two other months. Temperature across the three months peaked between 12:30 pm and 4:00 pm.

Figure 4.5 below display the average hourly prevailing wind conditions at the selected distribution site located in Montego Bay for three separate months of January, May, and September representing a sample of the yearlong wind conditions.

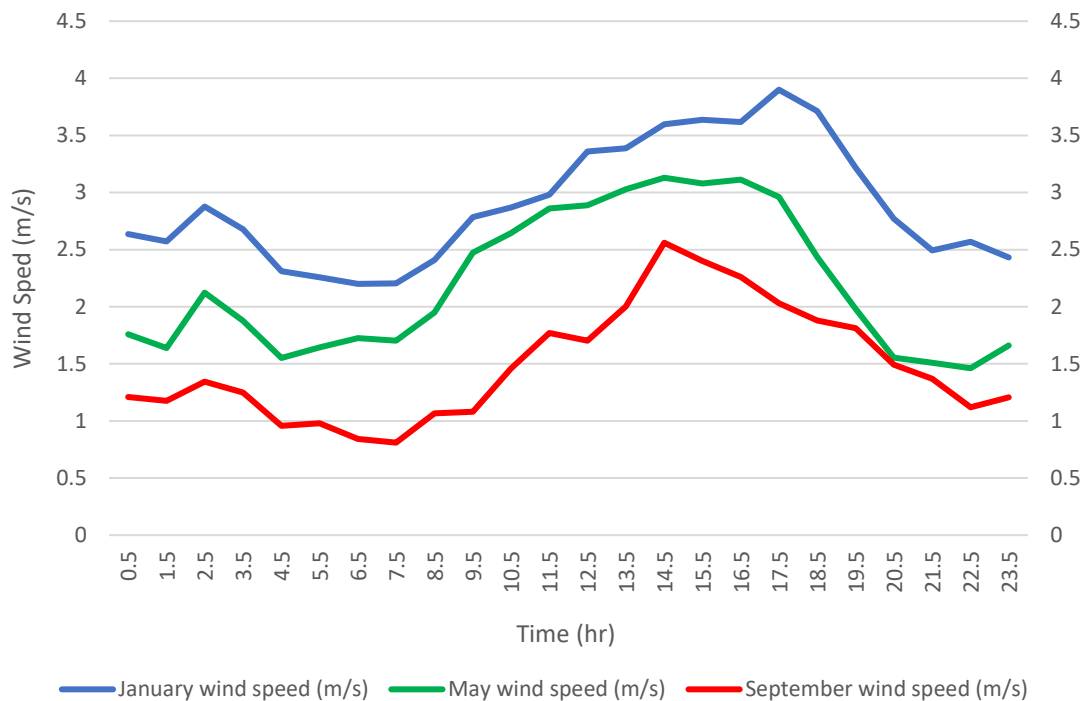


**Figure 4.5: Average hourly wind speed for Montego Bay**

The highest wind speeds are recorded in January, with May having the second highest values. During the period between 9:30 am and 11:30 am, May has prevailing winds which closely approximate to values recorded in January during that period. September has consistently recorded the lowest wind speeds.

#### 4.2.2.2 Tracking System Performance Comparison

Figure 4.6 below shows the average annual hourly plane of area irradiance data for the selected site at Montego Bay with mounted and tracking systems. The recorded data spans fixed-tilt mounting systems, 1-axis and 2-axis tracking technology to identify the optimal performance of the PV modules of the 120MW PV power plant.

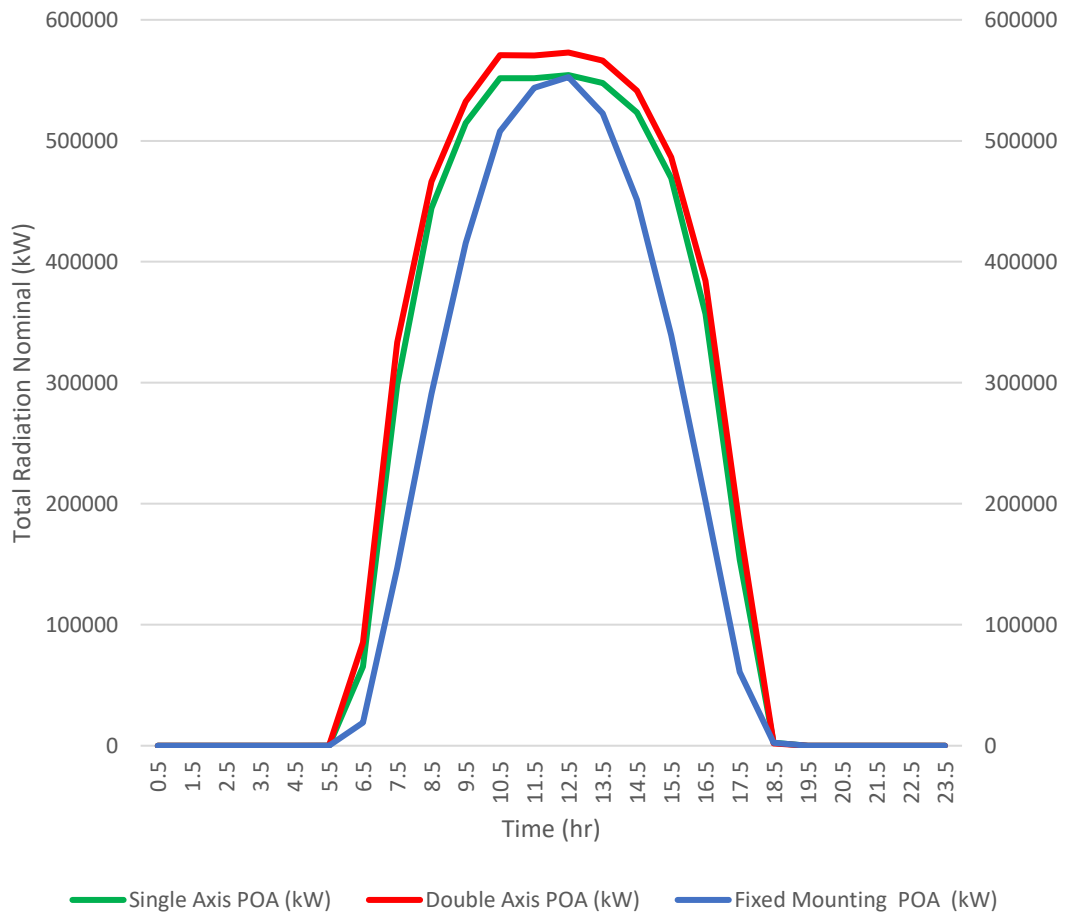


**Figure 4.6: Plane of array irradiance for tracking systems**

The 1-axis tracker yields a 24% increase in the annual solar irradiation energy capture in comparison to fixed-tilt. There is a 31% increase for the 2-axis tracker as opposed to the fixed-tilt configuration.

Figure 4.7 below shows the average annual hourly power generation output data for the selected site, Montego Bay, with mounted and tracking systems. The data measures the

generation output from fixed-tilt mounting systems, 1-axis, and 2-axis tracking technology for the 120MW PV power plant.

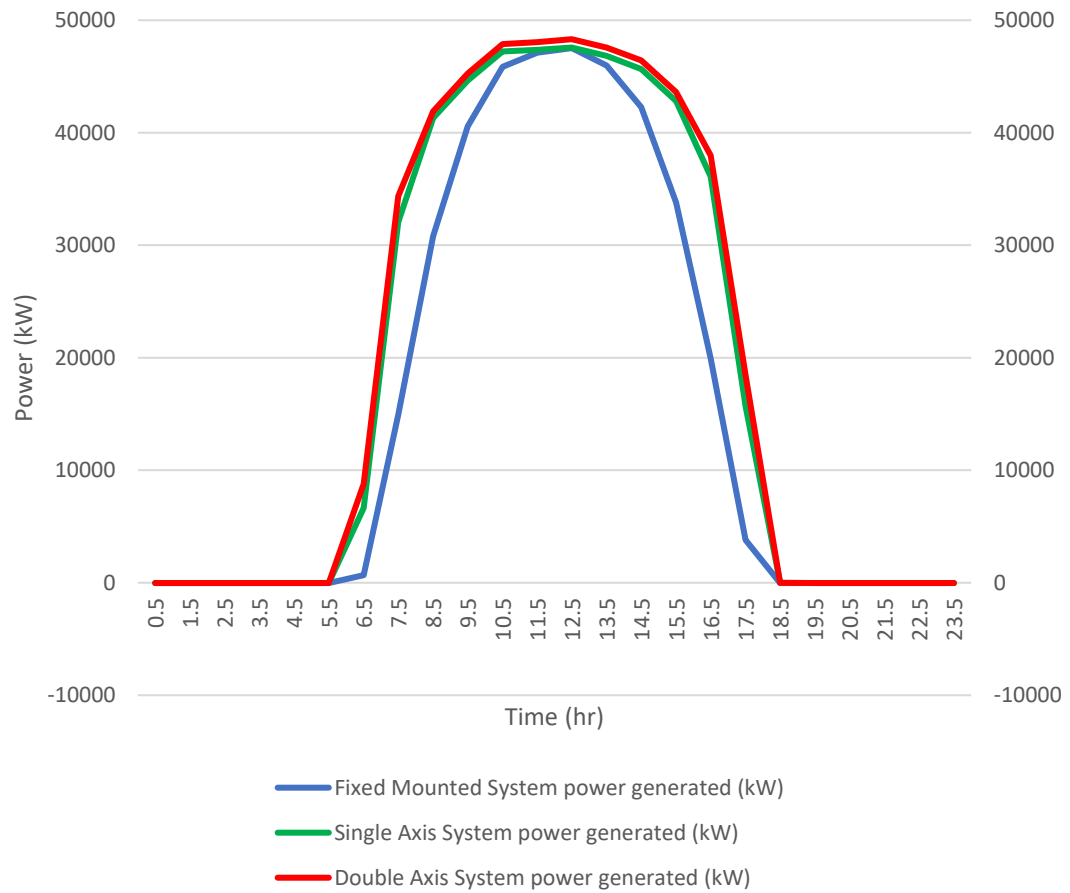


**Figure 4.7: 120MW PV power plant power generation output for tracking systems**

The 1-axis tracker yields 22% increase in the performance of annual power generation output in comparison to fixed-tilt. In contrast, there is a 26% increase for the 2-axis tracker as opposed to the fixed-tilt configuration.

Table 4.2 below outlines the overall annual output for the 120MW PV system after 8,760 hours of operation located at Montego Bay for fixed-tilt mounting systems, 1-axis, and 2-axis tracking systems.

*Table 4.2: Annual system output of 120MW PV power plant for tracking systems*

Metric	Value		
	Fixed	Single Axis	Double Axis
Annual energy (year 1) (kWh)	136,005,520	165,390,688	170,750,256
Capacity factor (year 1) (%)	12.9	15.7	16.2
Energy yield (year 1) (kWh/kW)	1,133	1,378	1,423
Increase in Energy yield (%)	—	21.6	25.6
Performance ratio (year 1)	0.58	0.57	0.56

The table reflects the annual energy transmitted to the electricity network, the capacity factor and performance ratio of the facility across the three system configurations. The table characterises energy yield relative to the installed size of the system and demonstrates the increase in performance of the tracking systems relative to the fixed-tilt arrangement.

#### 4.2.2.3 Distributed Facility Systems

Figure 4.8 below reflects the hourly power generation output of the fixed-tilt mounted 120MW PV plant distributed across four sites: Montego Bay, Mandeville, Spanish Town and Kingston. The plots itemise three separate months to represent the sample hourly generation across the entire year for each location.

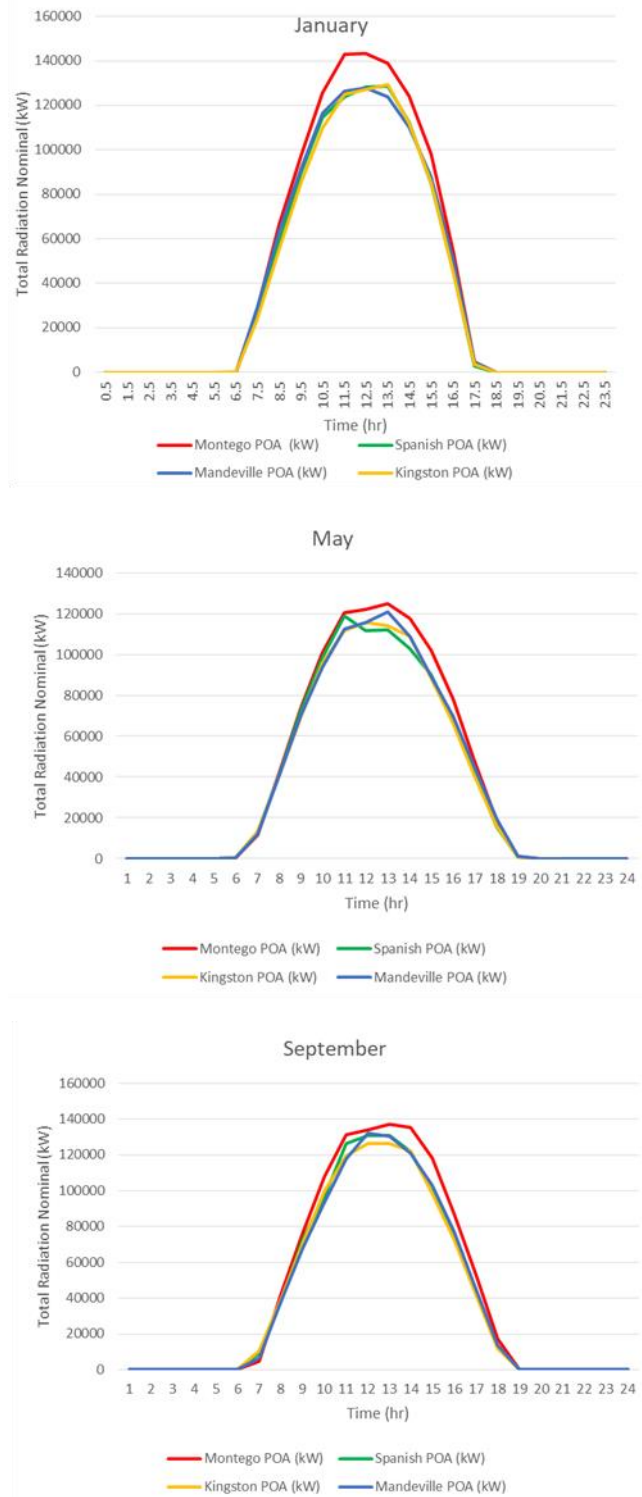


**Figure 4.8: Plane of array irradiance data for distributed sites**

The data above shows January and September have consistently high irradiance values, with the Montego Bay site having the highest POA capture in January. May displays longer sun hour periods but has lower irradiance concentration across all four sites.



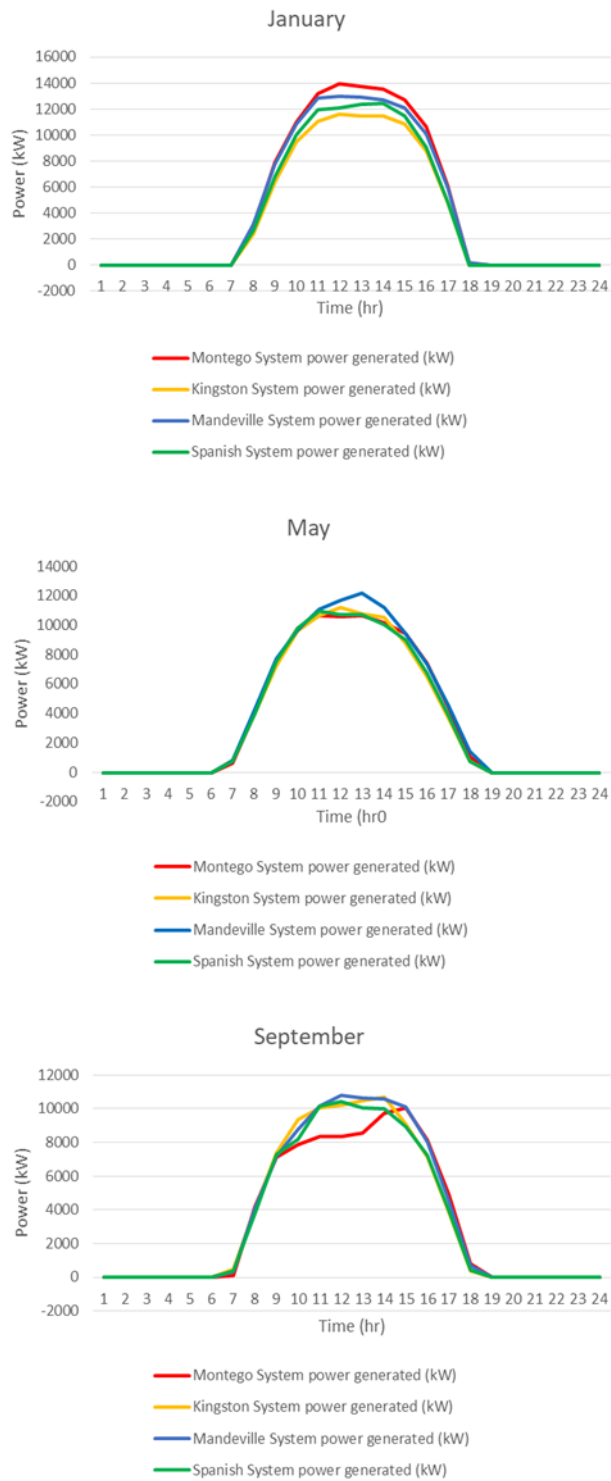


**Figure 4.9: 120MW PV power generation output from distributed sites**

Figure 4.9 expresses the hourly power generation output of the fixed-tilt mounted 120MW PV plant distributed across four sites: Montego Bay, Mandeville, Spanish Town and Kingston. The three selected months represent the sample hourly generation across the entire year. The data illustrates that January has the highest generation performance

across the four locations, with May being the next best performing month. September consistently had the lowest generation output across all four sites with Montego Bay recording a peak of 10MW at 2:30 pm.

Table 4.3 below outlines the overall annual output for the fixed-tilt mounted 120MW PV system after 8,760 hours of operation distributed across four sites: Montego Bay, Mandeville, Spanish Town and Kingston.

*Table 4.3: Combined annual output of distributed sites*

Metric	Values			
	Montego Bay	Spanish Town	Kingston	Mandeville
Annual energy (year 1) (kWh)	33,997,884	32,130,006	31,696,562	34,687,932
Capacity factor (year 1) (%)	12.9	12.2	12.1	13.2
Energy yield (year 1) (kWh/kW)	1,133	1,071	1,057	1,156
Performance ratio (year 1)	0.58	0.60	0.60	0.65

The table reflects the annual energy transmitted to the electricity network by each system, the capacity factor and performance ratio of each facility and the energy yield relative to the installed size of the system at each location.

#### 4.2.2.4 Net Energy Savings

The installed electricity capacity of Jamaica is 925.2MW, with a peak demand of 627.5MW, Figure 4.10 below provides a snapshot of the daily load profile. The figure also shows the energy output of the 120MW PV power plant simulated in SAM by NREL.

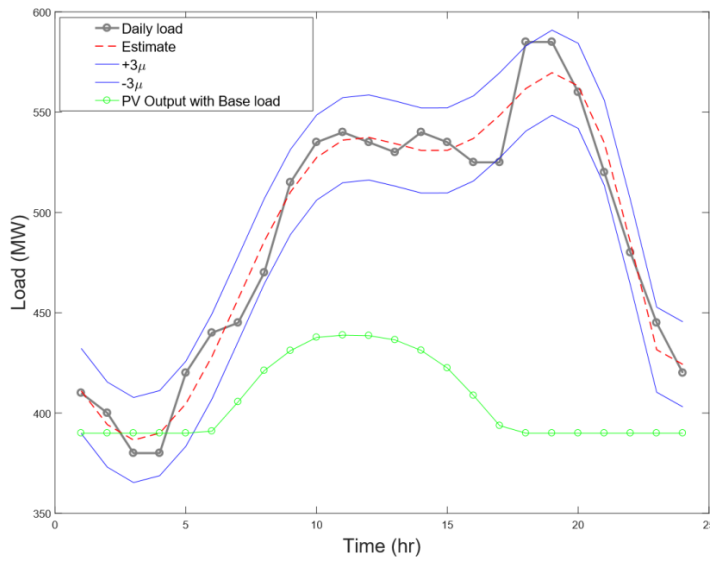


**Figure 4.10: Combination daily load profile for Jamaica**

The evening peak is the highest, but there is a consistent daytime demand of approximately 550MW. The plot lists an approximate annual daily average, and this has an error of  $\pm 3$  standard deviations to account for error and possible increases in energy consumption since 2015.

The combination of the daily demand and the daily PV output results in the net impact on the thermal output delivered by conventional units, which is shown in Figure 4.11 below.

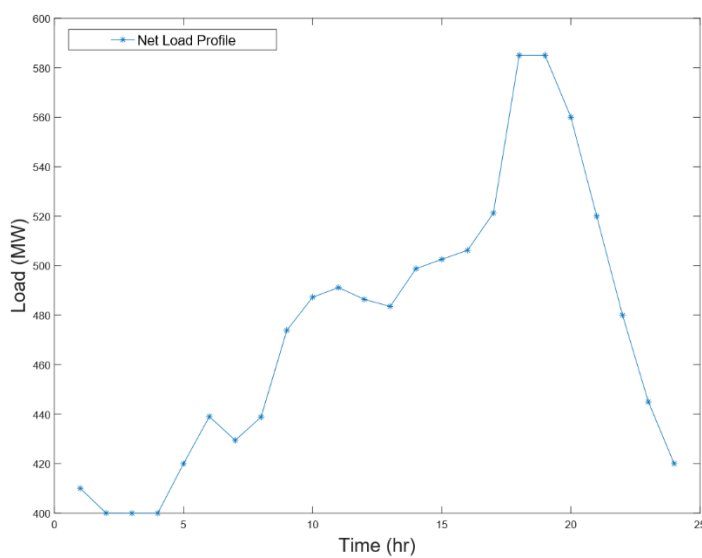


**Figure 4.11: Net daily load profile**

This figure demonstrates a decrease in the daytime load demand which could translate into oil savings per day. MATLAB code was used to accept the daily input from an Excel file then and compare the output of the 120MW PV system and calculate the daily net energy saved from thermal generation. This is only a skeleton of code to provide the quantified output of the integrated PV system. This code could be expanded to provide more detailed calculations and could be incorporated into a real-time algorithm. The code can be seen in Appendix A Figure A.1 with the output results of the system comparison.

Given the annual energy output of the 120MW PV system in Table 4.1 above and the energy equivalent of one barrel of oil [31], the annual saving in barrels is:

$$OilSavings = \frac{AnnualEnergy(kWh)}{Energy_{barrel}(kWh)} = \frac{136005520}{1700} = 80003.24$$

The resulting saving of approximately 80,000 barrels represent a 3.3% reduction in imported petroleum and will have a positive impact on the nation's GDP.

### 4.3 Load-Flow Analysis

This section introduces the load-flow analysis of an approximate model of Jamaica's transmission network. Technically, given the load demanded at consumption buses and the power supplied by generators, this analysis solves all bus voltages and, all real and reactive power injections on each bus of the system. The simulation presented in this section involved a load-flow of the current configuration of the transmission network being benchmarked against a load flow of the transmission network with the 120MW PV system integrated. The section describes the software used and provides a brief overview of the data processing for the networks that were analysed. The simulation models of the networks were built and analysed in the Xendee cloud computing platform.

### 4.3.1 Modelling of Transmission Network

The aim of this grid assessment is to benchmark the consistency of the approximated system model, inclusive of the characteristics of all the equipment and elements within the networks. The load-flow analysis was executed with the cloud computing platform software Xendee by EPRI (see section 1.7). The load-flow calculation is a quantitative analysis of the flow of electrical power throughout the electrical network. The load-flow calculation is done to analyse the power system in its steady-state operation. This provides the best sequence of power operation and information for planning for future expansion. Another critical function of a load-flow calculation is to calculate the voltage magnitude and angle for each bus, the P and Q power carried by each line, and the losses of each line and the whole system. The load-flow output report presents real-time data of a possible snapshot of the operating condition of the current Jamaican electricity grid versus the system with the theoretical 120MW PV system integrated to the electricity grid.

The models for the Jamaica Transmission network were built in the Xendee cloud computing software environment. The first model represented the approximate network as currently configured; a section is shown in Figure 4.12 below. The template for the network construction was laid out in the Jamaica all-island electricity grid provided by Jamaica Public Service Company Limited (JPSCo) [32]. Due to the private and confidential nature of the information required to represent the network accurately, the researcher was unable to gain access to that data. As such, operating element data were selected from the catalogue of the Xendee software tool to create an approximate network. This was conducted in an iterative process to provide a stable benchmark for the current network configuration. If this system data had been available, it would have improved the process, and this would have provided more precise and accurate output reports to match Jamaica's electricity network.

The second model is a near replication of the first model, with the exception that 120MW of fossil fuel generating units are replaced with 120MW of PV generation; a section is shown in Figure 4.13 below. The size of the PV generation system at 120MW was identified as this represents approximately 20% of Jamaica's peak demand, which averages 617.7MW [1], and this would meet the goal of 20% renewable generation by 2030 as stated in the NEP [33]. In addition, 20% PV penetration level is below high penetration level to prevent excessive short-circuit fault current values [9].

The existing Jamaican transmission network model consists of 34 sources, 170 branches/transmission lines, 55 loads, 63 bus bars, 97 transformers, and 3 cables. This is a large network model, as displayed in the software. Figure 4.12 below presents a snapshot of a small section of the network, to represent a few generators, transformers and a bus bar to indicate what the model looks like. This was used to generate the load-flow output report and associated data in Appendix B (note this is just raw data, which is then analysed, interpreted and synthesised).

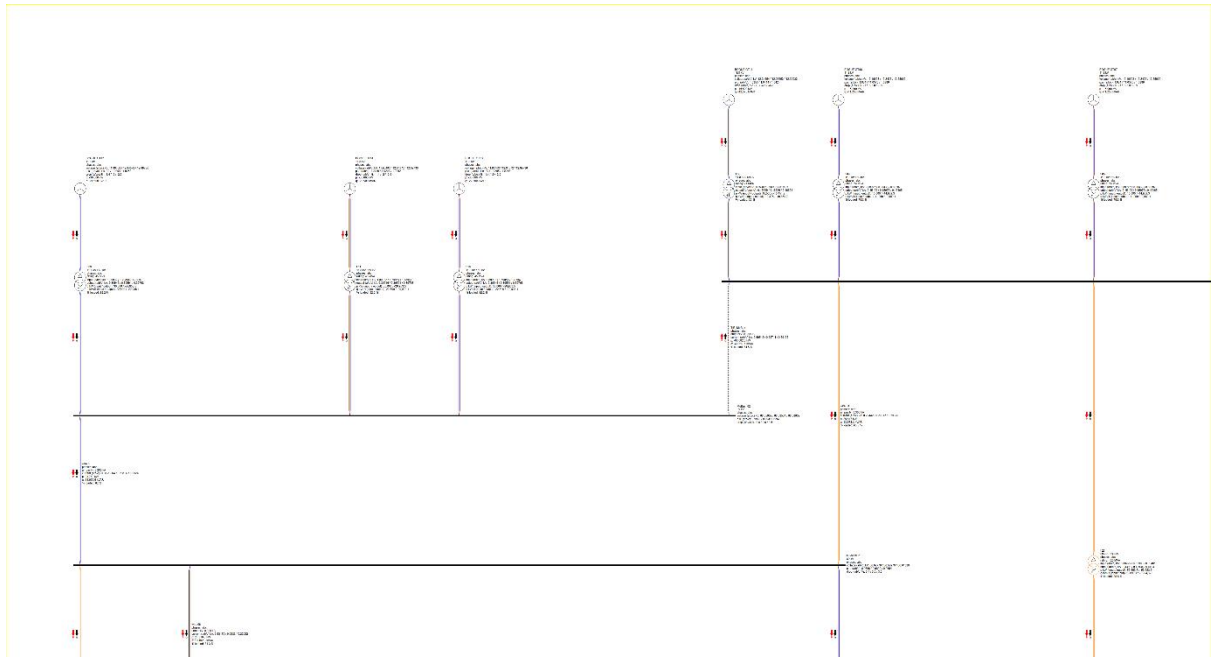


**Figure 4.12: Section of the Jamaican transmission network**

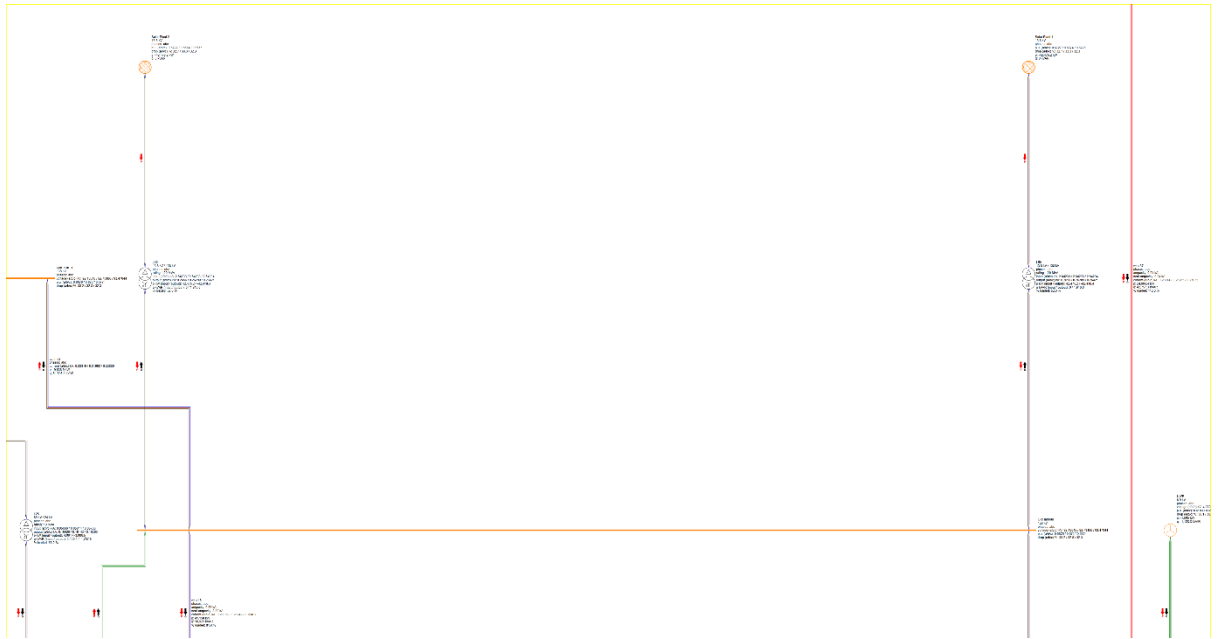


**Figure 4.13: Section of the Jamaican transmission network with integrated PV system**



Figure 4.12 and Figure 4.13 above are approximations of the existing Jamaican transmission network, with the necessary system specifications from the Xendee catalogue for real-world applications. Figure 4.13 has 120MW of fossil fuel energy replaced by a 120MW PV power plant. These two models will now form the basis of a comparison. The first step is to see how the present conventional network will work by assessing the load-flow of the network. This will then be compared to the load-flow of the transmission network with the 120MW PV system integrated into the grid.

### 4.3.2 Load-Flow Calculation

Information listed in the tables in Appendix B was gathered from a load-flow simulation of the two models, the conventional network, and the network with the 120MW PV system integrated. The data in the tables give an overall representation of all the various aspects of AC power parameters, such as real power (P), reactive power (Q), percentage loading for each element and equipment in the construct of the model simulation. The data demonstrates a clear contrast between the conventional system and the system with the theoretical 120MW PV network connection.

The report provides estimated losses, voltages, voltage angles, current flows, and other information for the total network and for each component. The report outlines the estimated output of all generating units; the also estimated active and reactive power flow through all transmission lines, generating unit step-up transformers, 138/69 kV transformers, and 69/24 transformers; and all estimated active and reactive loads.

The percentage loading in Table 4.4 below describes the operating parameters and the maximum tolerances of each piece of equipment as they are operating under load, which is moving electricity from the generating unit to the load elements that will be using the electricity. The percentage loading is quite critical to identifying the operating tolerance

of each element and what is optimal, which should be between 85 and 100%, at which point an element is classified as fully-loaded.

**Table 4.4: Comparison of congested transmission line data**

Name	P (kW)	Q (kVAR)	Solar - P (kW)	Solar - Q (kVAR)	% Loaded	Solar – % Loaded
04	29,447.0	18,672.8	31,004.2	21,032.0	96.5	104.5
07	16,449.3	4,258.3	19,619.4	8,618.2	83.2	106.7
08	52,523.9	84,323.0	48,367.4	129,226.3	83.9	120.0
11	8,575.2	34,190.7	10,224.9	64,650.3	96.3	193.7
37	31,061.3	34,475.9	24,993.4	42,757.3	96.2	112.6

**Table 4.5: Comparison of congested transformer data**

Name	P input (kW)	Q input (kW)	Solar – P input (kW)	Solar – Q input (kW)	P output (kW)	Q output (kW)	Solar – P output (kW)	Solar - Q output (kW)	% loaded	Solar – % loaded
T 12	19,874.1	9,898.8	48,654.2	138,864.6	19,830.9	-8,744.1	48,367.4	129,226.3	83.7	126.8

Given the large number of elements, 170 branches, 51 loads, 97 transformers and the comparative analysis between the conventional network and the PV integrated network, there were only six elements that were overloaded or negatively affected as it pertains to the theoretical PV system. This was in part due to the fact that the PV system does not contribute any reactive power to the overall network. This is needed to allow all elements to be in synchronisation, given the fact that there are so many reactive elements throughout the network that would be required to balance and be compensated by other conventional units within the network. Since the PV system will only contribute real power (P), there are other elements that would require reactive power values and will be compensated by other conventional generating units. Hence, the lines that are closer to a large cluster of generating units connected to the *MoBay\_01* Bus are now under excessive strain because the entire network is drawing reactive power from these conventional units and the line ratings for the network under the conventional measurement are significantly

excessive. This leads to these five transmission lines becoming overloaded and one transformer being overloaded by 126.8% because of where it is positioned. The overloading occurs as the network and the accompanying network elements are trying to balance themselves by absorbing the requisite reactive power to allow the network to stabilise. This data is all captured from the load-flow information from both conventional and theoretical PV integrated network and is reflected in the tables in Appendix B. The elements are shown, and their load values are compared to show how they would work under the conventional network, as well as the new values as the network is trying to compensate and balance for the absence of the reactive power from the solar generating system.

#### 4.3.3 Contingency Analysis

Given the comparison data between the load-flow simulations that is presented Table 4.4 and Table 4.5 above, which outline the specifics of the six parameters across such a large network, Appendix B Table B.1 outlines some technically feasible solutions for grid reinforcement. These recommendations will attempt to fill the gap by discussing the technical, economic and environmental aspects of various power transmission improvement technologies that can play an important role in Jamaica's transmission grid of the future.

The outcome of the simulation study highlights the requirement for infrastructure upgrades to make the electrical network compatible with a large utility-scale solar power plant. With the increasing availability of technologies and the rising environmental challenges, the options in Appendix B Table B.1 aid in the selection of the most appropriate technology for a given scenario. They can all be used in theory, but they have varying degrees of applicability to Jamaica, as indicated by their global advantages and disadvantages. It is also important to state that these solutions are presented in order of

their technical merit, that is, from what is most feasible and practical/efficient/effective to that which would not be deemed technically/economically feasible at Jamaica's present electrical infrastructure level. It is impossible to indicate an overall best solution for network reinforcement, but these possibilities frame not only short- to medium-term solutions but also long-term solutions as well. The choice for a particular technology strongly depends on contingencies but, clearly, research is needed in order to make economic efficient use of technologies in a wider range of situations.

## 4.4 Short-Circuit Study

This section presents a study of the power system operation during abnormal conditions due to faults occurring within the system. The results are obtained from the fault analysis study of a 20% scale model of Jamaica's transmission network. The fault analysis of the approximate current network configuration is the point of comparison for the fault analysis of the PV integrated system. This section describes the software used and provides a brief overview of the data processing for the networks that were analysed. The simulation models of the networks were built and analysed on the Xendee cloud computing platform.

### 4.4.1 Building the 20% Scale Model Transmission Network

Load-flow studies are conducted to assess the steady-state behaviour of a power network during normal operating states. In this operating condition, a network will be exposed to interruptions; as such, this behaviour is assessed during and after a short-circuit occurrence. In very broad terms, a fault is characterised as a flow of substantial current through a low resistive path created by the fault. These current surges through an improper path could cause enormous equipment damage which will lead to the interruption of power, personal injury or death. In addition, there could be fluctuations in the voltage

level, which will influence equipment insulation in the case of over-voltage; or could cause a failure in the start-up of equipment in the condition of under-voltage [9].

The existing transmission network as described in Section 4.3.1 is a very large network and is outside the calculation scope of the Xendee software tool. With a simulation model of the same size as that described in Figure 4.12 above, the output under fault conditions reported an error. Then several iterations were carried out to establish a smaller configuration to achieve a viable output. A viable output was reported after the system was approximately 21% of the model in Figure 4.12 above. Given the limitations of the Xendee software tool, the researcher then constructed a 20% model to provide a whole number multiplying factor of five to approximate across the existing transmission network.

The scale models for the short-circuit analysis were built in the Xendee cloud computing software environment. Figure 4.14 below represents the current configuration without PV integration into Jamaica's electricity network. Figure 4.15 below represents the second scenario with the PV system integrated into the near replica of Figure 4.14. The components of the 20% scale model are 5 sources, 12 branches/transmission lines, 5 loads, 3 bus bars, and 10 transformers.

This model was used to determine the magnitudes of fault currents, to design fault mitigation schemes as well as to recommend the application of equipment for overcurrent protection to isolate these faults. This was done to choose suitable power system management, with reference to the configuration of the transmission or distribution network, and the determination point of the required load and short-circuit ratings of the power system plant.

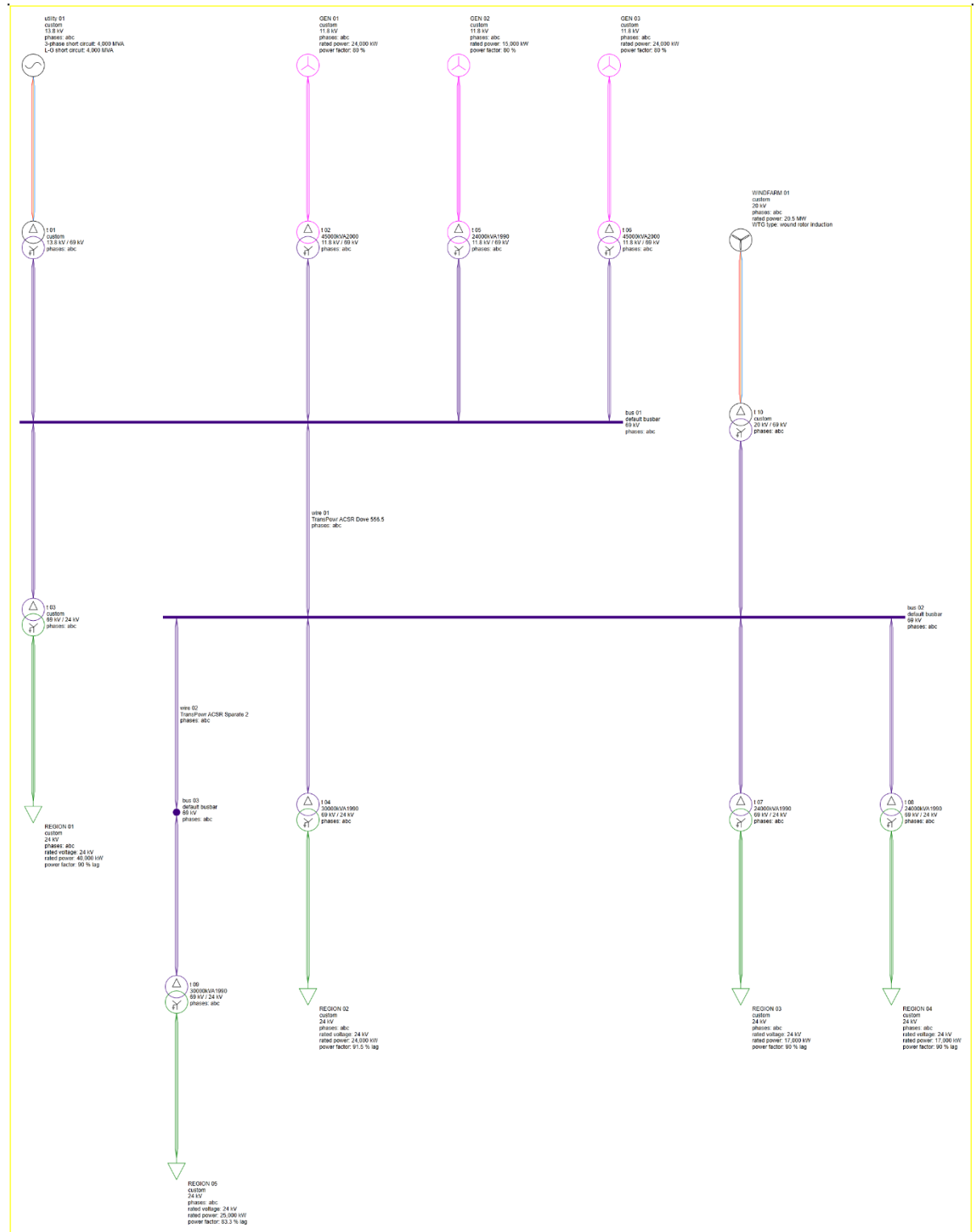


**Figure 4.14: Scaled network model for short circuit analysis**

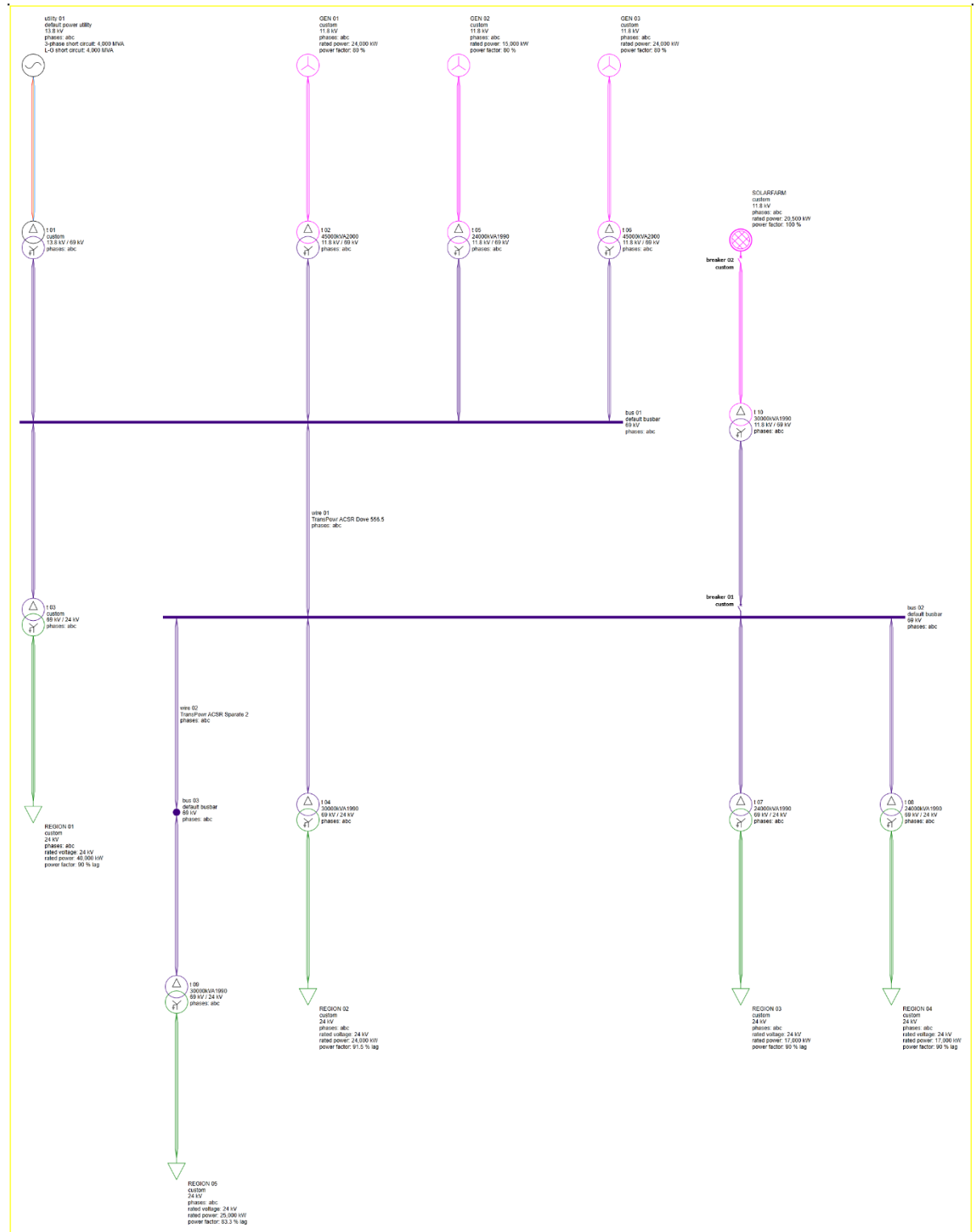


*Figure 4.15: Scaled network model for short-circuit analysis with integrated PV system*

#### 4.4.2 Fault Current Calculation

In this section, the Xendee software tool fault analysis calculations, carried out using the symmetrical components method, are discussed. The fault analysis calculations were done at the Region 5 load location connected to Bus 3 for three-phase, line-to-line, double-line-to-ground and single-line-to-ground faults using pre-determined functions and parameters within the Xendee cloud platform.

##### 4.4.2.1 Bolted Three-Phase Fault

The results of the three-phase bolted fault analysis are given in Table 4.6 below which lists the comparison of symmetrical and asymmetrical fault currents recorded within the conventional generation system and the PV integrated system. The faulted location is the load labelled Region 5 connected to Bus 3; all data are provided in Appendix C.

*Table 4.6: Comparison of three-phase bolted fault currents at Region 5*

Fault Cycle	Conventional		Solar	
	Symmetrical Fault (kA)	Asymmetrical Fault (kA)	Symmetrical Fault (kA)	Asymmetrical Fault (kA)
1/2	1.5817	2.7339	1.6101	1.6108
	1.5145	2.6177	1.5413	1.5420
	1.5285	2.6419	1.5560	1.5567
1 ½	1.5817	2.7056	1.6101	1.6101
	1.5145	2.5906	1.5413	1.5413
	1.5285	2.6145	1.5560	1.5560
8	1.6506	1.6506	1.6046	1.6046
	1.5864	1.5864	1.5362	1.5362
	1.5963	1.5963	1.5511	1.5511
30	1.5881	1.5881	1.5796	1.5796
	1.5208	1.5208	1.5130	1.5130
	1.5345	1.5345	1.5287	1.5287

Figure 4.16 shows the plot of the time response of the three-phase bolted symmetrical fault analysis of the conventional generation system versus the PV integrated system. The



symmetrical fault values of the PV integrated configuration are approximately 1.8% higher during the sub-transient period across the three phases of the network. During the transient period, the PV integrated configuration has approximately 3% lower fault currents across all 3 phases.

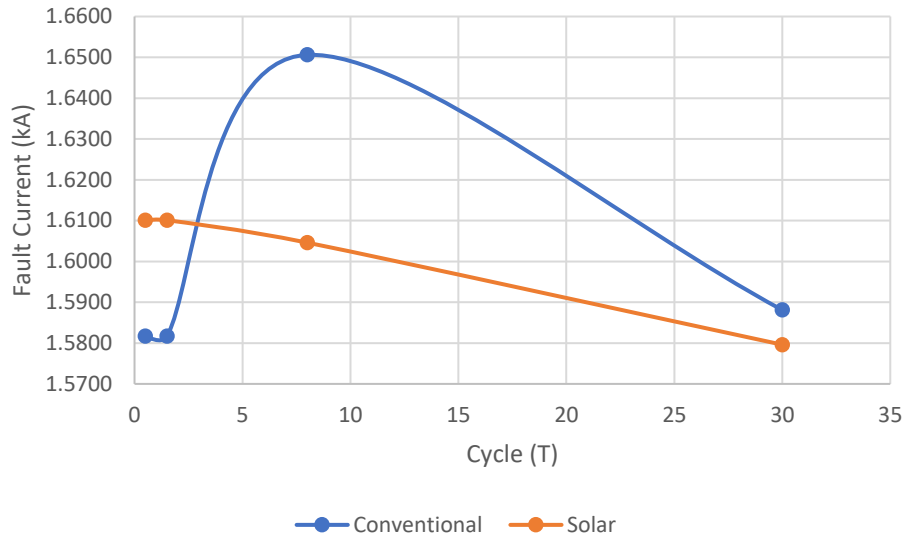


**Figure 4.16: Symmetrical fault analysis of 3-phase bolted fault at Region 5**

The fault currents settle at approximately 0.5% difference between the two configurations during the steady-state period, with the PV integrated configuration having the lower fault values across all three phases.

Figure 4.17 shows the plot of the time response of the three-phase bolted asymmetrical fault analysis of the conventional generation system versus the PV integrated system. In an asymmetrical assessment across all three phases, the fault current values of the sub-transient period of the PV integrated system are approximately 69% lower than the network without PV.

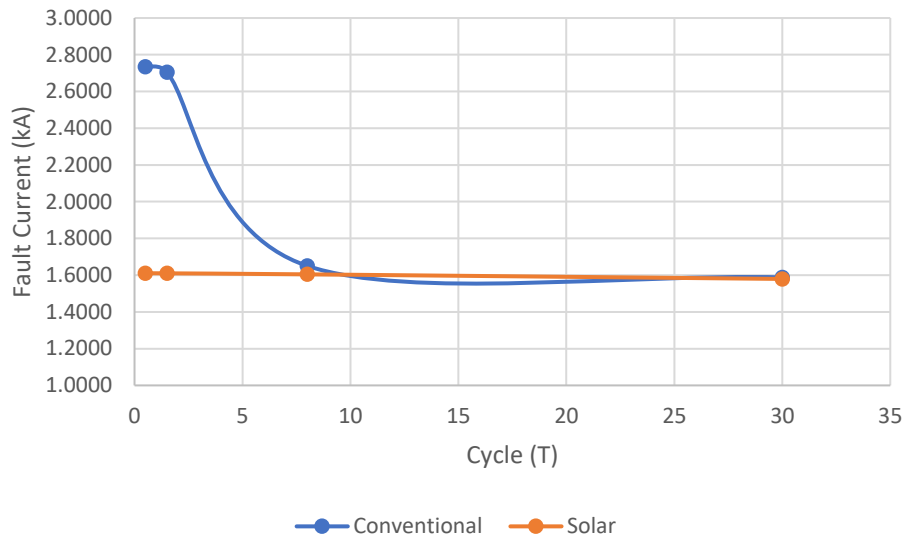


**Figure 4.17: Asymmetrical fault analysis of three-phase bolted fault at Region 5**

During the transient period, as the ride through of the fault is occurring, there are approximately 3% lower recorded fault currents in the PV integrated system. Subsequently, during the steady-state period, the fault currents showed a similar pattern to that of the symmetrical analysis to settle at approximately 0.5% difference with the PV integrated configuration having the lower fault values across all three phases.

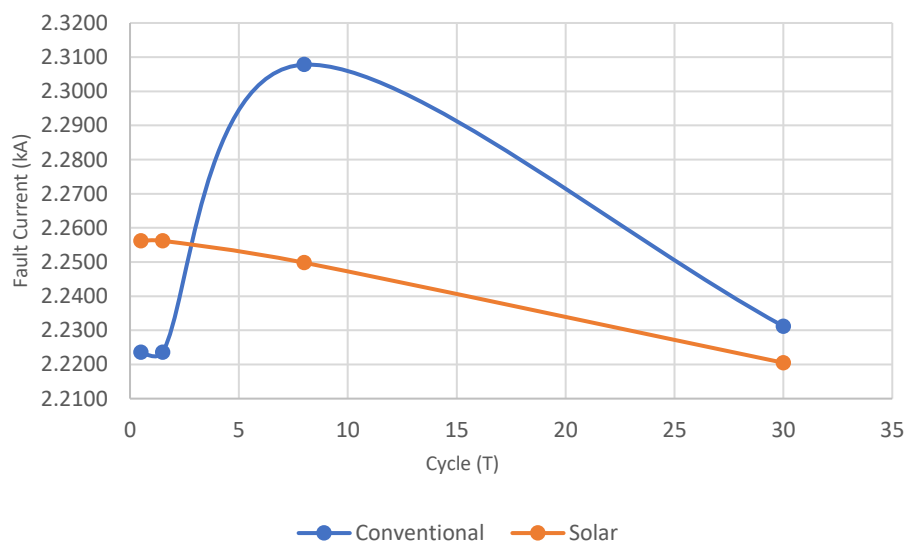
#### 4.4.2.2 Double-Line-to-Ground Fault

The results of the double-line-to-ground fault analysis are given in Table 4.7 below which lists the comparison of symmetrical and asymmetrical fault currents recorded within the conventional generation system and the PV integrated system. The faulted location is the load labelled Region 5 connected to Bus 3; all data are provided in Appendix C.

**Table 4.7: Comparison of double-line-to-ground fault currents at Region 5**

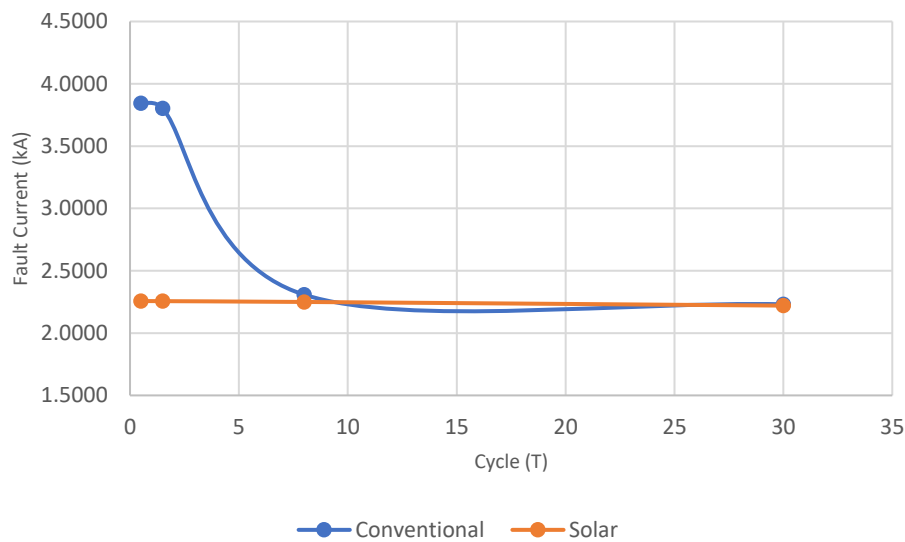
Fault Cycle	Conventional		Solar	
	Symmetrical Fault (kA)	Asymmetrical Fault (kA)	Symmetrical Fault (kA)	Asymmetrical Fault (kA)
1/2	2.2236	3.8433	2.2562	2.2572
	2.5756	4.4517	2.6322	2.6334
	0.0000	0.0000	0.0000	0.0000
1 ½	2.2236	3.8035	2.2562	2.2562
	2.5756	4.4056	2.6322	2.6322
	0.0000	0.0000	0.0000	0.0000
8	2.3078	2.3078	2.2498	2.2498
	2.6931	2.6931	2.6230	2.6230
	0.0000	0.0000	0.0000	0.0000
30	2.2312	2.2312	2.2205	2.2205
	2.5865	2.5865	2.5800	2.5800
	0.0000	0.0000	0.0000	0.0000

Figure 4.18 shows the plot of the time response of the double-line-to-ground symmetrical fault analysis of the conventional generation system set against the PV integrated system. The double-line-to-ground fault is executed on Phase B and Phase C, and the faulted current is flowing through both phases only.

**Figure 4.18: Symmetrical fault analysis of double-line-to-ground fault at Region 5**

During the symmetrical fault, the PV integrated configuration has fault current values 1.5% higher on Phase B and 2.2% higher on Phase C during the sub-transient period. During the transient period, the PV integrated configuration has fault currents of 2.6% and 2.7% lower on Phase B and Phase C respectively. In the steady-state period, the fault currents settle to within 0.48% difference between the two configurations on Phase B and 0.25% difference between the two configurations on Phase C, with the PV integrated configuration having the lower fault current values.

Figure 4.19 shows the plot of the time response of the double-line-to-ground asymmetrical fault analysis of the conventional generation system set against the PV integrated system. In the asymmetrical assessment, the fault current values of the sub-transient period of the PV integrated system are approximately 69% lower than the network without PV across Phase B and Phase C.



**Figure 4.19: Asymmetrical fault analysis of double-line-to-ground fault at Region 5**

During the transient period, the ride through stage Phase B and Phase C has 2.6% and 2.7% lower recorded fault currents within the PV integrated system respectively. Subsequently, during the steady-state period, the fault currents demonstrate a similar

pattern to that of the symmetrical analysis to settle at 0.48% difference between the two configurations on Phase B and 0.25% difference between the two configurations on Phase C, with the PV integrated configuration having the lower fault values.

#### 4.4.2.3 Line-to-Line Fault

The results of the line-to-line fault analysis are given in Table 4.8 below which lists the comparison of symmetrical and asymmetrical fault currents recorded within the conventional generation system and the PV integrated system. The faulted location is the load labelled Region 5 connected to Bus 3; all data are provided in Appendix C.

**Table 4.8: Comparison of line-to-line fault currents at Region 5**

Fault Cycle	Conventional		Solar	
	Symmetrical Fault (kA)	Asymmetrical Fault (kA)	Symmetrical Fault (kA)	Asymmetrical Fault (kA)
1/2	1.3234	2.2875	1.3479	1.3485
	0.0000	0.0000	0.0000	0.0000
	0.0000	0.0000	0.0000	0.0000
1 ½	1.3234	2.2638	1.3479	1.3479
	0.0000	0.0000	0.0000	0.0000
	0.0000	0.0000	0.0000	0.0000
8	1.3861	1.3861	1.3436	1.3436
	0.0000	0.0000	0.0000	0.0000
	0.0000	0.0000	0.0000	0.0000
30	1.3292	1.3292	1.3225	1.3225
	0.0000	0.0000	0.0000	0.0000
	0.0000	0.0000	0.0000	0.0000

Figure 4.20 shows the plot of the time response of the line-to-line symmetrical fault analysis of the conventional generation system set against the PV integrated system. Throughout the line-to-line-phase fault, Phase B and Phase C are in contact, which has the voltages at both phases equal. The fault current is passing from Phase B to Phase C, and in Phase A the current is equal to 0 compared to the fault current.

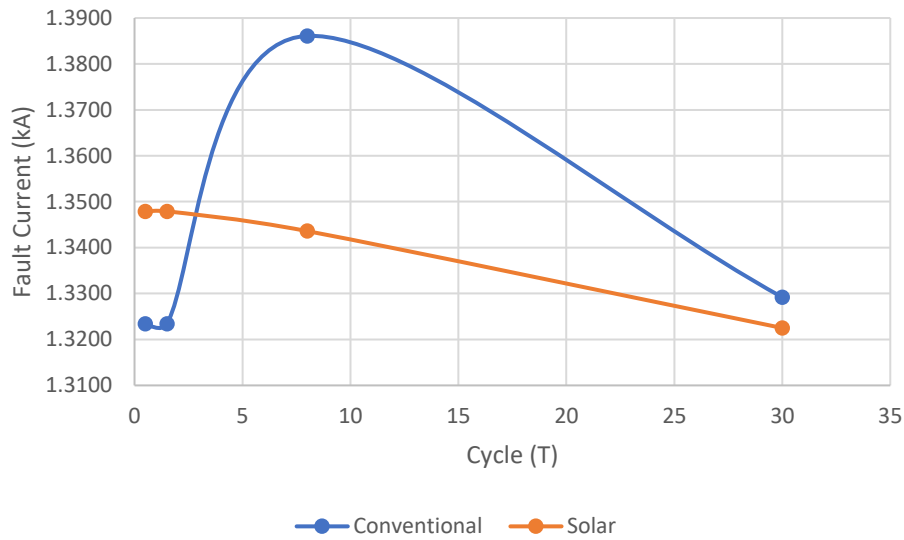


**Figure 4.20: Symmetrical fault analysis of line-to-line fault at Region 5**

The symmetrical fault current of the PV integrated configuration is 1.85% higher during the sub-transient period. During the transient period, the PV integrated configuration has the fault current 3.2% lower than the configuration without PV. While in the steady-state period, the fault currents settle to at approximately 0.5% difference between the two configurations, with the PV integrated configuration having a lower fault current.

Figure 4.21 shows the plot of the time response of the line-to-line asymmetrical fault analysis of the conventional generation system set against the PV integrated system.

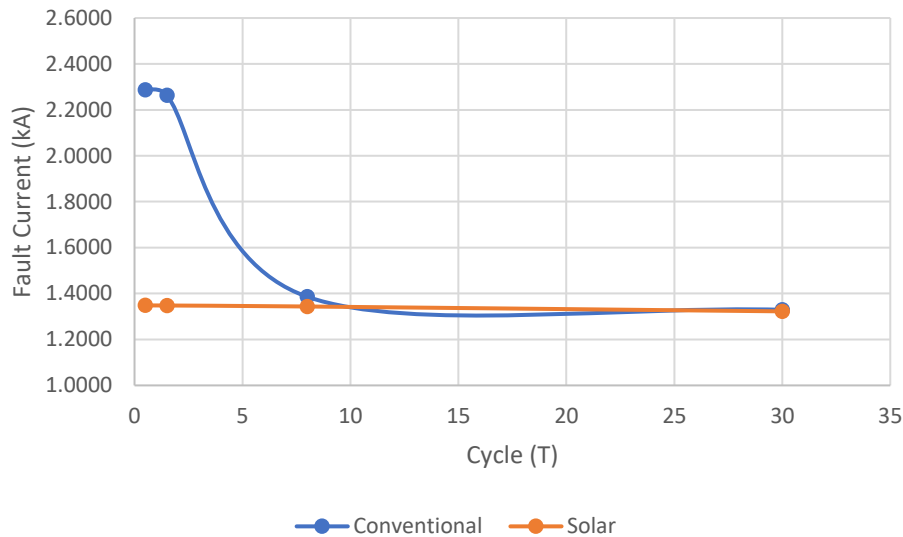


**Figure 4.21: Asymmetrical fault analysis of line-to-line fault at Region 5**

In the asymmetrical assessment, the fault current of the sub-transient period of the PV integrated system is 70% lower than the network without PV. During the transient period, the fault current is 3.2% lower within the PV integrated system. Subsequently, during the steady-state period, the fault currents settle at 0.5%, difference between the two configurations with the PV integrated configuration having the lower fault current.

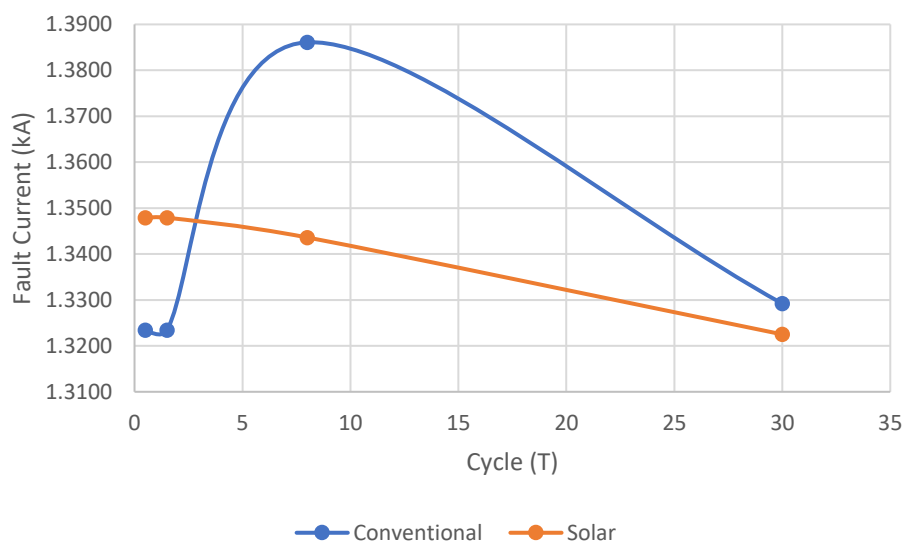
#### 4.4.2.4 Single-Line-to-Ground Fault

The results of the single-line-to-ground fault analysis are given in Table 4.9 below which lists the comparison of symmetrical and asymmetrical fault currents recorded within the conventional generation system and the PV integrated system. The faulted location is the load labelled Region 5 connected to Bus 3; all data are provided in Appendix C.

**Table 4.9: Comparison of single-line-to-ground fault currents at Region 5**

Fault Cycle	Conventional		Solar	
	Symmetrical Fault (kA)	Asymmetrical Fault (kA)	Symmetrical Fault (kA)	Asymmetrical Fault (kA)
1/2	2.1816	3.7707	2.2230	3.5711
	0.0000	0.0000	0.0000	0.0000
	0.0000	0.0000	0.0000	0.0000
1 ½	2.1816	3.7317	2.2230	2.7111
	0.0000	0.0000	0.0000	0.0000
	0.0000	0.0000	0.0000	0.0000
8	2.2857	2.3381	2.2158	2.2666
	0.0000	0.0000	0.0000	0.0000
	0.0000	0.0000	0.0000	0.0000
30	2.1912	2.3381	2.1813	2.1813
	0.0000	0.0000	0.0000	0.0000
	0.0000	0.0000	0.0000	0.0000

Figure 4.22 shows the plot of the time response of the line-to-line symmetrical fault analysis of the conventional generation system set against the PV integrated system. During the single-line-to-ground fault, only Phase B has a current since it is the faulted phase.

**Figure 4.22: Symmetrical fault analysis of single-line-to-ground fault at Region 5**



The symmetrical fault current of the PV integrated configuration is 1.9% higher during the sub-transient period. During the transient period, the PV integrated configuration has a fault current 3.2% lower than the configuration without PV. Then, during the steady-state period, the fault currents settle at approximately 0.5% difference between the two configurations, with the PV integrated configuration having the lower fault current.

Figure 4.23 shows the plot of the time response of the line-to-line asymmetrical fault analysis of the conventional generation system set against the PV integrated system. During the asymmetrical assessment, the fault current within the PV integrated system at the instant of the fault occurrence is 5.6% lower than the network without PV.

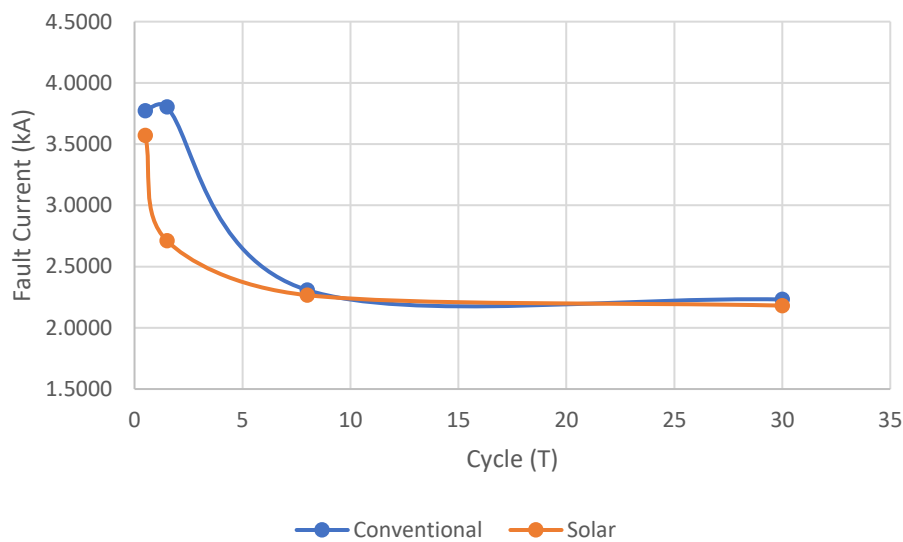


**Figure 4.23: Asymmetrical fault analysis of single-line-to-ground fault at Region 5**

During the next time period within the sub-transient stage, the fault current displays a sharp decline to be 38% lower than the configuration without PV. During the transient period the fault current, starting to settle, is 3.2% lower within the PV integrated system. Subsequently, during the steady-state period, the fault currents settle at 7.2% difference between the two configurations, with the PV integrated configuration having the lower fault current.

The above tables and figures present the comparison and evaluation of the conventional generation system and a PV integrated system in terms of symmetrical and asymmetrical faults. In the investigation, a 20% scale model of Jamaica's transmission network was utilised within a realistic parameter set to compare the fault ride through each configuration.

## Chapter 5                      Discussion and Implications

In the previous four chapters, this study examined the technical implications of integrating a 120MW PV power plant into the Jamaican electricity grid using a quantitative algorithm and simulation model. As a foundational study examining the phenomenon, it established the optimised performance of the 120MW PV system in environmental conditions typical of Jamaica. Additionally, in analysing the system performance, a technical analysis was done which highlighted viable infrastructural improvements. The implications of this study are threefold, and comprise macro-economic benefits, stimulation of energy competitiveness and spill-over benefits for other comparable SIDS.

Having obtained the results of the simulation studies for the performance of the PV power plant and the analysis of the integration of a 120MW PV power plant into the electrical transmission network in Jamaica, their implications are discussed in the following paragraphs. Section 5.1 discusses the implications of the simulated electrical generation performance of the 120MW PV power plant. The technical implications of integrating the 120MW PV system into the electricity network of Jamaica is reviewed in Section 5.2. The chapter concludes with a summary in Section 5.3.

### 5.1 System Performance Implications

This section outlines the implications of technical feasibility performance considerations for a 120MW PV power plant in conditions typical of Jamaica. The implications identified when conducting the appropriate site analysis are detailed in Section 5.1.1, while the implications of the results from assessing a single site study are discussed in Section 5.1.2, and in Section 5.1.3 the implications of a four site distributed study are presented.

### 5.1.1 Site Analysis

A simulation model was conducted in Section 4.2 of the daytime peak generation of a 120MW PV power plant, which corresponds to the daytime increase in load demand in Jamaica. The simulation accounted for the topography and other shading factors to generate the energy output for a single site system. The point of connection was selected out of four options, Kingston, Spanish Town, Mandeville, and Montego Bay. All are large load centres as they have high concentrations of population. Correspondingly, these are close connection points to the transmission network hence the potential for losses is significantly reduced. To test the robustness of the simulation model, a sensitivity analysis was conducted with conservative efficiency levels for the PV modules and inverters. This analysis sought to identify the connection between model inputs and predictions with a measured scope of uncertainty.

One of the implications of this simulation is the ideal site location of potentially high-value land area and its future use as it pertains to selecting a site. Fast forwarding a few years into the future, the growth, and expansion of a large load centre could have an impact on such a situation. While the findings strongly imply that the selection of a site around a load centre is a viable option for the development of a PV system, the implications attached to the future use of land is something that must also be considered. As it pertains to site selection implication, not just the future use of the specific land to serve a high-value purpose but the fact that other projects may have an influence on an established PV site should also be factored in. This implies that the passage of a highway or road network could add to or change the topography or the environmental conditions by creating more dust or other inhibitors to impact on the overall efficient performance of a PV system. Another factor to consider is a project being constructed in close vicinity to the PV facility. The landscape could change and alter the original components to

introduce shading, which was not initially calculated at different points in the day for the overall performance of a PV system. Hence these factors must be taken into consideration when identifying and selecting a site.

### 5.1.2 Implications of the Results of Single Site

The input for any solar system requires sunlight. The input in Figure 4.2 represents the POA conditions in Montego Bay for three separate months during the course of the year. The conditions favour January as it has the highest irradiance concentration, with May being the lowest. However, as it pertains to generation output shown in Figure 4.3, January correlates with the same trend, but there is a dip in September's performance. This may be due to factors that speak to the higher ambient temperature seen in Figure 4.4, as September and May show similar temperature values. Given the efficiency of a solar module is adversely affected by increasing temperature [21], this accounts for the underperformance in generation output for September. Results for May are supported by the wind data in Figure 4.5, as May has higher prevailing winds over the daytime period in contrast to September. This means the higher prevailing winds cause cooler overall ambient temperatures. This accounts for the increased performance of the generation output of May relative to September. This is taking into consideration the environmental conditions as they affect the overall performance of a single site location PV plant. The efficiency of PV modules tested in Oman had a 5% decrease with a 10 °C increase in temperature above STC although the modules were exposed to a high concentration of solar radiance [17]. Conversely, in an intensive monitoring programme in Germany 100 systems had a PR between 55% and 80% with more than half exceeding 70% as Germany conditions are cooler, hence solar modules require limited sunlight exposure to provide good quality and efficient electrical energy output [34].

In order to optimise the performance of the PV power plant, tracking systems are categorised as either fixed-tilt mounted, 1-axis tracking or 2-axis tracking, as discussed in Section 4.2.2.2. Figure 4.6 demonstrates the comparison between the solar irradiance captured by the modules given the three tracking conditions. The benchmark of the fixed configuration is outperformed by 24% by the 1-axis tracking and is outperformed by 31% by the 2-axis tracking. This correlates to 21% and 25% increases in generation performance respectively, as seen in Figure 4.7. In comparison to fixed-tilt mounted array, the standard increase for a 1-axis system generation performance is 12–29% [35], while the 2-axis system has a standard generation performance increase of 30–45% [36]. These performance values indicate that the geographical position of Jamaica is not heavily influenced or affected by the seasonal movement of the sun. As such, the gap in performance increase between 1-axis and 2-axis tracking is relatively small. These findings imply that, for optimisation, it would be more viable to use 1-axis tracking as the overall increase in investment capital, for 2-axis tracking equipment and maintenance would not outweigh the increase in performance.

### 5.1.3 Implications of the Results from Four Distributed sites

A four site distributed configuration simulation model of the daytime peak generation of a 120MW PV power plant aimed at assessing the impact on the generation capacity on-line but unloaded was undertaken. This simulation highlights the results of a distributed configuration PV system across four regions/cities – Kingston, Spanish Town, Mandeville, and Montego Bay. As indicated previously, they are all large load centres and have close connection points to the transmission network. Figure 4.8 illustrates the POA irradiance for each option/location during the course of a year. Montego Bay has the highest irradiance concentration consistently throughout the measured months, with January outperforming the other months – similar to the single site system configuration.

The other three locations record lower irradiance concentrations in comparison, but all perform above a 120,000 kW radiation concentration except in the month of May. As it pertains to output generation for the distributed systems, Figure 4.9 demonstrates that Montego Bay in January records the highest power generation and the trend in September reveals a drop in power generation among all locations. Factors that contribute to this drop in September throughout all distributed locations coincide with the conclusion highlighted in the single site system – underperformance in power generation coincides with environmental factors such as temperature increase and changes in the wind. Mandeville produces the highest energy generation overall of the four locations with a consistent plane of irradiance concentration and the highest energy generation in May and September. This is due to topography as the Mandeville region is on average 600 m above sea level which contributes to lower ambient temperatures, whereas by comparison the Montego Bay site is 120 m above sea level.

Table 4.3 illustrates the breakdown of power generated across the four locations in a distributed systems configuration. The September output profile highlights a general decline in performance which corresponds with environmental changes already outlined. Under the plane of irradiance concentration measurements and the system power generated from these measurements, Montego Bay and Mandeville generate the highest energy levels with a total of 26% each and Kingston and Spanish Town produce the remaining output with 24% each.

It is important to note that the total energy generation created by the distributed systems configuration using four locations around Jamaica does not produce as much energy as the single site configuration. As shown in Table 4.1, the single site produces 136GWh per annum, compared 130GWh per annum from the distributed systems configuration as shown in Table 4.3. Nevertheless, the data implies, that for optimisation of the PV plant

array configuration, a distributed systems configuration would be indicated. The overall environment of this configuration produces less technical strain on the electricity network and provides an opportunity more efficient dispatch management. An efficient dispatch management accommodates for losses, limited power flow, and frequency variations. The utility reserves in Jamaica as of 2015 is 29MW [37], therefore the loss of 120MW could have disastrous impacts on the electricity network in single site configuration. A distributed system configuration would mitigate the risk of such impacts occurring on Jamaica's utility reserves.

A non-technical implication of these findings that correlates to energy output in implementing a distributed systems configuration would be the significant difference in usable land space required to establish such an operation. A distributed systems configuration only requires the use of 155 usable acres of land per site. Meanwhile, a single site configuration requires the use of approximately 620 usable acres of land on one site. The use of such a large area of usable land for a single site configuration would have a much larger impact on future development in comparison to the usable land required for the distributed configuration system.

## 5.2 Implications of Technical Analysis

This section discusses the inferences arising from assessing the performance of a 120MW PV system integrated into the electricity network of Jamaica as well as the implications of possible solutions. The merits of grid reinforcement are outlined in Section 5.2.1, while the implications of what is technically feasible and infeasible for a SIDS such as Jamaica are discussed in Sections 5.2.2 and 5.2.3. Finally, the responsibility of establishing a performance limit on PV penetration into the electricity grid is presented in Section 5.2.4.



### 5.2.1 Grid Infrastructure Improvement

Load-flow analysis assesses the electricity network under normal operating conditions. A load-flow analysis was conducted on an approximate model of Jamaica's electricity network without PV integration. Then a similar analysis was done on an almost identical model with integration of a 120MW PV plant. The output of the first load-flow analysis, conducted through an iterative process, established a benchmark for the load-flow analysis with PV integration. The outcome of the load-flow analysis with PV integration had five transmission lines and one transformer operating beyond their rated parameters, as seen in Table 4.4 and Table 4.5. This was due to congestion from reactive compensation throughout the system. This constant strain on the network could further result in damage to the lines and other equipment and could lead to cascading collapse of the entire electrical network.

Solutions for situations similar to this imply the need for grid reinforcement. This speaks of improving the physical electrical grid or improving the monitoring and control of electrical elements within the electrical grid. Appendix B Table B.1 outlines various technological solutions for grid reinforcement that incorporate environmental concerns as well as techno-economic considerations. The implications of these recommended solutions and their relevant feasibility or infeasibility with respect to Jamaica are reviewed in Sections 5.2.2 and 5.2.3.

### 5.2.2 Technically Feasible Grid Reinforcement for Jamaica

The technological solutions identified in the contingency analysis allow for an increase in the flexibility and reliability, and improvement in the energy efficiency and power quality of the transmission grid, while integrating renewable sources such as PV power plants. From the results presented in Table 4.4, it was recognised that the PV integrated network introduced power quality issues onto the power grid. To help mitigate these

issues, control-technology-based power quality improvements are recommended in the form of power conditioning devices and phase shift transformers. Capacitors or other reactive sources will be required in the PV plant as they work in conjunction with the inverters to meet reactive power capability and requirements at the PCC. Inverters have a low short-circuit current contribution, high bandwidth controls and lack mechanical inertia. Therefore, PV power plants do not have inherent inertial or frequency response capabilities to react to system fluctuations. At low penetration levels (17–23%) [38], the power quality issue is on the renewable side and at the local grid level, and the solution is usually device specific. During the load-flow analysis, as the PV injects current on the utility line, the utility's voltage regulation devices will continue to operate normally to maintain nominal voltage levels at 88–110% under IEEE standard 929-2000 [39]. Voltage variation is related to reactive power flow while frequency variation is determined by the rate of change in real power flow. The smoothing out of voltage and frequency fluctuations can, therefore, be achieved by controlling reactive power and real power respectively. Reactive power compensation is one method for voltage control based on the addition of advanced power electronic technologies to improve capacity and stability. Power control devices such as flexible AC transmission systems (FACTS), thyristor-controlled series compensators, STATCOMs or controllable shunt reactors increase dampening and mitigate system oscillations [40]. The combination of these methods has significant future potential to maintain nominal voltage levels with the PV current injection into the system for overall stability.

The traditional approach for network reinforcement is the construction and addition of new transmission lines. As listed in Appendix B Table B.1, to ease the congestion on the conventional network, adding new lines will provide redundancy paths and create the ability to increase ampacity without increasing the weight. Investing in new transmission

lines technology or replacing transmission lines better utilises the current transmission network infrastructure and minimises environmental scarring. This is an extremely cost-effective approach because of the reutilization of network infrastructure resources. There are no current alternative technologies that can economically compete with overhead transmission lines, especially in rural areas. However, due to the relatively low technological impact of transmission lines, the present case for conventional network reinforcement faces tough opposition. In other word, this method of upgrade could become obsolete and could be unable to mitigate potential challenges as PV penetration level increase.

The results from the above analysis would, therefore, imply the implementation of a planned mitigation scheme that incorporates more technologically advanced elements listed in the power control devices discussion combined with the economic advantage of utilizing new transmission lines technology.

### 5.2.3 Technically Infeasible Grid Reinforcement for Jamaica

The SIDS are small island countries that share similar challenges such as vulnerability to external shocks, extensive dependence on international trade and little to no opportunity to create economies of scale [41]. Jamaica is listed in the group of SIDS and is afflicted by these conditions, and growth and developmental challenges. Given the economic constraints of such a country, some of the technological solutions presented in Appendix B Table B.1 would face extreme challenges to their implementation. High-temperature superconductors, line commutated converter high voltage direct current (LCC HVDC) conductors, voltage sourced converter high voltage direct current (VSC HVDC) conductors and gas insulated lines all require large amounts of investment capital and large capacity installations that create would tremendous complexity in Jamaica's present technological and economic condition. These options, therefore, rank lowest in solution

recommendations and instead would be considered in an environment where there is greater growth and development.

#### 5.2.4 Establish a Cap on PV Penetration

The short-circuit calculation is the analysis of a power system electrical network under fault conditions, with particular reference to the effects of these conditions on power system current and voltages. Combined with other aspects of the network analysis, fault calculation forms an indispensable component of the whole process of power system design. Correct mitigation schemes depend essentially on a full understanding of system behaviour and the ability to predict the complete range of possible system conditions. The analysis of these conditions and their effects on the power system is of particular relevance to the following conditions: firstly, the choice of suitable power system management, with particular reference to the configuration of the transmission network; secondly, the determination of the required load and short-circuit ratings of the power system plant; and finally, the design and description of the application of equipment for the control and protection of the power system.

According to several European grid codes, a PV power plant must be able to ride through specific disturbances without disconnection [39]. As was stated previously, at low penetration levels the power quality issue is at the device and local level while at high penetration levels, grid-level technologies and strategies are needed. With the integration of PV systems, short-circuit currents at the PCC are increased, as reflected by the results in Tables 4.6–4.9. If the penetration level becomes high, the short-circuit capacity increases across the entire transmission network. These increased fault values could reach significant levels which could exceed the rupturing capacity of overcurrent circuit breakers at the customers' end [42]. These excess values could also lead to miscoordination of overcurrent relays and circuit breakers [43]. In the study of fault

analysis here, overcapacity is unlikely to occur due to the fact that it is sized to be 20% of the peak capacity of Jamaica. The results imply that a threshold on PV penetration should be establishing to safeguard the network against potential excessive short-circuit fault values. Hence the short-circuit fault values should be the same as or lower than the rating of overcurrent protective devices; and therefore, should be capable of clearing system faults.

### 5.3 Summary

The research aimed to discover if whether is technically feasible for PV generation to be integrated into Jamaican grid. The outcome of the data analysis implies that the standard performance expectation of a PV system with 1-axis tracking under Jamaican conditions, is on par with international standards with a CF of 12.9% as well as a PR of 58%. Additionally, such a system could perform equally consistently across the country given its environmental conditions.

The findings also imply that, given the existing conditions of the Jamaican electricity grid, integrating a PV system would result in a network failure under the exact configuration at present. The data from the simulation identified the overloading of six crucial elements, as discussed in chapter four. However, there are possible improvements that could be made to streamline an efficient integration of a PV system. The simulations highlighted certain inadequacies in the system and led to the suggestion potential improvements such as physical grid reinforcement by improving transmission lines, as well as adding power conditioning devices to offset reactive power compensation. This combination would be capable of being conformed to operate within the country's infrastructure.

The findings from the review of literature and previous studies implied two key obstacles to increasing PV utility-scale penetration into the Jamaican grid. Firstly, there is a lack of technological integration for such intermittent levels of power generation. Secondly, the country is not equipped with the monitoring or the control that would allow for compensation on such a system if a utility-scale PV system was integrated. However, to minimise the effect of intermittence, the use of weather prediction models would be vital in the deployment of such a facility. Additionally, grid modernisation activities to incorporate smart technology would establish greater communication between generating units and elements within the transmission network to quickly respond to any signal fluctuation.

These systems and technical analyses shed light on the important yet neglected issues of energy generation and diversification. They provide a basis for comprehensive examination of these energy considerations in Jamaica and similarly uncompetitive countries. The International Renewable Energy Agency (IRENA) works closely with island countries to accelerate their shift to renewables and help ensure a sustainable energy future [44]. These studies have prompted policymakers to adopt more progressive approaches to energy analysis and diversification. Grid studies completed in Antigua and Barbuda, Cook Islands, Samoa, and Palau have formed the basis of sound technical policy and viable recommendations for infrastructure changes [45]. This lends itself to a new era of energy security, economic development, social progress, and environmental integrity.

Additionally, from the implications of the study, an unintended non-technical benefit was noted. From the utilisation of solar energy as a renewable source, thereby replacing approximately 80,000 barrels or 3.3% of the country's oil usage per annum, a potential reduction in the nation's oil bill would be realized. There are wider implications for the Jamaican economy, of which energy competitiveness is a major consideration. This could

improve Jamaica's current ranking from having the highest cost in the region [1] to becoming more competitive in terms of price per kWh for electricity. One spill-over benefit could be an improvement in the current level of foreign direct investment through global competitiveness which could stimulate further job creation and GDP growth.

These findings may be of interest to other small island states with the duality of similar environmental conditions and limited energy diversification. In that regard, this study provides the basis for particular small island states to conduct further research on the implications of system performance and technical analysis of utility-scale PV integration.

## Chapter 6                      Conclusions and Recommendations

The first five chapters of this thesis have presented a study of the technical feasibility of integrating a 120MW PV power plant, as well as the obstacles to increasing utility-scale PV penetration into the electricity grid in Jamaica. This chapter highlights the viable conclusions of the study and summarises ideas for future research work.

### 6.1 Conclusions

91% of Jamaica's energy is generated by imported fuel oil which creates an unsustainable environment for the nation's development goals. The Government of Jamaica created a national development policy for 2009–2030 which requires 20% renewable energy mix for energy diversification and energy security. The purpose of this research was to assess the feasibility of this renewable source being solar PV generation by integrating a 120MW PV power plant into Jamaica's electricity grid. From the simulation study carried out with environmental conditions typical of Jamaica, across four potential sites the CF ranged from 12.9–13.9% and PR was 58%. This falls within the global standard for PV facility CF which ranges from of 12–15% and the PR which ranges from of 55–80%. Given environmental conditions such as sunlight, irradiance, wind and ambient temperature, a 120MW PV power plant is projected to perform well in Jamaica.

After assessing how the system performed under environmental conditions, the next step was to assess how the PV power plant interacts with the power delivery system, in other words, the transmission network. For a PV power plant at a single site, due to reactive power compensation by the other conventional units, 6 out of 321 elements were operating well outside of their nominal operating parameters. This situation created weak points in the system that could potentially lead to catastrophic failure of the entire Jamaican electricity network. Given a four site PV power plant assessment, the reactive



power compensation was less overall, hence the network parameters were able to operate closer to their nominal values. Furthermore, from assessing the system under abnormal conditions, it was seen that the fault response values were generally lower with 20% PV integration compared to conventional generation network.

The integration of a PV power plant as a renewable source would benefit Jamaica by reducing the 91% proportion of the thermal dependent generating units and this by extension reduces the importation in the quantity of oil, thus reducing the CO<sub>2</sub> emissions as well as contributing to the energy diversity and security for the country. To curb the congestion impacts and increase the hosting capacity for reactive power compensation, line feeder upgrades, distributed/optimal location of utility PV facilities and grid voltage control solutions should be implemented. These involve the use of reactors, on-load tap-changers, inverter control, transmission line upgrade, static VAR compensation, STATCOM, and the virtual synchronous machine method. Based on evidence presented in the study, it is technically feasible for PV generation to be integrated in Jamaica's power grid with four sites.

### 6.1.1 Limitations of the Study

Throughout this research, there was a lack of information provided officially from Jamaica. The information from JPSCo was deemed sensitive and could not be shared for the completion of this thesis given the monopoly status of the utility company. The models used in this study were created based on an approximation and built from the data library within the software tool. An iterative process was used to establish the benchmark network parameters for the Jamaican network in its current configuration to develop definitive data for Jamaica.

## 6.2 Recommendations

Considering the research study and conclusions, it is recommended that the study can be repeated to get specified data if real-time parameters are provided from JPSCo, and additional recommendations for further exploration are as follows:

- **Energy storage options:** To further effectively utilise renewable energy, energy storage options provide the ability to store energy when supply exceeds demand. This storage will be useful to minimise the effect of the intermittent nature of renewables and therefore energy will be available at times when needed. The study can be further extended to incorporate the various available storage options to further the overall stability of energy delivery in Jamaica through the electricity grid.
- **Virtual inertia:** Renewable energy sources with inverter-based generation do not provide any mechanical inertia response, which compromises frequency stability. Therefore, it can be shown that, fundamentally, the objective of virtual inertia is to provide dynamic frequency response to an electrical network. The study could be expanded to include virtual inertia topologies and investigate how they would enhance the dynamics and overall stability of the Jamaican electricity grid.
- **Dismantle time:** SIDS are more vulnerable to shocks in the environment which are worsened by climate change. Renewable energy resource mechanics would require protection during any potential catastrophic events caused by climate anomalies. Expanding on this study and conducting research on the implementation and execution of dismantling procedures in emergency situations would help give insight into the durability of solar PV energy systems.

## References

- [1] S. Makhijani, A. Ochs, M. Weber, M. Konold, M. Lucky, and A. Ahmed, *Jamaica Sustainable Energy Roadmap: Pathways to an Affordable, Reliable, Low-Emission Electricity System*. Washington, DC: Worldwatch Institute, 2013.
- [2] J. Ferris, *Jamaica's Smart Grid Roadmap: Enabling the Nation's Smarter Energy Future*. New York, NY: IBM, 2013.
- [3] L. Partain, R. Hansen, S. Hansen, D. Bennett, A. Newlands, and L. Fraas, "'Swanson's Law' plan to mitigate global climate change," in *2016 IEEE 43rd Photovoltaic Specialists Conference (PVSC)*, Portland, OR 2016, pp. 3335-3340.
- [4] L. Partain, and L. Fraas, "Displacing California's coal and nuclear generation with solar PV and wind by 2022 using vehicle-to-grid energy storage," in *2015 IEEE 42nd Photovoltaic Specialist Conference (PVSC)*, New Orleans, LA, 2015, pp. 1-6.
- [5] B. Dudley, *BP Statistical Review of World Energy 2016*. London, UK: BP 2015.
- [6] C. McFadden. (2017). *Top 10 performing countries for solar energy* [Online] Available: <http://interestingengineering.com/top-10-performing-countries-for-solar-energy/>
- [7] S. Jothibasu, A. Dubey, and S. Santoso (2016). *Integrating photovoltaic generation: Cost of integrating distributed photovoltaic generation to the utility distribution circuits* [Online]. Available: [http://www.researchgate.net/publication/325766441\\_Cost\\_of\\_Integrating\\_Distributed\\_Photovoltaic\\_Generation\\_to\\_the\\_Utility\\_Distribution\\_Circuits](http://www.researchgate.net/publication/325766441_Cost_of_Integrating_Distributed_Photovoltaic_Generation_to_the_Utility_Distribution_Circuits)

- [8] M. Singh, V. Khadkikar, A. Chandra, and R. K. Varma, "Grid Interconnection of Renewable Energy Sources at the Distribution Level With Power-Quality Improvement Features," *IEEE Transactions on Power Delivery*, vol. 26, pp. 307-315, 2011.
- [9] M. Mirhosseini and V. G. Agelidis, "Interconnection of large-scale photovoltaic systems with the electrical grid: Potential issues," in *2013 IEEE International Conference on Industrial Technology (ICIT)*, Cape Town, South Africa, 2013, pp. 728-733.
- [10] J. Redway, P. Musilek, S. Mišák, L. A. S. Prokop, P. Bilík, and V. A. Snášel, "Towards prediction of photovoltaic power quality," presented at the 26th IEEE Canadian Conference on Electrical and Computer Engineering (CCECE), Regina, Saskatchewan, Canada, 2013.
- [11] A. Cabrera-Tobar, E. Bullich-Massagué, M. Aragüés-Peñalba, and O. Gomis-Bellmunt, "Review of advanced grid requirements for the integration of large scale photovoltaic power plants in the transmission system," *Renewable and Sustainable Energy Reviews*, vol. 62, pp. 971-987, Sept. 2016.
- [12] T. F. Wu, C. H. Chang, Y. D. Chang, and K. Y. Lee, "Power loss analysis of grid connection photovoltaic systems," in *2009 International Conference on Power Electronics and Drive Systems (PEDS)*, Taipei, Taiwan 2009, pp. 326-331.
- [13] R. Bakhshi and J. Sadeh, "A comprehensive economic analysis method for selecting the PV array structure in grid-connected photovoltaic systems," *Renewable Energy*, vol. 94, pp. 524-536, Aug. 2016.
- [14] M. Hammad, M. S. Ebaid, G. Halaseh, and B. Erekat, "Large scale grid connected (20MW) photovoltaic system for peak load shaving in Sahab

- Industrial District," *Jordan Journal of Mechanical & Industrial Engineering*, vol. 9, pp. 45-59, 2015.
- [15] IRENA, (2012) Renewable energy country profiles - Caribbean, [Online]. Available:  
[http://www.irena.org/documentdownloads/publications/\\_caribbeancomplete.pdf](http://www.irena.org/documentdownloads/publications/_caribbeancomplete.pdf)
- [16] I. N. S. Kumara, W. G. Ariastina, I. W. Sukerayasa, and I. A. D. Giriantari, "1 MWp grid connected PV systems in the village of Kayubihi Bali; Review on location's characteristics and its technical specifications," in *2013 International Conference on Information Technology and Electrical Engineering (ICITEE)*, Yogyakarta, Indonesia, 2013, pp. 306-311.
- [17] H. A. Kazem, M. H. Albadi, A. H. A. Al-Waeli, A. H. Al-Busaidi, and M. T. Chaichan, "Techno-economic feasibility analysis of 1MW photovoltaic grid connected system in Oman," *Case Studies in Thermal Engineering*, vol. 10, pp. 131-141, Sept. 2017.
- [18] S. Rehman, M. A. Ahmed, M. H. Mohamed, and F. A. Al-Sulaiman, "Feasibility study of the grid connected 10MW installed capacity PV power plants in Saudi Arabia," *Renewable and Sustainable Energy Reviews*, vol. 80, pp. 319-329, Dec. 2017.
- [19] S. Deambi, *Photovoltaic System Design: Procedures, Tools and Applications*. Boca Raton, FL: CRC Press, 2016.
- [20] R. L. Boylestad and L. Nashelsky, *Electronic Devices and Circuit Theory* 11<sup>th</sup> internat. ed. Upper Saddle River, N.J.: Pearson Prentice Hall, 2013.
- [21] G. M. Masters, *Renewable and Efficient Electric Power Systems* 2nd ed Hoboken, NJ: Wiley, 2013.

- [22] A. Sace, "Technical Application Papers No. 10–Photovoltaic plants," *A Division of ABB SpALV Breakers*, 2010.
- [23] H. Saadat, *Power System Analysis*: 3rd ed. USA PSA Pub., 2010.
- [24] K. Nallaperumal and A. Krishnan, (2013). *Engineering research methodology: A Computer Science and Engineering and Information and Communication Technologies Perspective*, [Online]. Available:  
[https://edisciplinas.usp.br/pluginfile.php/4125670/mod\\_resource/content/1/engineering\\_research\\_methodology.pdf](https://edisciplinas.usp.br/pluginfile.php/4125670/mod_resource/content/1/engineering_research_methodology.pdf)
- [25] N. Blair, A. P. Dobos, J. Freeman, T. Neises, M. Wagner, T. Ferguson, *et al.*, *System advisor model, sam 2014.1. 14*: General description NREL, Golden, CO, 2014.
- [26] L. Feng, L. Wei, X. Feng, F. Yongjie, S. Tao, and Z. Lingzhi, "Modeling and simulation of large-scale grid-connected photovoltaic system," in *2010 International Conference on Power System Technology*, Hangzhou, China, 2010, pp. 1-6.
- [27] B. Parsons, *et al.* (2014). *Variability of power from large-scale solar photovoltaic scenarios in the State of Gujarat*. [Online]. Available:  
<https://www.nrel.gov/docs/fy14osti/61555.pdf>
- [28] J. S. Remund, B. Huguenin-Landl, C. Studer, D. Klauser, C. Schilter, R. Lehnher, *Meteonorm global meteorological database: Handbook Part 1: Software, Version 7.1*, Meteotest, Bern, Switzerland, 2016
- [29] X. Corporation. *XENDEE: Cloud computing for microgrids*. [Online]. Available: <https://www.xendee.com>

- [30] J. Remund, S. Müller, S. Kunz, B. Huguenin-Landl, C. Studer, and C. Schilte, *Meteonorm global meteorological database: Handbook Part II: Theory, Version 7.1*, Meteotest, Bern, Switerzerland, 2014.
- [31] *Barrel of oil equivalent (BOE)* (n.d.) [Online]. Available:  
<https://www.investopedia.com/terms/b/barrelofoilequivalent.asp>
- [32] *About Jamaica Public Service* (2013).[Online]. Available:  
[http://myjpsco.gccnow.com/about\\_us/the\\_grid.php](http://myjpsco.gccnow.com/about_us/the_grid.php)
- [33] Ministry of Science, Energy and Technology *Jamaica National Energy Policy 2009–2030 Securing Jamaica's Energy Future... Advancing Competitiveness... Promoting Sustainable Prosperity*, Kingston, Jamaica: Author, 2009.
- [34] T. Erge, V. U. Hoffmann, and K. Kiefer, "The German experience with grid-connected PV-systems," *Solar Energy*, vol. 70, pp. 479-487, Jan. 2001.
- [35] A. Dolara, F. Grimaccia, S. Leva, M. Mussetta, R. Faranda, and M. Gualdoni, "Performance analysis of a single-axis tracking PV system," *IEEE Journal of Photovoltaics*, vol. 2, pp. 524-531, 2012.
- [36] R. Eke and A. Senturk, "Performance comparison of a double-axis sun tracking versus fixed PV system," *Solar Energy*, vol. 86, pp. 2665-2672, Sept 2012.
- [37] R. Case. (2015). *The merits of integrating renewables with smarter grid carimet*. [Online] Available: [https://www.slideshare.net/Rick\\_Case/the-merits-of-integrating-renewables-with-smarter-grid-carimet](https://www.slideshare.net/Rick_Case/the-merits-of-integrating-renewables-with-smarter-grid-carimet)
- [38] D. Hung, M. Nadarajah, and K. Y. Lee, "Determining PV penetration for distribution systems with time-varying load models," *IEEE Transactions on Power Systems*, vol.29, no. 6, pp. 3048-3057, 2014.

- [39] 929-2000 - *IEEE recommended practice for utility interface of photovoltaic (PV) systems - IEEE standard*. (n.d.) [Online] Available:  
<https://ieeexplore.ieee.org/stamp/stamp.jsp?arnumber=836389>
- [40] B. Gudimetla, S. Teleke, and J. Castaneda, "Application of energy storage and STATCOM for grid quality issues," in *Power and Energy Society General Meeting, 2011 IEEE*, Detroit, MI, 2011, pp. 1-8.
- [41] D. Weisser, "On the economics of electricity consumption in small island developing states: A role for renewable energy technologies?," *Energy Policy*, vol. 32, pp. 127-140, Jan 2004.
- [42] J. He and Y. W. Li, "Analysis, design, and implementation of virtual impedance for power electronics interfaced distributed generation," *IEEE Transactions on Industry Applications*, vol. 47, pp. 2525-2538, 2011.
- [43] Z. Zeng, R. Zhao, and H. Yang, "Coordinated control of multi-functional grid-tied inverters using conductance and susceptance limitation," *IET Power Electronics*, vol. 7, pp. 1821-1831, 2014.
- [44] IRENA. (2017). *National Energy Roadmaps For Islands*. [Online] Available:  
[https://www.irena.org/-/media/Files/IRENA/Agency/Publication/2017/IRENA\\_National\\_Energy-Roadmaps\\_for\\_Islands\\_2017.pdf](https://www.irena.org/-/media/Files/IRENA/Agency/Publication/2017/IRENA_National_Energy-Roadmaps_for_Islands_2017.pdf)
- [45] IRENA. (n.d.). *SIDS lighthouse Grid Integration*. [Online] Available:  
<http://islands.irena.org/grid.aspx>
- [46] S. Colel, D. Van Hertem, L. Meeus, and R. Belmans, "The influence of renewables and international trade on investment decisions in the grid of the future," in *ICREPQ'06 International Conference on Renewable Energies and Power Quality*, Palma de Mallorca, Spain, 2006.



- [47] S. Cole, D. Van Hertem, L. Meeus, and R. Belmans, "Technical developments for the future transmission grid," in 2005 *International Conference on Future on Power Systems*, 2005.
- [48] Y. Xiao, Y. Song, C.-C. Liu, and Y. Sun, "Available transfer capability enhancement using FACTS devices," *IEEE Transactions on Power Systems*, vol. 18, pp. 305-312, 2003.
- [49] J. Verboomen, D. Van Hertem, P. H. Schavemaker, W. L. Kling, and R. Belmans, "Phase shifting transformers: Principles and applications," in 2005 *International Conference on Future Power Systems*, Amsterdam, Netherlands, 2005.
- [50] N. Takinami and S.-I. Kobayashi, "Gas insulated line takes power to the people- Japan's Shinmeika-Tokai GIL, the longest in the world, carries 3000 MW of electricity to the suburbs of Nagoya," *Transmission and Distribution World*, vol. 56, pp. 88-91, 2004.
- [51] R. Silbergliitt, E. Ettegui, and A. Hove, "Strengthening the grid: effect of high-temperature superconducting power technologies on reliability, power transfer capacity, and energy use," Science and Technology Policy Institute, Rand Corporation, Washington, DC, 2002.
- [52] J. Oestergaard, J. Okholm, K. Lomholt, and O. Toennesen, "Energy losses of superconducting power transmission cables in the grid," *IEEE Transactions on Applied Superconductivity*, vol. 11, pp. 2375-2378, 2001.
- [53] A. Wolsky, "Environment, safety, and health impact of HTS power equipment," *IEEE Power Engineering Review*, vol. 20, pp. 12-15, 2000.

- [54] O. Gomis-Bellmunt, J. Liang, J. Ekanayake, R. King, and N. Jenkins, "Topologies of multiterminal HVDC-VSC transmission for large offshore wind farms," *Electric Power Systems Research*, vol. 81, pp. 271-281, 2011.
- [55] R. Rudervall, J. Charpentier, and R. Sharma, "High voltage direct current (HVDC) transmission systems technology review paper," *Energy Week*, vol. 2000, p. 2, 2000.
- [56] P. Fischer de Toledo, "Feasibility of HVDC for city infeed," Licentiate thesis, Royal Institute, Sweden, 2003.

## Appendix A      PV Plant Data

*Table A.1: Electrical characteristics of SUNARRAY-S6B3613-300T*

Standard Test Conditions	S6B3613-300T
Optimum operating Voltage ( $V_{mp}$ )	37.8 Vdc
Optimum operating Current ( $I_{mp}$ )	8.2 Adc
Open Circuit Voltage ( $V_{oc}$ )	45.4 Vdc
Short Circuit Current ( $I_{sc}$ )	8.7 Adc
Maximum power at STC ( $P_{mp}$ )	310.716 Wdc
Module efficiency	15.9342 %
Operating Module Temperature	-40°C ~ +85°C
Type	Mono Crystalline

*Table A.2: Temperature characteristics of SUNARRAY-S6B3613-300T*

Nominal Operating Cell Temperature	S6B3613-300T
Temperature Coefficient of $P_{mp}$	-0.457 %/°C
Temperature Coefficient of $V_{oc}$	-0.344 %/°C
Temperature Coefficient of $I_{sc}$	0.055 %/°C

*Table A.3: Datasheet Information for FS1000CU [CEC 2016]*

Inverter Model	Power Electronics: FS1000CU [CEC 2016]
<b>Inputs</b>	
Maximum DC Power	1150 kW
MPP Voltage Range	642 - 800 Vdc
Maximum Input Voltage	800 Vdc
Maximum Input Current	1437.5 Adc
Number of MPP Trackers	2
<b>Outputs</b>	
Rated AC Power at 25°C	1110 kW
Maximum AC Output Current	1608.7 Aac
Rated AC Voltage	690 Vac
AC Grid Frequency	50 Hz
<b>Efficiency</b>	
Maximum Efficiency	96.9430 %
Euro Efficiency	96.7280 %
Standby Consumption	281 Wac
Operation Consumption	4572.9 Wdc

```

% Author: O'Neil Nelson   Date: 1/09/2018

% This is a skelton code that takes as the input data associated with daily energy
% demand of Jamaica in an Excel form. This is compared against a theoretical
% 120MW PV power plant to estimate the approximate energy savings and project oil
% savings

% This calls and loads the output data of the PV plant
DATA='Daily DATA.xlsx';
A=xlsread(DATA);

% Variable to accept Daily Demand Data
daily_load=A(3:end,3);
% Variable to represent Time in hrs
time=1:24;
hour=time';
% Ouput of the PV System
% A(3:end,4) represents original PV_out
% A(3:end,5) represents the output of the software.
PV_out=A(3:end,5);
% Ouput of the PV System with System Base Load
PV_out_390=PV_out+390;
% PV_out_soft=A(3:end,5);
% PV_out_soft_390=PV_out_soft+390;

% Variable to represent the Energy consumed
area_diff=abs(daily_load-PV_out_390)+390;

% Polyfit fits an 8 order polynomial to the data given in daily load depending
% on the nature of the data, one can fit a lesser ordered polynomial if required
% eqn gives the symbolic representation of the 8th order polynomial
[p,S,mu]=polyfit(hour,daily_load,8);
eqn=poly2sym(p);
% Evaluates the polynomial to give the best fit to the data
% f+3*mu(2), f-3*mu(2) gives the line of plus/minus 3 standard deviations
f = polyval(p,hour,[1,mu]);

% Plot of hourly daily load, polynomial esitmate with plus/minus three
% standard deviations and PV output with base load
figure(1)
plot(hour,daily_load,'-ko',hour,f,'r--',hour,f+3*mu(2),'b',hour,f-3*mu(2),'b',hour,PV_out_390,'g-o')
legend('Daily load','Estimate','+3\mu','-3\mu','PV Output with Base load')

% Plot of net result of PV integrated to the system.
figure(2)
plot(hour,area_diff,'-*')
legend('Net Load Profile')

actual = trapz(daily_load)           % Energy consumed per day
estimate=trapz(f)                   % Energy consumed by best fit
upr_est = trapz(f+3*mu(2))           % Upper limit of energy consumed
lwr_est= trapz(f-3*mu(2))           % Lower limit of energy consumed
energy_diff=trapz(area_diff)         % Net energy consumed

```

**Figure A.1: MATLAB Code**

*Table A.4: Net Output Jamaica Daily Load with 120MW Power Plant*

<b>Daily Energy Forecast</b>	<b>Energy Consumed (MWh)</b>
Daily Energy Consumed	11305
Estimate Daily avg	11302
Upper Estimate Daily avg	11790
Lower Estimate daily avg	10814
Net Conventional Energy	10969

## Appendix B      Grid Data

**Table B.1** *Grid upgrade options available to Jamaica for Utility-Scale PV integration*

Technology	Advantage	Disadvantage	Applicability to Jamaica	Current Implementations in Jamaica	References
New AC Transmission Line	<ul style="list-style-type: none"> <li>• Low cost</li> <li>• Simple technology</li> </ul>	<ul style="list-style-type: none"> <li>• Long permit process (ranging from 3 to 15 years) evaluating socioeconomic before constructing new overhead lines</li> </ul>	<ul style="list-style-type: none"> <li>• Increases the efficient utilization of the network.</li> <li>• Control the power flow of existing lines.</li> <li>• Improves the monitoring of voltage level per section of line for given distances.</li> </ul>	<ul style="list-style-type: none"> <li>• Current electrification rate 98%</li> <li>• Network voltages are 69kV and 138kV.</li> </ul>	[46]
Adding or replacing conductors	<ul style="list-style-type: none"> <li>• Increases capacity with minimal environmental impact</li> <li>• Light weight</li> <li>• Cost-effective</li> </ul>	<ul style="list-style-type: none"> <li>• Need for transmission tower modifications to support increased forces due to additional weight</li> </ul>	<ul style="list-style-type: none"> <li>• For maintenance of conductors as some conductors may have passed useful service.</li> <li>• Adding conductors enables more current to be carried, hence more power to be delivered.</li> </ul>	<ul style="list-style-type: none"> <li>• Existing facilities are aging with a commission range from 1973 to 2006.</li> <li>• Significant transmission and distribution losses.</li> </ul>	[47]
New Conductor types	<ul style="list-style-type: none"> <li>• Offers up to double the ampacity in comparison to traditional Aluminium conductor steel-reinforced cable (ACSR)</li> </ul>	<ul style="list-style-type: none"> <li>• Significantly higher cost</li> <li>• Increases in losses due to higher operating temperature.</li> </ul>	<ul style="list-style-type: none"> <li>• New line constructed with the use of ACSR would allow less and shorter transmission towers.</li> </ul>	<ul style="list-style-type: none"> <li>• No technology data on life-cycle deployment.</li> </ul>	[47]
Power Conditioning Devices	<ul style="list-style-type: none"> <li>• Help to reduce the flows in heavily loaded lines, resulting in an increased load ability.</li> <li>• Low system losses improve grid stability and reliability.</li> <li>• Provide a raised transient stability limit.</li> <li>• Limited short-circuit current.</li> <li>• Improved power oscillation damping (POD).</li> <li>• Switchable technology enables full control of the injected voltages and currents.</li> </ul>	<ul style="list-style-type: none"> <li>• Forces the power to follow certain paths results in the occurrence of higher losses in that part of the network.</li> <li>• Injection of harmonics at high power levels, requiring the introduction of expensive filter devices</li> <li>• Limited experience with thyristor-based FACTS at the transmission level</li> <li>• High investment cost</li> </ul>	<ul style="list-style-type: none"> <li>• Introduce controllable reactive power to maintain high power factor.</li> <li>• Maintain voltage stability for the overall system.</li> <li>• Produce less transmission losses.</li> </ul>	<ul style="list-style-type: none"> <li>• No remote monitoring of voltage regulators and capacitor banks</li> <li>• Low voltage power quality (PQ) is investigated manually.</li> </ul>	[48]

Technology	Advantage	Disadvantage	Applicability to Jamaica	Current Implementations in Jamaica	References
Phase Shifting Transformer (PST)	<ul style="list-style-type: none"> <li>Possible to control both active and reactive power.</li> <li>Limited cost and lower losses favour the use of PST over FACTS devices.</li> </ul>	<ul style="list-style-type: none"> <li>PSTs are not flexible</li> <li>Have longer reaction times than FACTS</li> </ul>	<ul style="list-style-type: none"> <li>Regulate voltage phase angle by control active power flow.</li> </ul>	<ul style="list-style-type: none"> <li>No technology data on life-cycle deployment.</li> </ul>	[49]
Underground Cables	<ul style="list-style-type: none"> <li>Aesthetically and environmentally appealing</li> <li>faster permit process</li> <li>Less right-of-way space needed.</li> <li>Reduced health risks of electromagnetic fields</li> <li>Lower operating and maintenance cost.</li> <li>The mean tie between failures is also considerably lower, especially at lower voltages.</li> </ul>	<ul style="list-style-type: none"> <li>Higher capital cost</li> <li>Higher detection and repair cost</li> <li>Failure can take longer to repair.</li> <li>limited to distances of a few kilometres</li> </ul>	<ul style="list-style-type: none"> <li>Suited for where is difficult to use overhead lines.</li> </ul>	<ul style="list-style-type: none"> <li>Electrical network is essentially exclusively serviced by overhead transmission lines.</li> </ul>	[46]
Gas Insulated Lines (GIL)	<ul style="list-style-type: none"> <li>Better insulation</li> <li>Operates at voltages up to 550kV.</li> <li>The capacity is smaller than ordinary underground cables.</li> <li>Load current is much lower.</li> </ul>	<ul style="list-style-type: none"> <li>More complex placement</li> <li>Environmental impact pressurized gas which is poisonous.</li> </ul>	<ul style="list-style-type: none"> <li>GIL can be cost-effective for bulk power transmission systems, (3000 – 4000 MW)</li> </ul>	<ul style="list-style-type: none"> <li>925.2 MW of installed capacity, this applies for long-term forecasting.</li> </ul>	[50]
High Temperature Superconductors (HTS)	<ul style="list-style-type: none"> <li>HTS cables are relatively safe.</li> <li>Environmentally friendly.</li> <li>Carries three to five times more power without increasing voltages.</li> </ul>	<ul style="list-style-type: none"> <li>Significantly more expensive.</li> <li>Capital cost of cryogenic equipment is pricey.</li> <li>Power is needed for cooling.</li> <li>Losses are higher if utilization is below 33%.</li> </ul>	<ul style="list-style-type: none"> <li>Running powerful superconducting electromagnets.</li> <li>Apt for fast digital circuits in Superconducting Quantum Interface Devices.</li> </ul>	<ul style="list-style-type: none"> <li>Limited communication support and lack of technology integration.</li> <li>Network constraints in the form of lack of capacity and lack of redundant feeder paths.</li> </ul>	[51-53]
Line Commutated Converter High-Voltage Direct Current (LCC HVDC)	<ul style="list-style-type: none"> <li>Lower cost of overhead lines or cables, right-of-way, operating and maintenance.</li> <li>Advantageous over longer distance of transmission.</li> </ul>	<ul style="list-style-type: none"> <li>Higher investment cost for converter stations</li> </ul>	<ul style="list-style-type: none"> <li>Submarine and underground cable transmission.</li> <li>Asynchronous link between AC systems.</li> <li>Long distance bulk power transmission using overhead lines.</li> </ul>	<ul style="list-style-type: none"> <li>925.2 MW of installed capacity, this applies for long-term forecasting.</li> </ul>	[54, 55]
Voltage Sourced Converters HVDC (VSC HVDC)	<ul style="list-style-type: none"> <li>Voltage controlled turn-on and turn-off capability offers black start capability</li> </ul>	<ul style="list-style-type: none"> <li>The losses in the converters are higher</li> <li>DC line faults are critical.</li> </ul>	<ul style="list-style-type: none"> <li>Supply electric power from shore to offshore installations</li> </ul>	<ul style="list-style-type: none"> <li>No large offshore installations but will be via if future exploration projects are investigated.</li> </ul>	[47, 56]



Technology	Advantage	Disadvantage	Applicability to Jamaica	Current Implementations in Jamaica	References
	<ul style="list-style-type: none"> <li>• Eliminate flicker and reduce harmonics in the AC systems.</li> <li>• Reactive power control independent of the active power flow.</li> </ul>	<ul style="list-style-type: none"> <li>• DC line faults require the opening of AC circuit breaker at both ends.</li> <li>• Overall cost of converter stations is higher</li> </ul>			

**Table B.2: Transmission Line Data**

Line No.	From Bus	To Bus	Voltage (kV - LL)	Length (m)	P (kW)	Q (kVAR)	Ampacity (kA)	% Loaded
01	MoBay_01	Orange Bay	69	28,000	46,995.3	36,479.1	0.725	69.7
02	Orange Bay	Paradise	69	30,670	24,554.1	19,784.5	0.360	83.5
03	Paradise	Maggoty	69	47,550	2,368.2	5,468.8	0.140	50.5
04	MoBay_01	QueenDr	69	5,440	29,447.0	18,672.8	0.305	96.5
05	MoBay_02	QueenDr	69	7,360	23,768.0	14,090.5	0.285	82.0
06	QueenDr	Rosehall	69	8,350	24,516.3	10,102.3	0.285	81.3
07	Rosehall	GrnWood	69	11,390	16,449.3	4,258.3	0.185	83.2
08	Kendal_M	Kendal_D	138	40,880	52,523.9	84,323.0	0.525	83.9
09	GrnWood	MarthaBrae	69	12,800	7,988.6	795.7	0.140	55.4
10	MarthaBrae	Duncans	69	9,100	838.9	-1,731.0	0.140	13.8
11	Kendal_D	Kendall138	138	48,430	8,575.2	34,190.7	0.185	96.3
12	Kendall138	Ken_138_2	138	17,000	-1,060.3	4,347.3	0.140	17.5
13	Ken_138_2	Ken_138_3	138	36,000	526.0	-2,652.3	0.140	10.5
14	Maggoty	Old_SpurT	69	36,860	-5,838.0	-94.7	0.140	53.5
15	Kendall_69	New_SpurT	69	10,670	-92.2	3,123.4	0.140	24.3
16	Porus	Toll Gate	69	15,600	5,120.0	2,562.4	0.140	44.5
17	Paranassus	MonyMusk	69	18,000	6,361.4	6,230.5	0.140	68.5
18	OldHarbour	Tredegar13	138	28,300	52,263.4	26,693.6	0.330	96.7
19	OldHarbour	Duhaney	138	38,100	47,889.5	68,739.6	0.640	71.8
20	Tredegar13	Duhaney	138	11,900	24,545.0	9,804.4	0.185	85.1
21	MarthaBrae	Duncans	69	9,100	838.9	-1,731.0	0.140	13.8
22	Duncans	Rio Bueno	69	12,000	3,456.6	345.5	0.140	24.9
23	Rio Bueno	CardiffHal	69	15,540	6,419.0	2,666.7	0.140	50.8
24	CardiffHal	RoarRiver	69	20,270	6,036.6	2,650.0	0.140	51.1
25	RoarRiver	Ocho Rios	69	8,500	8,140.6	4,526.9	0.140	78.5
26	Ocho Rios	LWR SS	69	5,120	-3,800.5	-3,295.3	0.140	44.9
27	Bellevue69	Oracabessa	69	12,800	16,669.3	12,980.6	0.330	79.5
28	LWR SS	Bellevue69	69	12,800	846.2	187.8	0.140	7.7
29	Oracabessa	AnnottoBay	69	22,300	5,989.6	4,716.5	0.140	73.2
30	AnnottoBay	HighGate	69	13,400	-2,885.7	-1,784.5	0.140	37.8
31	AnnottoBay	PortAntoni	69	45,500	2,737.2	1,882.6	0.140	37.2
32	Bellevue69	BlackStone	69	13,500	-7,007.4	-4,423.1	0.140	87.5
33	Ewarton	Michelton	69	10,720	11,496.6	11,348.2	0.245	82.0
34	Ewarton	Michelton	69	2,400	-2,012.9	2,903.5	0.140	33.9
35	Michelton	Tredegar69	69	18,000	-5,523.8	584.4	0.140	52.7
36	Tredegar13	Bellevue13	138	40,100	3,019.1	-5,880.3	0.140	28.5
37	Kendal_D	Bellevue13	138	56,800	31,061.3	34,475.9	0.240	96.2
38	Tredegar69	Bushy Park	69	19,500	-7,806.1	2,003.1	0.140	69.8
39	Bushy Park	JABoilers	69	3,300	13,648.4	11,209.2	0.285	68.4
40	Bushy Park	RhodesPen	69	5,900	-22,365.0	-9,396.9	0.285	94.1
41	New_Twack	Duhaney69	69	8,200	5,869.2	1,880.0	0.140	53.9
42	MonyMusk	OldHarb_69	69	24,600	-6,550.1	-3,870.8	0.140	63.9
43	OldHarb_69	RhodesPen	69	7,700	28,909.9	14,119.0	0.640	52.4
44	Duhaney69	NaggosHead	69	10,900	28,225.9	25,454.4	1.815	26.5

Line No.	From Bus	To Bus	Voltage (kV - LL)	Length (m)	P (kW)	Q (kVAR)	Ampacity (kA)	% Loaded
45	Duhaney69	New Port	69	9,100	913.6	920.6	0.140	12.1
46	Duhaney69	HuntsBay	69	5,000	1,611.3	1,684.9	0.140	21.9
47	HuntsBay	GreenwishR	69	400	18,331.2	15,823.8	0.570	54.3
48	GreenwishR	Rockfort	69	7,700	2,879.2	2,396.8	0.140	34.7
49	Rockfort	UpParkCamp	69	4,700	15,660.5	8,588.0	0.285	81.8
50	UpParkCamp	WKingsHous	69	4,800	3,841.0	-887.3	0.140	38.9
51	WKingsHous	Wash_Boul	69	5,100	-9,673.2	-13,265.7	0.245	92.5
52	Wash_Boul	ThreeMiles	69	4,800	-11,474.7	-1,026.5	0.245	62.9
53	Hunt dBay	ThreeMiles	69	2,500	15,314.0	3,744.0	0.280	72.5
54	Duhaney69	Wash_Boul	69	5,500	25,895.3	26,518.3	0.535	88.1
55	Rockfort	CaneRiver	69	8,200	13,815.4	9,537.1	0.285	77.1
56	CaneRiver	OldHopeRd	69	13,500	-77.9	-8,664.0	0.140	8.9
57	WKingsHous	OldHopeRd	69	5,100	13,449	12,377.2	0.285	87.8
58	CaneRiver	GoodYear	69	36,700	4,884.0	2,766.7	0.140	55.2
59	GoodYear	Lyssons	69	5,600	2,043.2	1,044.2	0.140	28.0

**Table.B.3: Load Transformer Data**

Name	Rating (MVA)	P input (kW)	Q input (kW)	From Bus	P output (kW)	Q output (kW)	To Bus	% loaded
T 02	60	40,053.6	21,173.6	MoBay_01	-40,000.0	-19,382.9	MoBay	76.0
T 12	30	19,874.1	9,898.8	Orange Bay	-19,830.9	-8,744.1	OrgBay_Loa	83.7
T 13	24	9,360.9	5,327.0	Paradise	-9,334.9	-4,521.1	Paradise_1	60.9
T 14	24	9,360.9	5,327.0	Paradise	-9,334.9	-4,521.1	Paradise_2	60.9
T 18	30	10,647.2	7,796.6	Maggoty	-10,619.4	-7,053.3	Magg_Load	67.3
T 19	15	7,990.9	5,852.2	QueensDr	-7,965.9	-5,290.9	HalfMoon	68.5
T 20	30	19,348.0	15,711.8	QueensDr	-19,301.7	-14,476.3	Ironshore	86.2
T 21	10	7,388.7	5,333.2	Rosehall	-7,360.3	-4,561.5	Rhall_Load	97.7
T 22	10	7,600.6	3,154.9	GrnWood	-7,550.7	-2,481.8	GrnWood_L	93.4
T 25	10	5,496.0	2,923.6	Kendall_69	-5,475.6	-2,414.4	Kendall_L	80.4
T 31	24	11,386.6	8,881.8	Old_SpurT	-11,343.1	-7,534.0	Old_Spur_L	78.2
T 32	10	4,601.2	3,922.1	Porus	-4,581.7	-3,436.3	Porus_L	78.6
T 33	10	4,823.3	2,561.8	Toll Gate	-4,805.6	-2,118.9	TollGate_L	75.1
T 38	10	5,947.4	4,242.6	MarthaBrae	-5,904.2	-3,659.1	MarthaBr_L	87.0
T 39	10	6,355.7	3,686.8	Duncans	-6,333.0	-3,067.2	Duncans_L	87.6
T 42	30	11,442.9	7,700.0	Ocho Rios	-11,413.9	-6,923.4	Ocho_Load	68.6
T 45	15	2,131.4	1,803.4	PortAntoni	-2,121.9	-1,591.5	PortAn_Loa	42.4
T 46	24	5,013.4	4,325.0	AnnottoBay	-4,994.7	-3,746.0	Annotto_Lo	51.5
T 50	30	9,626.5	7,172.8	Orcaabessa	-9,601.4	-6,502.2	Oraca_Loada	63.9
T 51	15	5,010.1	3,442.8	Blackstone	-4,988.6	-2,960.1	Blkstone_L	63.9
T 52	15	3,941.6	2,624.4	HighGate	-3,925.1	-2,256.0	HGate_Load	55.8
T 54	24	8,580.5	7,448.9	Tredegar69	-8,547.0	-6,410.2	Trede_Load	68.8
T 55	24	3,485.7	2,321.8	Michelton	-3,480.4	-2,157.0	MicHel_Loa	27.4
T 56	30	13,457.6	11,062.8	JABoilers	-13,420.3	-10,065.2	JA_Boil	77.7

Name	Rating (MVA)	P input (kW)	Q input (kW)	From Bus	P output (kW)	Q output (kW)	To Bus	% loaded
T 60	10	5,532.4	3,204.5	RhodesPen	-5,512.7	-2,669.9	Rhodes_Lea	81.5
T 62	30	12,101.4	9,941.4	MonyMusk	-12,068.0	-9,051.0	MonyMusk_L	73.4
T 63	24	8,580.3	7,448.7	New_Twick	-8,546.8	-6,410.1	NewTwick_L	68.8
T 67	45	14,000.6	11,424.6	NaggosHead	-13,972.4	-10,479.3	Naggos_01	64.0
T 68	45	14,000.6	11,424.6	NaggosHead	-13,972.4	-10,479.3	Naggos_02	64.0
T 69	60	21,426.7	15,781.7	New Port	-21,384.7	-14,370.6	NewPort_1	67.6
T 70	60	21,426.7	15,781.7	New Port	-21,384.7	-14,370.6	NewPort_2	67.6
T 76	24	7,747.7	6,718.6	HuntsBay	-7,717.6	-5,788.2	HB_T1	65.1
T 77	10	3,436.9	2,625.9	HuntsBay	-3,412.2	-2,293.0	HB_T1_13_8	65.9
T 78	10	3,436.9	2,625.9	HuntsBay	-3,412.2	-2,293.0	HB_T2_13_8	65.9
T 79	24	7,716.3	6,691.1	GreenwichR	-7,686.4	-5,764.8	GR_T1	65.0
T 80	24	7,716.3	6,691.1	GreenwichR	-7,686.4	-5,764.8	GR_T2	65.0
T 83	24	8,181.2	6,008.6	Rockfort	-8,150.3	-5,051.1	CementCo	66.1
T 84	24	8,513.6	5,016.6	Rockfort	-8,484.3	-4,109.1	Rockfort_L	64.3
T 85	24	11,430.1	9,152.3	UpParkCamp	-11,362.1	-7,041.6	JDF Camp	98.2
T 86	10	3,433.2	2,436.9	ThreeMiles	-3,409.2	-2,112.8	3Miles	65.1
T 87	24	7,890.5	6,843.8	Constant S	-7,859.9	-5,894.9	C Spring	65.8
T 88	24	9,143.8	5,393.4	Duhaney69	-9,112.1	-4,413.2	Duhaney_T3	66.9
T 89	15	4,204.4	3,570.3	CanRiver	-4,185.1	-3,138.9	CanRiver1	60.4
T 90	15	4,204.4	3,570.3	CanRiver	-4,185.1	-3,138.9	CanRiver2	60.4
T 91	24	6,678.8	5,782.1	OldHopeRd	-6,653.2	-4,989.9	OHR_01	60.2
T 92	24	6,678.8	5,782.1	OldHopeRd	-6,653.2	-4,989.9	OHR_02	60.2
T 93	24	8,832.4	4,171.2	Wash_Boul	-8,803.2	-3,267.6	WB_T1	64.2
T 94	24	8,832.4	4,171.2	Wash_Boul	-8,803.2	-3,267.6	WB_T2	64.2
T 95	24	8,832.4	4,171.2	Wash_Boul	-8,803.2	-3,267.6	WB_T3	64.2
T 96	10	1,771.9	1,489.6	GoodYear	-1,759.3	-1,319.5	Good_Year	47.2
T 97	10	2,001.6	1,045.3	Lyssons	-1,989.1	-877.1	Lyssons_L	47.0

**Table.B.4: Generating Unit Transformer Data**

Name	Rating (MVA)	P input (kW)	Q input (kW)	Generating Unit	P output (kW)	Q output (kW)	To Bus	% loaded
T 47	30	302.8	227.1	Alcan	-302.8	-226.4	Ewarton	2
T 15	2.5	1,194.1	895.6	MAGGOTY01	-1,178.3	-781.4	Maggoty	86.7
T 16	2.5	1,194.1	895.6	MAGGOTY02	-1,178.3	-781.4	Maggoty	86.7
T 17	2.5	1,194.1	895.6	MAGGOTY03	-1,178.3	-781.4	Maggoty	86.7
T 40	45	3,033.5	2,277.1	RioBueno	-3,032.8	-2,250.7	Rio Bueno	10.2
T 41	30	2,611.8	1,958.9	RR_Hydro	-2,610.4	-1,920.6	RoarRiver	15.2
T 43	30	2,840.3	2,130.2	LWR	-2,838.5	-2,081.5	WR Tie	17.2
T 44	30	1,906.5	1,429.9	UWR	-1,905.7	-1,407.8	WR Tie	11.6
T 01	450	5,501.2	50,912.6	Swing Bus	-5,492.1	-50,668.0	MoBay_01	11.6
T 03	5	3,360.0	2,520.0	BOGUE GT03	-3,333.4	-2,280.6	MoBay_01	81.7
T 04	24	15,000.0	11,250.0	BOGUE GT06	-14,959.3	-9,989.1	MoBay_01	75.8
T 05	24	15,000.0	11,250.0	BOGUE GT07	-14,959.3	-9,989.1	MoBay_01	75.8
T 06	24	16,500.0	12,375.0	BOGUE GT11	-16,451.2	-10,860.7	MoBay_01	83.0

Name	Rating (MVA)	P input (kW)	Q input (kW)	Generating Unit	P output (kW)	Q output (kW)	To Bus	% loaded
T 07	30	24,000.0	18,000.0	BOGUE GT08	-23,940.8	-16,419.3	MoBay_01	97.9
T 08	30	24,000.0	18,000.0	BOGUE GT09	-23,940.8	-16,419.3	MoBay_01	97.9
T 09	45	30,000.0	22,500.0	BOGUE GT12	-29,953.5	-20,938.1	MoBay_02	82.2
T 10	45	30,000.0	22,500.0	BOGUE GT13	-29,953.5	-20,938.1	MoBay_02	82.2
T 11	45	30,000.0	22,500.0	BOGUE ST14	-29,953.5	-20,938.1	MoBay_02	82.2
T 71	24	8,985.3	6,739.0	HUNTSB GT4	-8,953.0	-5,738.5	HuntsBay	67.7
T 73	24	8,985.3	6,739.0	HUNTSB GT5	-8,953.0	-5,738.5	HuntsBay	67.7
T 74	45	18,899.1	14,174.3	WESTK_01	-18,858.0	-12,795.2	West Kgn	77.4
T 75	45	18,899.1	14,174.3	WESTK_02	-18,858.0	-12,795.2	West Kgn	77.4
T 64	75	47,538.8	35,654.1	Old_H_01	-47,434.8	-32,158.7	OldHarb_69	95.0
T 66	120	43,313.6	32,485.2	Old_H_03	-43,254.3	-30,494.6	Oldharbour	56.6
T 65	120	43,313.6	32,485.2	Old_H_02	-43,254.3	-30,494.6	Oldharbour	56.6
T 72	120	53,601.8	40,201.3	HUNTSB B6	-53,478.5	-36,058.6	HuntsBay	82.1
T 81	24	11,813.3	8,859.9	ROCDiesel1	-11,756.7	-7,106.2	Rockfort	89.6
T 82	24	11,813.3	8,859.9	ROCDiesel2	-11,756.7	-7,106.2	Rockfort	89.6
T 27	15	9,188.0	2,302.7	Wigon01	-9,153.6	-1,531.9	New_SpurT	80.5
T 28	15	9,188.0	2,302.7	Wigon02	-9,153.6	-1,531.9	New_SpurT	80.5
T 29	15	9,188.0	2,302.7	Wigon03	-9,153.6	-1,531.9	New_SpurT	80.5
T 30	5	2,286.9	573.1	BMR	-2,272.4	-442.7	New_SpurT	60.2
T 36	24	8,970.2	6,727.6	Jamalco	-8,946.5	-5,995.2	Parnassus	57.7

**Table.B.5: Generation Plant Data**

Name	Rated Power (MW)	Measured MW	Measured MVAR
BOGUE GT03	3.36	3.36	2.52
BOGUE GT06	15.00	15.00	11.25
BOGUE GT07	15.00	15.00	11.25
BOGUE GT08	<b>24.00</b>	24.00	18.00
BOGUE GT09	24.00	24.00	18.00
BOGUE GT11	16.50	16.50	12.38
BOGUE GT12	30.00	30.00	22.50
BOGUE GT13	30.00	30.00	22.50
BOGUE ST14	30.00	30.00	22.50
MAGGOTTY01	2.00	1.19	0.89
MAGGOTTY02	2.00	1.19	0.89
MAGGOTTY03	2.00	1.19	0.89
JAMALCO	11.00	8.97	6.73
RIOBUENO A	2.50	2.11	1.58
RIOBUENO B	1.10	0.93	0.70
RR_HYDRO	4.10	2.61	1.96
LWR	4.80	2.84	2.13
UWR	3.24	1.91	1.43
ALCAN	0.60	0.30	0.23
OLD_H_01	55.00	47.54	35.65
OLD_H_02	55.00	43.31	32.49

Name	Rated Power (MW)	Measured MW	Measured MVAR
OLD_H_03	55.00	43.31	32.49
HUNTSB B6	92.50	53.60	40.20
HUNTSB GT4	15.00	8.99	6.74
HUNTSB GT5	15.00	8.99	6.74
WESTK_01	32.75	18.90	14.17
WESTK_02	32.75	18.90	14.17
ROCDIESEL 1	20.00	11.81	8.86
ROCDIESEL 2	20.00	11.81	8.86
WIGTON 01	12.00	9.19	2.30
WIGTON 02	12.00	9.19	2.30
WIGTON 03	12.00	9.19	2.30
BMR	3.00	2.29	0.57

**Table.B.6: Transmission Line Data – Solar System Network**

Line No.	From Bus	To Bus	Voltage (kV - LL)	Length (m)	P (kW)	Q (kVAR)	Ampacity (kA)	% Loaded
01	MoBay_01	Orange Bay	69	28,000	47,143.5	39,099.6	0.725	72.2
02	Orange Bay	Paradise	69	30,670	25,132.4	22,173.7	0.360	90.1
03	Paradise	Maggoty	69	47,550	3,745.1	7,985.9	0.140	75.9
04	MoBay_01	QueenDr	69	5,440	31,004.2	21,032.0	0.305	104.5
05	MoBay_02	QueenDr	69	7,360	25,051.0	15,909.9	0.285	88.8
06	QueenDr	Rosehall	69	8,350	27,696.2	14,517.6	0.285	96.8
07	Rosehall	GrnWood	69	11,390	19,619.4	8,618.2	0.185	106.7
08	Kendal_M	Kendal_D	138	40,880	48,367.4	129,226.3	0.525	120.0
09	GrnWood	MarthaBrae	69	12,800	11,182.0	5,122.5	0.140	87.8
10	MarthaBrae	Duncans	69	9,100	2,576.2	634.1	0.140	20.8
11	Kendal_D	Kendall138	138	48,430	10,224.9	64,650.3	0.185	193.7
12	Kendall138	Ken_138_2	138	17,000	-669.8	1,578.6	0.140	7.9
13	Ken_138_2	Ken_138_3	138	36,000	321.9	-1,194.9	0.140	5.6
14	Maggoty	Old_SpurT	69	36,860	-4,351.4	3,087.2	0.140	55.3
15	Kendall_69	New_SpurT	69	10,670	-371.1	1,440.2	0.140	13.5
16	Porus	Toll Gate	69	15,600	3,765.2	1,876.2	0.140	37.9
17	Paranassus	MonyMusk	69	18,000	5,004.9	4,208.8	0.140	58.6
18	OldHarbour	Tredegar13	138	28,300	41,158.0	10,921.0	0.330	81.4
19	OldHarbour	Duhaney	138	38,100	37,115.0	43,650.8	0.640	57.3
20	Tredegar13	Duhaney	138	11,900	15,428.7	10,551.5	0.185	68.4
21	MarthaBrae	Duncans	69	9,100	2,576.2	634.1	0.140	20.8
22	Duncans	Rio Bueno	69	12,000	3,281.9	1,476.8	0.140	28.2
23	Rio Bueno	CardiffHal	69	15,540	5,723.3	3,404.2	0.140	53.3
24	CardiffHal	RoarRiver	69	20,270	5,302.3	3,355.3	0.140	53.7
25	RoarRiver	Ocho Rios	69	8,500	6,843.1	4,814.9	0.140	78.8
26	Ocho Rios	LWR SS	69	5,120	-2,595.6	-1,320.4	0.140	29.3
27	Bellevue69	Oracabessa	69	12,800	12,719.8	10,123.0	0.330	69.6
28	LWR SS	Bellevue69	69	12,800	1,108.4	1,441.5	0.140	18.2

Line No.	From Bus	To Bus	Voltage (kV - LL)	Length (m)	P (kW)	Q (kVAR)	Ampacity (kA)	% Loaded
29	Oracabessa	AnnottoBay	69	22,300	4,637.1	3,878.6	0.140	66.0
30	AnnottoBay	HighGate	69	13,400	-2,235.7	-1,132.9	0.140	31.9
31	AnnottoBay	PortAntoni	69	45,500	2,109.1	1,450.6	0.140	32.6
32	Bellevue69	BlackStone	69	13,500	-5,341.3	-3,118.0	0.140	74.6
33	Ewarton	Michelton	69	10,720	7,950.6	11,962.1	0.245	82.9
34	Ewarton	Michelton	69	2,400	-2,446.2	5,701.6	0.140	67.8
35	Michelton	Tredegar69	69	18,000	-5,146.5	3,947.9	0.140	70.8
36	Tredegar13	Bellevue13	138	40,100	5,645.8	-15,270.2	0.140	79.2
37	Kendal_D	Bellevue13	138	56,800	24,993.4	42,757.3	0.240	112.6
38	Tredegar69	Bushy Park	69	19,500	-4,913.4	2,142.3	0.140	53.3
39	Bushy Park	JABoilers	69	3,300	9,778.7	8,013.4	0.285	57.4
40	Bushy Park	RhodesPen	69	5,900	-15,220.8	-5,962.3	0.285	74.5
41	New_Twack	Duhamney69	69	8,200	3,707.1	2,867.4	0.140	46.8
42	MonyMusk	OldHarb_69	69	24,600	-4,312.2	-3,060.7	0.140	51.9
43	OldHarb_69	RhodesPen	69	7,700	19,796.7	9,180.2	0.640	42.0
44	Duhamney69	NaggosHead	69	10,900	21,217.5	19,050.9	1.815	22.8
45	Duhamney69	New Port	69	9,100	205.9	472.8	0.140	5.7
46	Duhamney69	HuntsBay	69	5,000	335.3	867.9	0.140	10.4
47	HuntsBay	GreenwishR	69	400	13,923.0	11,989.7	0.570	46.8
48	GreenwishR	Rockfort	69	7,700	2,182.0	1,820.2	0.140	29.9
49	Rockfort	UpParkCamp	69	4,700	12,110.5	6,694.4	0.285	71.9
50	UpParkCamp	WKingsHous	69	4,800	3,116.6	-475.7	0.140	35.1
51	WKingsHous	Wash_Boul	69	5,100	-7,063.0	-9,755.9	0.245	77.1
52	Wash_Boul	ThreeMiles	69	4,800	-9,162.9	-1,441.8	0.245	57.6
53	HuntDBay	ThreeMiles	69	2,500	12,103.6	3,519.1	0.280	65.7
54	Duhamney69	Wash_Boul	69	5,500	18,719.3	18,897.8	0.535	72.4
55	Rockfort	CaneRiver	69	8,200	10,648.1	7,350.2	0.285	67.5
56	CaneRiver	OldHopeRd	69	13,500	2.9	-587.1	0.140	6.9
57	WKingsHous	OldHopeRd	69	5,100	10,125.7	9,278.2	0.285	75.0
58	CaneRiver	GoodYear	69	36,700	3,797.1	2,150.8	0.140	48.7
59	GoodYear	Lyssons	69	5,600	1,588.5	811.8	0.140	24.7

**Table.B.7: Load Transformer Data – Solar System Network**

Name	Rating (MVA)	P input (kW)	Q input (kW)	From Bus	P output (kW)	Q output (kW)	To Bus	% loaded
T 02	60	40,054.4	21,200.7	MoBay_01	-40,000.0	-19,372.9	MoBay	76.6
T 12	30	48,654.2	138,864.6	Orange Bay	-48,367.4	-129,226.3	OrgBay_Loa	126.8
T 13	24	8,677.7	4,934.3	Paradise	-8,653.7	-4,191.2	Paradise_1	58.6
T 14	24	8,677.7	4,934.3	Paradise	-8,653.7	-4,191.2	Paradise_2	58.6
T 18	30	8,415.3	6,151.1	Maggoty	-8,393.8	-5,575.1	Magg_Load	59.4
T 19	15	7,823.9	5,729.3	QueensDr	-7,799.3	-5,180.3	HalfMoon	67.7
T 20	30	18,943.4	15,381.9	QueensDr	-18,898.1	-14,173.6	Ironshore	85.2
T 21	10	7,114.2	5,133.5	Rosehall	-7,086.9	-4,392.1	Rhall_Load	95.8

Name	Rating (MVA)	P input (kW)	Q input (kW)	From Bus	P output (kW)	Q output (kW)	To Bus	% loaded
T 22	10	7,018.9	2,910.6	GrnWood	-6,973.1	-2,291.9	GrnWood_L	89.7
T 25	10	4,001.0	2,120.1	Kendall_69	-3,986.5	-1,757.8	Kendall_L	68.2
T 31	24	8,378.2	6,513.7	Old_SpurT	-8,346.9	-5,544.0	Old_Spur_L	66.7
T 32	10	3,385.0	2,877.8	Porus	-3,371.0	-2,528.3	Porus_L	67.0
T 33	10	3,551.8	1,879.1	Toll Gate	-3,539.0	-1,560.5	TollGate_L	64.0
T 38	10	5,107.7	3,639.0	MarthaBrae	-5,071.0	-3,142.7	MarthaBr_L	80.4
T 39	10	5,306.8	3,072.5	Duncans	-5,288.0	-2,561.1	Duncans_L	79.8
T 42	30	8,938.9	6,003.2	Ocho Rios	-8,916.6	-5,408.7	Ocho_Load	60.1
T 45	15	1,642.4	1,389.6	PortAntoni	-1,635.1	-1,226.3	PortAn_Loa	37.2
T 46	24	3,849.2	3,318.9	AnnottoBay	-3,834.9	-2,876.2	Annotto_Lo	45.0
T 50	30	7,276.2	5,409.5	Orcaabessa	-7,257.7	-4,915.0	Oraca_Loada	54.9
T 51	15	3,742.1	2,562.5	Blackstone	-3,726.4	-2,211.1	Blkstone_L	54.5
T 52	15	2,978.0	1,977.9	HighGate	-2,965.8	-1,704.6	HGate_Load	48.1
T 54	24	6,418.6	5,554.2	Tredegar69	-6,394.2	-4,795.6	Trede_Load	58.9
T 55	24	2,598.6	1,727.9	Michelton	-2,594.8	-1,608.1	MicHel_Loa	23.4
T 56	30	9,645.3	7,911.8	JABoilers	-9,619.1	-7,214.4	JA_Boil	65.3
T 60	10	3,943.2	2,275.1	RhodesPen	-3,929.6	-1,903.2	Rhodes_Lea	68.3
T 62	30	8,728.8	7,155.0	MonyMusk	-8,705.4	-6,529.0	MonyMusk_L	61.8
T 63	24	6,418.5	5,554.1	New_Twick	-6,394.0	-4,795.5	NewTwick_L	58.9
T 67	45	10,526.4	8,572.4	NaggosHead	-10,505.7	-7,879.3	Naggos_01	55.0
T 68	45	10,526.4	8,572.4	NaggosHead	-10,505.7	-7,879.3	Naggos_02	55.0
T 69	60	16,269.1	11,958.9	New Port	-16,238.0	-10,912.0	NewPort_1	58.3
T 70	60	16,269.1	11,958.9	New Port	-16,238.0	10,912.0	NewPort_2	58.3
T 76	24	5,886.8	5,088.8	HuntsBay	-5,864.6	-4,398.4	HB_T1	56.2
T 77	10	2,610.5	1,989.0	HuntsBay	-2,592.2	-1,742.0	HB_T1_13_8	56.9
T 78	10	2,610.5	1,989.0	HuntsBay	-2,592.2	-1,742.0	HB_T2_13_8	56.9
T 79	24	5,863.2	5,068.1	GreenwichR	-5,841.1	-4,380.8	GR_T1	56.1
T 80	24	5,863.2	5,068.1	GreenwichR	-5,841.1	-4,380.8	GR_T2	56.1
T 83	24	6,219.7	4,551.0	Rockfort	-6,196.8	-3,840.4	CementCo	57.0
T 84	24	6,471.0	3,797.0	Rockfort	-6,449.3	-3,123.5	Rockfort_L	55.5
T 85	24	8,693.1	6,920.6	UpParkCamp	-8,642.6	-5,356.2	JDF Camp	84.7
T 86	10	2,602.7	1,841.9	ThreeMiles	-2,584.9	-1,602.0	3Miles	56.1
T 87	24	5,927.8	5,124.6	Constant S	-5,905.4	-4,429.0	C Spring	56.4
T 88	24	6,867.4	4,033.4	Duhaney69	-6,844.2	-3,314.8	Duhaney_T3	57.3
T 89	15	3,194.5	2,704.7	CanRiver	-3,182.2	-2,385.2	CanRiver1	52.1
T 90	15	3,194.5	2,704.7	CanRiver	-3,180.2	-2,385.2	CanRiver2	52.1
T 91	24	5,060.1	4,365.8	OldHopeRd	-5,041.2	-3,780.9	OHR_01	51.8
T 92	24	5,060.1	4,365.8	OldHopeRd	-5,041.2	-3,780.9	OHR_02	51.8
T 93	24	6,667.7	3,132.5	Wash_Boul	-6,646.2	-2,467.0	WB_T1	55.2
T 94	24	6,667.7	3,132.5	Wash_Boul	-6,646.2	-2,467.0	WB_T2	55.2
T 95	24	6,667.7	3,132.5	Wash_Boul	-6,646.2	-2,467.0	WB_T3	55.2
T 96	10	1,377.6	1,158.1	GoodYear	-1,367.8	-1,025.8	Good_Year	41.7
T 97	10	1,556.2	812.7	Lyssons	-1,546.5	-681.9	Lyssons_L	41.5



Table.B.8: Generating Unit Transformer Data – Solar System Network

Name	Rating (MVA)	P input (kW)	Q input (kW)	Generating Unit	P output (kW)	Q output (kW)	To Bus	% loaded
T 47	30	231.6	173.7	Alcan	-231.5	-173.1	Ewarton	1.7
T 15	2.5	961.2	720.9	MAGGOTY01	-948.5	-629.0	Maggoty	78.0
T 16	2.5	961.2	720.9	MAGGOTY02	-948.5	-629.0	Maggoty	78.0
T 17	2.5	961.2	720.9	MAGGOTY03	-948.5	-629.0	Maggoty	78.0
T 40	45	2,532.2	1,899.1	RioBueno	-2,531.6	-1,878.8	Rio Bueno	9.4
T 41	30	2,100.5	1,575.4	RR_Hydro	-2,099.4	-1,544.6	RoarRiver	13.7
T 43	30	2,242.2	1,681.6	LWR	-2,240.7	-1,643.2	WR Tie	15.3
T 44	30	1,505.0	1,128.8	UWR	-1,504.4	-1,111.3	WR Tie	10.3
T 01	450	4,518.2	108,880.2	Swing Bus	-4,477.3	-107,505.4	MoBay_01	24.5
T 03	5	3,360.0	2,520.0	BOGUE GT03	-3,333.0	2,277.4	MoBay_01	82.3
T 04	24	15,000.0	11,250.0	BOGUE GT06	-14,958.8	-9,972.2	MoBay_01	76.4
T 05	24	15,000.0	11,250.0	BOGUE GT07	-14,958.8	-9,972.2	MoBay_01	76.4
T 06	24	16,500.0	12,375.0	BOGUE GT11	-16,450.5	-10,840.6	MoBay_01	83.6
T 07	30	24,000.0	18,000.0	BOGUE GT08	-23,940.0	-16,397.8	MoBay_01	98.7
T 08	30	24,000.0	18,000.0	BOGUE GT09	-23,940.0	-16,397.8	MoBay_01	98.7
T 09	45	30,000.0	22,500.0	BOGUE GT12	-29,952.9	-20,916.6	MoBay_02	83.0
T 10	45	30,000.0	22,500.0	BOGUE GT13	-29,952.9	-20,916.6	MoBay_02	83.0
T 11	45	30,000.0	22,500.0	BOGUE ST14	-29,952.9	-20,916.6	MoBay_02	83.0
T 71	24	6,972.0	5,229.0	HUNTSB GT4	-6,946.9	-4,452.7	HuntsBay	59.8
T 73	24	6,972.0	5,229.0	HUNTSB GT5	-6,946.9	-4,452.7	HuntsBay	59.8
T 74	45	14,664.4	10,998.3	WESTK_01	-14,632.6	-9,928.2	West Kgn	68.4
T 75	45	14,664.4	10,998.3	WESTK_02	14,632.6	9,928.2	West Kgn	68.4
T 64	75	27,858.9	20,894.2	Old_H_01	-27,809.0	-19,218.2	OldHarb_69	66.0
T 66	120	42,475.2	0.0	SolarFarm1	-42,418.4	1,910.6	Oldharbour	52.6
T 65	120	42,475.2	0.0	SolarFarm2	-42,418.4	1,910.6	Oldharbour	52.6
T 72	120	41,591.4	31,193.5	HUNTSB B6	-41,495.7	-27,979.0	HuntsBay	72.6
T 81	24	9,176.8	6,882.6	ROCDiesel1	-9,132.8	-5,520.2	Rockfort	79.2
T 82	24	9,176.8	6,882.6	ROCDiesel2	-9,132.8	-5,520.2	Rockfort	79.3
T 27	15	6,897.0	1,728.6	Wigon01	-6,871.2	-1,150.0	New_SpurT	70.0
T 28	15	6,897.0	1,728.6	Wigon02	-6,871.2	-1,150.0	New_SpurT	70.0
T 29	15	6,897.0	1,728.6	Wigon03	-6,871.2	-1,150.0	New_SpurT	70.0
T 30	5	1,716.7	430.2	BMR	-1,705.8	-332.3	New_SpurT	52.4
T 36	24	6,658.5	4,993.8	Jamalco	-6,640.9	-4,450.2	Parnassus	49.9

*Table.B.9: Generation Plant Data – Solar System Network*

<b>Name</b>	<b>Rated Power (MW)</b>	<b>Measured MW</b>	<b>Measured MVAR</b>
BOGUE GT03	3.36	3.36	2.52
BOGUE GT06	15.00	15.00	11.25
BOGUE GT07	15.00	15.00	11.25
BOGUE GT08	24.00	24.00	18.00
BOGUE GT09	24.00	24.00	18.00
BOGUE GT11	16.50	16.50	12.38
BOGUE GT12	30.00	30.00	22.50
BOGUE GT13	30.00	30.00	22.50
BOGUE ST14	30.00	30.00	22.50
MAGGOTTY01	2.00	0.96	0.72
MAGGOTTY02	2.00	0.96	0.72
MAGGOTTY03	2.00	0.96	0.72
JAMALCO	11.00	6.66	4.99
RIOBUENO A	2.50	1.76	1.32
RIOBUENO B	1.10	0.77	0.58
RR_HYDRO	4.10	2.10	1.58
LWR	4.80	2.24	1.68
UWR	3.24	1.51	1.13
ALCAN	0.60	0.23	0.17
OLD_H_01	55.00	27.86	20.89
Solar plant 1	60.00	42.47	0.00
Solar plant 2	60.00	42.47	0.00
HUNTSB B6	92.50	41.59	31.19
HUNTSB GT4	15.00	6.97	5.23
HUNTSB GT5	15.00	6.97	5.23
WESTK_01	32.75	14.66	11.00
WESTK_02	32.75	14.66	11.00
ROCDIESEL 1	20.00	9.18	6.88
ROCDIESEL 2	20.00	9.18	6.88
WIGTON 01	12.00	6.90	1.73
WIGTON 02	12.00	6.90	1.73
WIGTON 03	12.00	6.90	1.73
BMR	3.00	1.72	0.43

## Appendix C      Short-Circuit Fault Data

*Table C.1: Generator Data for 3-Phase Bolted Fault*

Fault Cycle	Name	MVA Rating	Voltage Rating (kV)	P (MW)	Q (MVAR)
SWING BUS	UTILITY 01	4000	13.8		
1/2	GEN 01		11.8	-0.024	-0.018
	GEN 02		11.8	-0.015	-0.011
	GEN 03		11.8	-0.024	-0.018
	WINDFARM 01		20.0	0.018	0.005
1 ½ - 4	GEN 01		11.8	-0.024	-0.018
	GEN 02		11.8	-0.015	-0.011
	GEN 03		11.8	-0.024	-0.018
	WINDFARM 01		20.0	0.018	0.005
8	GEN 01		11.8	-6.497	-4.123
	GEN 02		11.8	-3.238	-2.173
	GEN 03		11.8	-6.937	-4.428
	WINDFARM 01		20.0	-6.814	-6.689
30	GEN 01		11.8	-1.042	-0.637
	GEN 02		11.8	-0.636	-0.393
	GEN 03		11.8	-1.125	-0.688
	WINDFARM 01		20.0	-0.349	-0.358

Table C.2: Transformer Data for 3-Phase Bolted Fault

Fault Cycle	Name	MVA Rating	Voltage Rating (kV)	INPUT		OUTPUT	
				P (MW)	Q (MVAR)	P (MW)	Q (MVAR)
1/2	T 01	60	13.8 / 69	48.211	40.424	-48.107	-36.913
	T 02	45	11.8 / 69	0.024	0.018	-0.024	-0.018
	T 03	60	69 / 24	0.000	0.000	0.000	0.000
	T 04	30	69 / 24	0.000	0.000	0.000	0.000
	T 05	24	11.8 / 69	0.015	0.011	-0.015	-0.011
	T 06	45	11.8 / 69	0.024	0.018	-0.024	-0.018
	T 07	24	69 / 24	0.000	0.000	0.000	0.000
	T 08	24	69 / 24	0.000	0.000	0.000	0.000
	T 09	30	69 / 24	0.285	7.608	0.000	0.000
	T 10	150	20 / 69	-0.018	-0.005	0.018	0.005
1 ½ - 4	T 01	60	13.8 / 69	48.211	40.425	48.107	36.913
	T 02	45	11.8 / 69	0.024	0.018	-0.024	-0.018
	T 03	60	69 / 24	0.000	0.000	0.000	0.000
	T 04	30	69 / 24	0.000	0.000	0.000	0.000
	T 05	24	11.8 / 69	0.015	0.011	-0.015	-0.011
	T 06	45	11.8 / 69	0.024	0.018	-0.024	-0.018
	T 07	24	69 / 24	0.000	0.000	0.000	0.000
	T 08	24	69 / 24	0.000	0.000	0.000	0.000
	T 09	30	69 / 24	0.285	7.608	0.000	0.000
	T 10	150	20 / 69	-0.018	-0.005	0.018	0.005
8	T 01	60	13.8 / 69	28.218	21.755	-28.185	-20.640
	T 02	45	11.8 / 69	6.497	4.123	-6.495	-4.051
	T 03	60	69 / 24	0.000	0.000	0.000	0.000
	T 04	30	69 / 24	0.000	0.000	0.000	0.000
	T 05	24	11.8 / 69	3.238	2.173	3.236	2.112
	T 06	45	11.8 / 69	6.937	4.428	-6.935	-4.347
	T 07	24	69 / 24	0.000	0.000	0.000	0.000
	T 08	24	69 / 24	0.000	0.000	0.000	0.000
	T 09	30	69 / 24	0.311	8.309	0.000	0.000
	T 10	150	20 / 69	6.814	6.689	-6.813	-6.646
30	T 01	60	13.8 / 69	45.428	38.154	-45.335	-35.036
	T 02	45	11.8 / 69	1.042	0.637	-1.042	-0.635
	T 03	60	69 / 24	0.000	0.000	0.000	0.000
	T 04	30	69 / 24	0.000	0.000	0.000	0.000
	T 05	24	11.8 / 69	0.636	0.393	-0.636	-0.390
	T 06	45	11.8 / 69	1.125	0.688	-1.125	-0.685
	T 07	24	69 / 24	0.000	0.000	0.000	0.000
	T 08	24	69 / 24	0.000	0.000	0.000	0.000
	T 09	30	69 / 24	0.287	7.669	0.000	0.000
	T 10	150	20 / 69	0.349	0.358	-0.349	-0.358

*Table C.3: Generator Data for 3-Phase Bolted Fault with Solar Farm*

Fault Cycle	Name	MVA Rating	Voltage Rating (kV)	P (MW)	Q (MVAR)
SWING BUS	UTILITY 01	4000	13.8		
1/2	GEN 01		11.8	-8.343	-6.592
	GEN 02		11.8	-3.873	-3.243
	GEN 03		11.8	-8.343	-6.592
	SOLARFARM		11.8	0.000	0.000
1 1/2 - 4	GEN 01		11.8	-8.343	-6.592
	GEN 02		11.8	-3.873	-3.243
	GEN 03		11.8	-8.343	-6.592
	SOLARFARM		11.8	0.000	0.000
8	GEN 01		11.8	-6.846	-5.269
	GEN 02		11.8	-3.403	-2.761
	GEN 03		11.8	-7.308	-5.656
	SOLARFARM		11.8	0.000	0.000
30	GEN 01		11.8	0.989	-0.678
	GEN 02		11.8	-0.604	-0.417
	GEN 03		11.8	-1.067	-0.732
	SOLARFARM		11.8	0.000	0.000

Table C.4: Transformer Data for 3-Phase Bolted Fault with Solar Farm

Fault Cycle	Name	MVA Rating	Voltage Rating (kV)	INPUT		OUTPUT	
				P (MW)	Q (MVAR)	P (MW)	Q (MVAR)
1/2	T 01	60	13.8 / 69	26.736	24.786	-26.701	-23.617
	T 02	45	11.8 / 69	8.343	6.592	-8.339	-6.455
	T 03	60	69 / 24	0.000	0.000	0.000	0.000
	T 04	30	69 / 24	0.000	0.000	0.000	0.000
	T 05	24	11.8 / 69	3.873	3.243	-3.870	-3.142
	T 06	45	11.8 / 69	8.343	6.592	-8.339	-6.455
	T 07	24	69 / 24	0.000	0.000	0.000	0.000
	T 08	24	69 / 24	0.000	0.000	0.000	0.000
	T 09	30	69 / 24	0.295	7.883	0.000	0.000
	T 10	30	20 / 69	2.519	1.695	-2.518	1.719
1 ½ - 4	T 01	60	13.8 / 69	26.736	24.786	-26.701	-23.617
	T 02	45	11.8 / 69	8.343	6.592	-8.339	-6.455
	T 03	60	69 / 24	0.000	0.000	0.000	0.000
	T 04	30	69 / 24	0.000	0.000	0.000	0.000
	T 05	24	11.8 / 69	3.873	3.243	-3.870	-3.142
	T 06	45	11.8 / 69	8.343	6.592	-8.339	-6.455
	T 07	24	69 / 24	0.000	0.000	0.000	0.000
	T 08	24	69 / 24	0.000	0.000	0.000	0.000
	T 09	30	69 / 24	0.295	7.883	0.000	0.000
	T 10	150	20 / 69	2.519	-1.695	-2.518	1.719
8	T 01	60	13.8 / 69	29.377	27.468	-29.335	-26.044
	T 02	45	11.8 / 69	6.846	5.269	-6.844	-5.178
	T 03	60	69 / 24	0.000	0.000	0.000	0.000
	T 04	30	69 / 24	0.000	0.000	0.000	0.000
	T 05	24	11.8 / 69	3.403	2.761	-3.401	-2.684
	T 06	45	11.8 / 69	7.308	5.656	-7.305	-5.552
	T 07	24	69 / 24	0.000	0.000	0.000	0.000
	T 08	24	69 / 24	0.000	0.000	0.000	0.000
	T 09	30	69 / 24	0.293	7.831	0.000	0.000
	T 10	150	20 / 69	2.558	-1.734	-2.557	1.759
30	T 01	60	13.8 / 69	42.659	39.714	-42.569	-36.702
	T 02	45	11.8 / 69	0.989	0.678	0.989	-0.676
	T 03	60	69 / 24	0.000	0.000	0.000	0.000
	T 04	30	69 / 24	0.000	0.000	0.000	0.000
	T 05	24	11.8 / 69	0.604	0.417	-0.604	-0.415
	T 06	45	11.8 / 69	1.067	0.732	-1.067	-0.730
	T 07	24	69 / 24	0.000	0.000	0.000	0.000
	T 08	24	69 / 24	0.000	0.000	0.000	0.000
	T 09	30	69 / 24	0.285	7.597	0.000	0.000
	T 10	150	20 / 69	2.728	-1.937	-2.727	1.967

*Table C.5: Generator Data for Double-Line-to-Ground Fault*

Fault Cycle	Name	MVA Rating	Voltage Rating (kV)	P (MW)	Q (MVAR)
SWING BUS   1/2	UTILITY 01	4000	13.8		
	GEN 01		11.8	-0.024	-0.018
	GEN 02		11.8	-0.015	-0.011
	GEN 03		11.8	-0.024	-0.018
	WINDFARM 01		20.0	0.018	0.005
1 ½ - 4	GEN 01		11.8	-0.024	-0.018
	GEN 02		11.8	-0.015	-0.011
	GEN 03		11.8	-0.024	-0.018
	WINDFARM 01		20.0	0.018	0.005
8	GEN 01		11.8	-5.672	-4.266
	GEN 02		11.8	-2.233	-2.173
	GEN 03		11.8	-6.055	-4.579
	WINDFARM 01		20.0	-5.708	-6.688
30	GEN 01		11.8	-0.916	-0.661
	GEN 02		11.8	-0.559	-0.407
	GEN 03		11.8	-0.989	-0.713
	WINDFARM 01		20.0	-0.290	-0.359

*Table C.6: Transformer Data for Double-Line-to-Ground Fault*

Fault Cycle	Name	MVA Rating	Voltage Rating (kV)	INPUT		OUTPUT	
				P (MW)	Q (MVAR)	P (MW)	Q (MVAR)
1/2	T 01	60	13.8 / 69	41.635	40.000	-41.545	-37.362
	T 02	45	11.8 / 69	0.024	0.018	-0.024	-0.018
	T 03	60	69 / 24	0.000	0.000	0.000	0.000
	T 04	30	69 / 24	0.000	0.000	0.000	0.000
	T 05	24	11.8 / 69	0.015	0.011	-0.015	-0.011
	T 06	45	11.8 / 69	0.024	0.018	-0.024	-0.018
	T 07	24	69 / 24	0.000	0.000	0.000	0.000
	T 08	24	69 / 24	0.000	0.000	0.000	0.000
	T 09	30	69 / 24	0.463	12.351	0.000	0.000
	T 10	150	20 / 69	-0.018	-0.005	0.018	0.005
1 ½ - 4	T 01	60	13.8 / 69	41.635	40.372	-41.546	-37.362
	T 02	45	11.8 / 69	0.024	0.018	-0.024	-0.018
	T 03	60	69 / 24	0.000	0.000	0.000	0.000
	T 04	30	69 / 24	0.000	0.000	0.000	0.000
	T 05	24	11.8 / 69	0.015	0.011	-0.015	-0.011
	T 06	45	11.8 / 69	0.024	0.018	-0.024	-0.018
	T 07	24	69 / 24	0.000	0.000	0.000	0.000
	T 08	24	69 / 24	0.000	0.000	0.000	0.000
	T 09	30	69 / 24	0.463	12.351	0.000	0.000
	T 10	150	20 / 69	-0.018	-0.005	0.018	0.005
8	T 01	60	13.8 / 69	24.320	21.938	-24.292	-20.986
	T 02	45	11.8 / 69	5.672	4.266	-5.670	-4.204
	T 03	60	69 / 24	0.000	0.000	0.000	0.000
	T 04	30	69 / 24	0.000	0.000	0.000	0.000
	T 05	24	11.8 / 69	2.821	2.233	-2.819	-2.181
	T 06	45	11.8 / 69	6.055	4.579	-6.053	-4.509
	T 07	24	69 / 24	0.000	0.000	0.000	0.000
	T 08	24	69 / 24	0.000	0.000	0.000	0.000
	T 09	30	69 / 24	0.503	13.418	0.000	0.000
	T 10	150	20 / 69	5.708	6.688	-5.707	-6.651
30	T 01	60	13.8 / 69	39.202	38.110	-39.122	-35.438
	T 02	45	11.8 / 69	0.916	0.661	-0.916	-0.659
	T 03	60	69 / 24	0.000	0.000	0.000	0.000
	T 04	30	69 / 24	0.000	0.000	0.000	0.000
	T 05	24	11.8 / 69	0.559	0.407	0.559	-0.405
	T 06	45	11.8 / 69	0.989	0.713	-0.988	-0.711
	T 07	24	69 / 24	0.000	0.000	0.000	0.000
	T 08	24	69 / 24	0.000	0.000	0.000	0.000
	T 09	30	69 / 24	0.466	12.447	0.000	0.000
	T 10	150	20 / 69	0.290	0.359	-0.290	-0.359



*Table C.7: Generator Data for Double-Line-to-Ground Fault with Solar Farm*

Fault Cycle	Name	MVA Rating	Voltage Rating (kV)	P (MW)	Q (MVAR)
SWING BUS  1/2	UTILITY 01	4000	13.8		
	GEN 01		11.8	-7.222	-6.668
	GEN 02		11.8	-3.343	-3.262
	GEN 03		11.8	-7.222	-6.668
	SOLARFARM		11.8	0.000	0.000
1 ½ - 4	GEN 01		11.8	-7.222	-6.668
	GEN 02		11.8	-3.343	-3.262
	GEN 03		11.8	-7.222	-6.668
	SOLARFARM		11.8	0.000	0.000
8	GEN 01		11.8	-5.936	-5.344
	GEN 02		11.8	-2.943	-2.785
	GEN 03		11.8	-6.334	-5.734
	SOLARFARM		11.8	0.000	0.000
30	GEN 01		11.8	-0.866	-0.696
	GEN 02		11.8	-0.528	-0.428
	GEN 03		11.8	-0.934	-0.751
	SOLARFARM		11.8	0.000	0.000

*Table C.8: Transformer Data for Double-Line-to-Ground Fault with Solar Farm*

Fault Cycle	Name	MVA Rating	Voltage Rating (kV)	INPUT		OUTPUT	
				P (MW)	Q (MVAR)	P (MW)	Q (MVAR)
1/2	T 01	60	13.8 / 69	22.849	24.619	-22.819	-23.618
	T 02	45	11.8 / 69	7.222	6.668	-7.218	-6.551
	T 03	60	69 / 24	0.000	0.000	0.000	0.000
	T 04	30	69 / 24	0.000	0.000	0.000	0.000
	T 05	24	11.8 / 69	3.343	3.262	-3.340	-3.174
	T 06	45	11.8 / 69	7.222	6.668	-7.218	-6.551
	T 07	24	69 / 24	0.000	0.000	0.000	0.000
	T 08	24	69 / 24	0.000	0.000	0.000	0.000
	T 09	30	69 / 24	0.480	12.822	0.000	0.000
	T 10	30	20 / 69	2.456	-1.356	-2.455	1.377
1 ½ - 4	T 01	60	13.8 / 69	22.849	24.619	-22.819	-23.618
	T 02	45	11.8 / 69	7.222	6.668	-7.218	-6.551
	T 03	60	69 / 24	0.000	0.000	0.000	0.000
	T 04	30	69 / 24	0.000	0.000	0.000	0.000
	T 05	24	11.8 / 69	3.343	3.262	-3.340	-3.174
	T 06	45	11.8 / 69	7.222	6.668	-7.218	-6.551
	T 07	24	69 / 24	0.000	0.000	0.000	0.000
	T 08	24	69 / 24	0.000	0.000	0.000	0.000
	T 09	30	69 / 24	0.480	12.822	0.000	0.000
	T 10	150	20 / 69	2.456	-1.356	-2.455	1.377
8	T 01	60	13.8 / 69	25.108	27.269	-25.072	-26.048
	T 02	45	11.8 / 69	5.936	5.344	-5.933	-5.266
	T 03	60	69 / 24	0.000	0.000	0.000	0.000
	T 04	30	69 / 24	0.000	0.000	0.000	0.000
	T 05	24	11.8 / 69	2.943	2.785	-2.941	-2.719
	T 06	45	11.8 / 69	6.334	5.734	-6.332	-5.644
	T 07	24	69 / 24	0.000	0.000	0.000	0.000
	T 08	24	69 / 24	0.000	0.000	0.000	0.000
	T 09	30	69 / 24	0.477	12.739	0.000	0.000
	T 10	150	20 / 69	2.496	-1.389	-2.495	1.411
30	T 01	60	13.8 / 69	36.579	39.430	-36.502	-36.843
	T 02	45	11.8 / 69	0.866	0.696	-0.866	-0.694
	T 03	60	69 / 24	0.000	0.000	0.000	0.000
	T 04	30	69 / 24	0.000	0.000	0.000	0.000
	T 05	24	11.8 / 69	0.528	0.428	-0.528	-0.426
	T 06	45	11.8 / 69	0.934	0.751	-0.934	-0.750
	T 07	24	69 / 24	0.000	0.000	0.000	0.000
	T 08	24	69 / 24	0.000	0.000	0.000	0.000
	T 09	30	69 / 24	0.463	12.361	0.000	0.000
	T 10	150	20 / 69	2.673	-1.563	-2.672	1.588

**Table C.9: Generator Data for Line-to-Line Fault**

Fault Cycle	Name	MVA Rating	Voltage Rating (kV)	P (MW)	Q (MVAR)
SWING BUS  1/2	UTILITY 01	4000	13.8		
	GEN 01		11.8	-0.023	-0.017
	GEN 02		11.8	-0.014	-0.011
	GEN 03		11.8	-0.023	-0.017
	WINDFARM		20.0	0.019	0.005
1 1/2 - 4	GEN 01		11.8	-0.023	-0.017
	GEN 02		11.8	-0.014	-0.011
	GEN 03		11.8	-0.023	-0.017
	WINDFARM		20.0	0.019	0.005
8	GEN 01		11.8	-3.195	-2.112
	GEN 02		11.8	-1.592	-1.112
	GEN 03		11.8	-3.410	2.268
	WINDFARM		20.0	-3.577	-3.209
30	GEN 01		11.8	-0.528	-0.330
	GEN 02		11.8	-0.323	-0.204
	GEN 03		11.8	-0.569	-0.356
	WINDFARM		20.0	-0.176	-0.169

Table C.10: Transformer Data for Line-to-Line Fault

Fault Cycle	Name	MVA Rating	Voltage Rating (kV)	INPUT		OUTPUT	
				P (MW)	Q (MVAR)	P (MW)	Q (MVAR)
1/2	T 01	60	13.8 / 69	23.653	19.796	-23.602	-18.072
	T 02	45	11.8 / 69	0.023	0.017	-0.023	-0.017
	T 03	60	69 / 24	0.000	0.000	0.000	0.000
	T 04	30	69 / 24	0.000	0.000	0.000	0.000
	T 05	24	11.8 / 69	0.014	0.011	-0.014	-0.011
	T 06	45	11.8 / 69	0.023	0.017	-0.023	-0.017
	T 07	24	69 / 24	0.000	0.000	0.000	0.000
	T 08	24	69 / 24	0.000	0.000	0.000	0.000
	T 09	30	69 / 24	0.140	3.737	0.000	0.000
	T 10	150	20 / 69	-0.019	-0.005	0.019	0.005
1 ½ - 4	T 01	60	13.8 / 69	23.653	19.796	-23.602	-18.072
	T 02	45	11.8 / 69	0.023	0.017	-0.023	-0.017
	T 03	60	69 / 24	0.000	0.000	0.000	0.000
	T 04	30	69 / 24	0.000	0.000	0.000	0.000
	T 05	24	11.8 / 69	0.014	0.011	-0.014	-0.011
	T 06	45	11.8 / 69	0.023	0.017	-0.023	-0.017
	T 07	24	69 / 24	0.000	0.000	0.000	0.000
	T 08	24	69 / 24	0.000	0.000	0.000	0.000
	T 09	30	69 / 24	0.140	3.737	0.000	0.000
	T 10	150	20 / 69	-0.019	-0.005	0.019	0.005
8	T 01	60	13.8 / 69	13.716	10.538	-13.700	-9.995
	T 02	45	11.8 / 69	3.195	2.112	-3.194	-2.077
	T 03	60	69 / 24	0.000	0.000	0.000	0.000
	T 04	30	69 / 24	0.000	0.000	0.000	0.000
	T 05	24	11.8 / 69	1.592	1.112	-1.591	-1.083
	T 06	45	11.8 / 69	3.410	2.268	-3.409	-2.228
	T 07	24	69 / 24	0.000	0.000	0.000	0.000
	T 08	24	69 / 24	0.000	0.000	0.000	0.000
	T 09	30	69 / 24	0.154	4.099	0.000	0.000
	T 10	150	20 / 69	3.577	3.209	-3.576	-3.186
30	T 01	60	13.8 / 69	22.274	18.671	-22.229	-17.141
	T 02	45	11.8 / 69	0.528	0.330	-0.528	-0.329
	T 03	60	69 / 24	0.000	0.000	0.000	0.000
	T 04	30	69 / 24	0.000	0.000	0.000	0.000
	T 05	24	11.8 / 69	0.323	0.204	0.323	-0.203
	T 06	45	11.8 / 69	0.569	0.356	-0.569	-0.355
	T 07	24	69 / 24	0.000	0.000	0.000	0.000
	T 08	24	69 / 24	0.000	0.000	0.000	0.000
	T 09	30	69 / 24	0.141	3.770	0.000	0.000
	T 10	150	20 / 69	0.176	0.169	-0.176	-0.169

**Table C.11: Generator Data for Line-to-Line Fault with Solar Farm**

<b>Fault Cycle</b>	<b>Name</b>	<b>MVA Rating</b>	<b>Voltage Rating (kV)</b>	<b>P (MW)</b>	<b>Q (MVAR)</b>
SWING BUS  1/2	UTILITY 01	4000	13.8		
	GEN 01		11.8	-4.129	-3.342
	GEN 02		11.8	-1.916	-1.644
	GEN 03		11.8	-4.129	-3.342
	SOLARFARM		11.8	0.000	0.000
1 1/2 - 4	GEN 01		11.8	-4.129	-3.342
	GEN 02		11.8	-1.916	-1.644
	GEN 03		11.8	-4.129	-3.342
	SOLARFARM		11.8	0.000	0.000
8	GEN 01		11.8	-3.393	-2.674
	GEN 02		11.8	-1.686	-1.401
	GEN 03		11.8	-3.621	-2.870
	SOLARFARM		11.8	0.000	0.000
30	GEN 01		11.8	-0.503	-0.352
	GEN 02		11.8	-0.307	-0.217
	GEN 03		11.8	-0.541	-0.379
	SOLARFARM		11.8	0.000	0.000

*Table C.12: Transformer Data for Line-to-Line Fault with Solar Farm*

Fault Cycle	Name	MVA Rating	Voltage Rating (kV)	INPUT		OUTPUT	
				P (MW)	Q (MVAR)	P (MW)	Q (MVAR)
1/2	T 01	60	13.8 / 69	13.117	12.008	-13.100	-11.436
	T 02	45	11.8 / 69	4.129	3.342	-4.127	-3.275
	T 03	60	69 / 24	0.000	0.000	0.000	0.000
	T 04	30	69 / 24	0.000	0.000	0.000	0.000
	T 05	24	11.8 / 69	1.916	1.644	-1.915	-1.594
	T 06	45	11.8 / 69	4.129	3.342	-4.127	-3.275
	T 07	24	69 / 24	0.000	0.000	0.000	0.000
	T 08	24	69 / 24	0.000	0.000	0.000	0.000
	T 09	30	69 / 24	0.145	3.877	0.000	0.000
	T 10	30	20 / 69	1.201	-0.932	-1.201	0.944
1 1/2 - 4	T 01	60	13.8 / 69	13.117	12.008	-13.100	-11.436
	T 02	45	11.8 / 69	4.129	3.342	-4.127	-3.275
	T 03	60	69 / 24	0.000	0.000	0.000	0.000
	T 04	30	69 / 24	0.000	0.000	0.000	0.000
	T 05	24	11.8 / 69	1.916	1.644	-1.915	-1.594
	T 06	45	11.8 / 69	4.129	3.342	-4.127	-3.275
	T 07	24	69 / 24	0.000	0.000	0.000	0.000
	T 08	24	69 / 24	0.000	0.000	0.000	0.000
	T 09	30	69 / 24	0.145	3.877	0.000	0.000
	T 10	150	20 / 69	1.201	-0.932	-1.201	0.944
8	T 01	60	13.8 / 69	14.413	13.360	-14.392	-12.662
	T 02	45	11.8 / 69	3.393	2.674	-3.392	-2.629
	T 03	60	69 / 24	0.000	0.000	0.000	0.000
	T 04	30	69 / 24	0.000	0.000	0.000	0.000
	T 05	24	11.8 / 69	1.686	1.401	-1.685	-1.363
	T 06	45	11.8 / 69	3.621	2.870	-3.620	-2.819
	T 07	24	69 / 24	0.000	0.000	0.000	0.000
	T 08	24	69 / 24	0.000	0.000	0.000	0.000
	T 09	30	69 / 24	0.144	3.851	0.000	0.000
	T 10	150	20 / 69	1.221	-0.951	-1.221	-0.963
30	T 01	60	13.8 / 69	20.939	19.508	-20.895	-18.031
	T 02	45	11.8 / 69	0.503	0.352	-0.503	-0.351
	T 03	60	69 / 24	0.000	0.000	0.000	0.000
	T 04	30	69 / 24	0.000	0.000	0.000	0.000
	T 05	24	11.8 / 69	0.307	0.217	-0.307	-0.216
	T 06	45	11.8 / 69	0.541	0.379	-0.514	-0.378
	T 07	24	69 / 24	0.000	0.000	0.000	0.000
	T 08	24	69 / 24	0.000	0.000	0.000	0.000
	T 09	30	69 / 24	0.140	3.732	0.000	0.000
	T 10	150	20 / 69	1.307	-1.049	-1.306	1.065

**Table C.13: Generator Data for Single-Line-to-Ground Fault**

<b>Fault Cycle</b>	<b>Name</b>	<b>MVA Rating</b>	<b>Voltage Rating (kV)</b>	<b>P (MW)</b>	<b>Q (MVAR)</b>
SWING BUS	UTILITY 01	4000	13.8		
	GEN 01		11.8	-0.024	-0.018
	GEN 02		11.8	-0.015	-0.011
	GEN 03		11.8	-0.024	-0.018
	WINDFARM		20.0	0.018	0.005
1 1/2 - 4	GEN 01		11.8	-0.024	-0.018
	GEN 02		11.8	-0.015	-0.011
	GEN 03		11.8	-0.024	-0.018
	WINDFARM		20.0	0.018	0.005
8	GEN 01		11.8	-2.930	-2.142
	GEN 02		11.8	-1.458	-1.123
	GEN 03		11.8	-3.127	-2.299
	WINDFARM		20.0	-3.172	-3.475
30	GEN 01		11.8	-0.487	-0.341
	GEN 02		11.8	-0.297	-0.210
	GEN 03		11.8	-0.524	-0.367
	WINDFARM		20.0	-0.152	-0.184

Table C.14: Transformer Data for Single-Line-to-Ground Fault

Fault Cycle	Name	MVA Rating	Voltage Rating (kV)	INPUT		OUTPUT	
				P (MW)	Q (MVAR)	P (MW)	Q (MVAR)
1/2	T 01	60	13.8 / 69	21.478	19.914	-21.431	-18.354
	T 02	45	11.8 / 69	0.024	0.018	-0.024	-0.018
	T 03	60	69 / 24	0.000	0.000	0.000	0.000
	T 04	30	69 / 24	0.000	0.000	0.000	0.000
	T 05	24	11.8 / 69	0.015	0.011	-0.015	-0.011
	T 06	45	11.8 / 69	0.024	0.018	-0.024	-0.018
	T 07	24	69 / 24	0.000	0.000	0.000	0.000
	T 08	24	69 / 24	0.000	0.000	0.000	0.000
	T 09	30	69 / 24	0.190	5.077	0.000	0.000
	T 10	150	20 / 69	-0.018	-0.005	0.018	0.005
1 1/2 - 4	T 01	60	13.8 / 69	21.478	19.914	-21.431	-18.354
	T 02	45	11.8 / 69	0.024	0.018	-0.024	-0.018
	T 03	60	69 / 24	0.000	0.000	0.000	0.000
	T 04	30	69 / 24	0.000	0.000	0.000	0.000
	T 05	24	11.8 / 69	0.015	0.011	-0.015	-0.011
	T 06	45	11.8 / 69	0.024	0.018	-0.024	-0.018
	T 07	24	69 / 24	0.000	0.000	0.000	0.000
	T 08	24	69 / 24	0.000	0.000	0.000	0.000
	T 09	30	69 / 24	0.190	5.077	0.000	0.000
	T 10	150	20 / 69	-0.018	-0.005	0.018	0.005
8	T 01	60	13.8 / 69	12.476	10.518	-12.462	-10.032
	T 02	45	11.8 / 69	2.930	2.142	-2.929	-2.111
	T 03	60	69 / 24	0.000	0.000	0.000	0.000
	T 04	30	69 / 24	0.000	0.000	0.000	0.000
	T 05	24	11.8 / 69	1.458	1.123	-1.457	-1.097
	T 06	45	11.8 / 69	3.127	2.299	-3.126	-2.263
	T 07	24	69 / 24	0.000	0.000	0.000	0.000
	T 08	24	69 / 24	0.000	0.000	0.000	0.000
	T 09	30	69 / 24	0.209	5.574	0.000	0.000
	T 10	150	20 / 69	3.172	3.475	-3.171	-3.454
30	T 01	60	13.8 / 69	20.221	18.773	-20.180	-17.390
	T 02	45	11.8 / 69	0.487	0.341	-0.487	-0.340
	T 03	60	69 / 24	0.000	0.000	0.000	0.000
	T 04	30	69 / 24	0.000	0.000	0.000	0.000
	T 05	24	11.8 / 69	0.297	0.210	-0.297	-0.209
	T 06	45	11.8 / 69	0.524	0.367	-0.524	-0.366
	T 07	24	69 / 24	0.000	0.000	0.000	0.000
	T 08	24	69 / 24	0.000	0.000	0.000	0.000
	T 09	30	69 / 24	0.192	5.122	0.000	0.000
	T 10	150	20 / 69	0.152	0.184	-0.152	-0.184



**Table C.15: Generator Data for Single-Line-to-Ground Fault with Solar Farm**

<b>Fault Cycle</b>	<b>Name</b>	<b>MVA Rating</b>	<b>Voltage Rating (kV)</b>	<b>P (MW)</b>	<b>Q (MVAR)</b>
SWING BUS  1/2	UTILITY 01	4000	13.8		
	GEN 01		11.8	-3.742	-3.384
	GEN 02		11.8	-1.733	-1.658
	GEN 03		11.8	-3.742	-3.384
	SOLARFARM		11.8	0.000	0.000
1 1/2 - 4	GEN 01		11.8	-3.742	-3.384
	GEN 02		11.8	-1.733	-1.658
	GEN 03		11.8	-3.742	-3.384
	SOLARFARM		11.8	0.000	0.000
8	GEN 01		11.8	-3.079	-2.712
	GEN 02		11.8	-1.528	-1.416
	GEN 03		11.8	-3.285	-2.910
	SOLARFARM		11.8	0.000	0.000
30	GEN 01		11.8	-0.460	-0.360
	GEN 02		11.8	-0.281	-0.221
	GEN 03		11.8	-0.495	-0.388
	SOLARFARM		11.8	0.000	0.000

Table C.16: Transformer Data for Single-Line-to-Ground Fault with Solar Farm

Fault Cycle	Name	MVA Rating	Voltage Rating (kV)	INPUT		OUTPUT	
				P (MW)	Q (MVAR)	P (MW)	Q (MVAR)
1/2	T 01	60	13.8 / 69	11.777	12.004	-11.762	-11.487
	T 02	45	11.8 / 69	3.742	3.384	-3.740	-3.322
	T 03	60	69 / 24	0.000	0.000	0.000	0.000
	T 04	30	69 / 24	0.000	0.000	0.000	0.000
	T 05	24	11.8 / 69	1.733	1.658	-1.732	-1.612
	T 06	45	11.8 / 69	3.742	3.384	-3.740	-3.322
	T 07	24	69 / 24	0.000	0.000	0.000	0.000
	T 08	24	69 / 24	0.000	0.000	0.000	0.000
	T 09	30	69 / 24	0.197	5.272	0.000	0.000
	T 10	30	20 / 69	1.271	-0.773	-1.271	0.785
1 1/2 - 4	T 01	60	13.8 / 69	11.777	12.004	-11.762	-11.487
	T 02	45	11.8 / 69	3.742	3.384	-3.740	-3.322
	T 03	60	69 / 24	0.000	0.000	0.000	0.000
	T 04	30	69 / 24	0.000	0.000	0.000	0.000
	T 05	24	11.8 / 69	1.733	1.658	-1.732	-1.612
	T 06	45	11.8 / 69	3.742	3.384	-3.740	-3.322
	T 07	24	69 / 24	0.000	0.000	0.000	0.000
	T 08	24	69 / 24	0.000	0.000	0.000	0.000
	T 09	30	69 / 24	0.197	5.272	0.000	0.000
	T 10	150	20 / 69	1.271	-0.773	-1.271	0.785
8	T 01	60	13.8 / 69	12.941	13.349	-12.923	-12.718
	T 02	45	11.8 / 69	3.079	2.712	-3.078	-2.671
	T 03	60	69 / 24	0.000	0.000	0.000	0.000
	T 04	30	69 / 24	0.000	0.000	0.000	0.000
	T 05	24	11.8 / 69	1.528	1.416	-1.526	-1.381
	T 06	45	11.8 / 69	3.285	2.910	-3.284	-2.863
	T 07	24	69 / 24	0.000	0.000	0.000	0.000
	T 08	24	69 / 24	0.000	0.000	0.000	0.000
	T 09	30	69 / 24	0.196	5.238	0.000	0.000
	T 10	150	20 / 69	1.291	-0.790	-1.290	0.802
30	T 01	60	13.8 / 69	18.845	19.488	-18.805	-18.150
	T 02	45	11.8 / 69	0.460	0.360	-0.460	-0.359
	T 03	60	69 / 24	0.000	0.000	0.000	0.000
	T 04	30	69 / 24	0.000	0.000	0.000	0.000
	T 05	24	11.8 / 69	0.281	0.221	-0.281	-0.220
	T 06	45	11.8 / 69	0.495	0.388	-0.495	-0.387
	T 07	24	69 / 24	0.000	0.000	0.000	0.000
	T 08	24	69 / 24	0.000	0.000	0.000	0.000
	T 09	30	69 / 24	0.190	5.076	0.000	0.000
	T 10	150	20 / 69	1.375	-0.877	-1.374	0.891

